QUANTITATIVE MODELS AND METHODS FOR RISK-INFORMED PHYSICAL ASSET MANAGEMENT

by

Zaki Syed

A thesis submitted in conformity with the requirements

for the degree of Doctor of Philosophy

Department of Chemical Engineering & Applied Chemistry

University of Toronto

ABSTRACT

Quantitative Models and Methods for Risk-informed Physical Asset Management

Zaki Syed

Doctor of Philosophy

Department of Chemical Engineering & Applied Chemistry

University of Toronto

2019

In the last decade, the management of physical assets has emerged as a crucial business function for companies operating in asset intensive industries. Risk, defined as the likelihood and consequence(s) of undesired events, is an integral part of asset management. In this work, we set out to develop quantitative models and methods to facilitate risk-informed decision-making for the management of physical assets in the natural gas industry. We develop a novel practical approach that can be used in reliability analysis of physical assets. A Bayesian framework is implemented to cohesively integrate objective data with expert opinion and tacit knowledge with the aim toward deriving predictive models for time to failure for physical assets. The methodology presented provides an elegant and powerful way of addressing uncertainty by allowing the analyst to take into consideration all types of available information. To quantitatively analyse potential production losses due to critical asset failures, we develop a physics-based system performance and reliability model for an underground gas storage facility. The model combines a thermo-hydraulic performance model for a gas storage facility consisting of a gathering system, compression system and transmission system with a Monte Carlo simulation of potential disruption events. The model captures interdependence of assets within the system and facilitates quantitative analysis of operational reliability risk for a gas storage system. Additionally, a framework and methodology for decision-making under risk and uncertainty is developed for prioritization of a portfolio of capital investment decisions. The methodology uses quantitative risk measures to prioritize projects based on a combination of risk tolerance criteria, cost-benefit analysis and uncertainty reduction metrics. We use multi-criteria decision analysis methods to integrate subjective decision-maker preferences with objective project performance measures to prioritize potential capital investments. The methodology provides a practical and transparent way of making decisions for the management of physical assets.

ACKNOWLEDGEMENTS

I thank my thesis supervisor, Professor Yuri Lawryshyn, for his guidance and support throughout my journey. Our discussions gave me interesting insights into my work and challenged me to consider many different avenues of research. I would also like to thank my supervising committee, professors Graeme Norval and Roy H. Kwon, for their valuable feedback, motivating me to expand my thesis work beyond my original scope.

I have pursued my PhD work with an aim towards applicability in industry. Working with dedicated and experienced industry professionals, Andy Ridpath and Marcello Oliverio, pushed me to pursue practical solutions to critical issues in the management of physical assets. I am grateful for their mentorship throughout my professional career.

Most importantly, I would like to thank my wonderful wife, Shahani Zarra, for her enduring love and support throughout this journey. This work would not have been possible without your dedication and patience.

To my beloved wife.

CONTENTS

List of Tables

List of Figures

List of Appendices

1 INTRODUCTION

In the last decade, the management of physical assets has emerged as a crucial business function for companies operating in asset intensive industries (van der Lei, Herder, & Wijnia, 2012). Aging of asset systems, increased performance expectations from stakeholders, more stringent requirements from a safety and environmental standpoint, and several other factors can be attributed to the recent emphasis on asset management. Furthermore, the increasing complexity of modern engineered systems has precipitated the need for asset management as a discipline (Hastings, 2015). The increased complexity of asset management has also expanded the field beyond its historical boundaries. Whereas traditionally asset management was confined to the realm of maintenance management, the discipline now encompasses the entire asset lifecycle from the identification of business needs to end-of-life/disposal (IAM, 2015). The ISO 55000 Asset Management standard defines asset management as the "co-ordinated activity of an organization to realize value from assets", where optimal value is obtained by balancing cost, performance and risk (ISO, 2014).

The Global Forum on Maintenance & Asset Management has produced a detailed review of the activities necessary to support the management of physical assets (GFMAM, 2014). Three of the activities identified by the GFMAM are reliability engineering, risk assessment and management, and capital investment decision-making, which are of interest for this thesis work. Practical application of reliability analysis methods can be challenging, especially when data availability and data quality is an issue. Consequently, there is a need for robust methods and tools that can incorporate all available information to facilitate informed decision-making (Mettas, 2013; Leimeister & Kolios, 2018). Modern engineered assets operate within complex asset systems. As such, risk assessment in the asset management

context requires a systemic view in order to support optimal decision-making (IAM, 2015). Risk and reliability analysis of asset systems, as opposed to individual assets, has been identified as an important area requiring further research (Parlikad & Jafari, 2016; Petchrompo & Parlikad, 2019). Decision-making in the asset management context must take into consideration the requirements of multiple stakeholders as well as multiple dimensions of cost, performance and risk (IAM, 2015). A recent review of multi-criteria decision-making methods has highlighted that contributions towards improving the managerial decision process, taking into consideration multi-dimensional criteria and decision-maker preferences are needed (de Almeida, Alencar, Garcez, & Ferreira, 2017).

We set out to address the challenges described above for the management of natural gas storage and transmission assets. Increasing demand for natural gas makes effective management of assets in this industry of critical importance. Global demand for natural gas has been growing every year since 2009 at a compound rate of 2.6%. In 2017, production hit a record high of 3,768 billion cubic metres (IEA, 2018). Inevitably this increasing demand will put a greater strain on assets in the natural gas industry, meaning the consequence of failure of critical assets will be higher than before.

Lastly, we note that while the contributions (summarized in Section 1.2) of this thesis have been applied for the management of physical assets in the natural gas industry, much of the work has broader applications. Many disciplines, including medical science and finance, rely on expert opinion to support the development of statistical models. The first thesis contribution may be applied in such cases. Risk and reliability analysis of asset systems is also of critical importance across nearly all industries, including electric and water utilities, discrete manufacturing, and transportation and logistics. The approach for integration of physics models with asset reliability models (second contribution) may be applied. The risk-informed decision-making framework presented in the third contribution may be applied for environmental and ecological management, process safety management, maintenance management, etc. Such applications are further discussed in Chapter 5 Conclusions and Future Work

1.1 Objective

The primary objective of this thesis is to develop a framework and computer models to facilitate risk-informed and data-driven management of physical assets for natural gas storage and transmission systems. We develop a reliability analysis methodology that incorporates expert opinion as well as objective failure data. A stochastic simulation model is developed

to quantify operational reliability risk of a natural gas storage facility. Lastly, we present a framework for the prioritization of asset investment options considering risk and uncertainty.

1.2 Contributions

The main contributions of the thesis are the methodologies and computer models discussed in the manuscripts summarized below. Each manuscript addresses significant gaps in the asset management literature by providing an effective means of incorporating tacit knowledge in asset reliability analysis, using simulation to facilitate system-level risk analysis of gas storage and transmission assets, and presenting a unified framework for risk-informed decision-making in the asset management context. In summary, the key contributions of this thesis are:

1. **A method for integrating expert knowledge with objective failure data in reliability analysis.**

   This contribution is discussed in the paper presented in Chapter 2. A Bayesian framework is implemented to cohesively integrate objective data with expert opinion and tacit knowledge with the aim toward deriving time to failure distributions for physical assets. The flexibility of the proposed methodology allows for efficiently dealing with missing and incomplete failure data. Subjective information is processed using the Analytic Hierarchy Process (AHP) to aggregate time to failure estimates from multiple experts to minimize biases and address inconsistencies in their estimates. These estimates are summarized in the form of informative priors that are implemented in a Bayesian update procedure for the Weibull distribution. This is particularly useful for the cases of limited objective data, which are poorly handled by classical reliability approaches.

2. **A model for quantitatively analysing operational reliability risk in a gas storage and transmission system.**

   This contribution is discussed in the paper presented in Chapter 3. The model combines a thermo-hydraulic performance model for a gas storage facility consisting of a gathering system, compression system and transmission system with a Monte Carlo simulation of potential disruption events. The disruption events can impact the availability of one or more critical assets within the gas storage facility, which in turn affect the gas flow capability. The flow capability is compared against externally derived gas flow demand patterns to determine if shortfalls in supply can occur. The model is highly configurable and can be used to quantitatively assess operational

reliability risk for natural gas storage and transmission assets. The model is unique in that it integrates a physics-based system performance model with stochastic simulation of critical asset failures, allowing for quantitative risk analysis at the system level.

3. **A framework for objectively prioritizing capital investments considering multi-dimensional risk and uncertainty.**

   This contribution is discussed in the paper presented in Chapter 4. The methodology uses quantitative risk measures to prioritize projects based on a combination of risk tolerance criteria, cost-benefit analysis and uncertainty metrics. We consider risk measures for loss of life, loss of production and loss of property. Risk reduction benefit of the capital investment options is quantified and cost-benefit analysis is performed to screen for viable projects. Viable projects are prioritized taking into consideration subjective decision-maker preferences as well as objective capital investment performance measures (i.e. risk reduction benefits, costs). This paper addresses a gap in the literature for risk-informed asset management decisions: a unified framework to facilitate asset management decision-making using quantitative and multi-dimensional risk measures and decision-maker preferences.

1.3 Document Outline

The remainder of this document is organized into five chapters. Chapter 2 presents the paper titled “A Novel Tool for Bayesian Reliability Analysis Using AHP as a Framework for Prior Elicitation”. Chapter 3 presents the paper “Risk Analysis of an Underground Gas Storage Facility using a Physics-based System Performance Model and Monte Carlo Simulation”. Chapter 4 includes the paper “Multi-Criteria Decision-Making Considering Risk and Uncertainty in Physical Asset Management”. Finally, Chapter 5 discusses the major conclusions of this thesis and proposes potential future work. In addition to the case studies presented in each chapter, a summary case study encompassing all the methodologies developed in this work is included in the Appendix.

2 A NOVEL TOOL FOR BAYESIAN RELIABILITY ANALYSIS USING AHP AS A FRAMEWORK FOR PRIOR ELICITATION

ABSTRACT

Over the last decade, many companies have realized the utility of reliability methods and predictive maintenance to facilitate informed decision-making. However, practical application of such methods can be challenging, especially when data availability and data quality is an issue. Consequently, there is a need for robust methods and tools that can incorporate all available information to facilitate informed decision-making. This paper presents a novel practical approach that can be used in reliability assessment and risk analysis. A Bayesian framework is implemented to cohesively integrate objective data with expert opinion and tacit knowledge with the aim toward deriving life distributions for physical assets. The flexibility of the proposed methodology allows for efficiently dealing with missing and incomplete failure data. Subjective information is processed using the Analytic Hierarchy Process to aggregate time to failure estimates from multiple experts to minimize biases and address inconsistencies in their estimates. These estimates are summarized in the form of informative priors that are implemented in a Bayesian update procedure for the Weibull distribution. This is particularly useful for the cases of limited objective data, which are poorly handled by classical reliability approaches. Application of the proposed approach is illustrated using a case study.

2.1 Introduction

The advent of easily accessible information coupled with ever increasing computing power solidifies the application of predictive analytics to facilitate efficient decision-making. Some industries, through numerous examples, have shown the advantage of using predictive analytics such as machine learning and artificial intelligence as a decision support tool (Knox, 2018). Such analytics are data centric at their core and may not require any knowledge of the underlying theory/process of a system under consideration. Thus, when good quality data is in abundance, these approaches can be employed to inform decision-making. However, despite the tremendous appetite for using such analytics, misleading results can be obtained if the analytics are based on limited, missing or poor-quality data (Redman, 2018).

The field of physical asset management is acutely aware of the problems of incomplete and poor-quality data. In practice, the data problems are common for many industries, including energy, oil and gas, utilities, etc. (Hong, Meeker, & McCalley, 2009). Many physical assets such as pipelines and rotating equipment are expensive to maintain or replace, making effective decision-making evermore critical. Nevertheless, asset managers must make decisions with limited data (and thus high uncertainty) about which assets to prioritize for maintenance/replacement and when to carry out such work on an asset. A method to incorporate all available information about an asset is necessary to facilitate decision-making when faced with data scarcity. The Bayesian paradigm offers a mathematically consistent way of augmenting the available data with other sources of information, and in turn reducing the amount of uncertainty faced by a decision-maker. In this paper, we apply Bayesian methods in reliability analysis in the context of decision-making for physical asset management.

Much of the research in reliability of engineered systems or components has successfully integrated multiple sources of information by applying informative prior distributions within the Bayesian paradigm. Wilson and Fronczyk (2016) showed how prior information can improve precision in reliability calculations for military application purposes. The authors applied laboratory test results to specify an informative prior, which was then used to supplement the experimental data. Wu (2017) implemented an outcome of fatigue analysis to rigorously construct informative priors in a Bayesian Hierarchical model for reliability of wind turbines. Such integration of prior information enabled reliability of engineered systems or components to be estimated even under significant data scarcity. Li and Meeker (2014) compared multiple cases of using informative prior, non-informative prior and maximum likelihood (MLE) methods for reliability studies. While non-informative and

traditional MLE methods provide almost identical results, informative priors, based on accelerated degradation tests, significantly contributed to uncertainty reduction in all reliability case studies. Furthermore, the authors argue that explicitly defined informative priors establish a better foundation for decision-making, due to its inherent transparency. Other researchers advocate that properly specified priors (even weakly informative) not only help to formally integrate various types of information, but also help to minimize convergence issues for numerical algorithms, such as Markov Chain Monte Carlo (MCMC) (McNeish, 2016; Lambert, 2018).

In this paper we present a methodology to incorporate expert opinion with actual failure data with the goal of obtaining a Weibull life distribution for a physical asset. The Analytic Hierarchy Process (AHP) is implemented to provide a structured approach for selecting experts from whom to elicit time to failure estimates (Saaty, 1980). AHP is also used to aggregate opinions of multiple experts to construct informative priors. A similar method was suggested by Cagno, et al. (2000). The authors used AHP in the Bayesian paradigm to obtain prior distributions for the failure rate of different low-pressure cast-iron gas pipelines. However, AHP was utilized for pairwise comparison of assets under different operating conditions rather than for expert selection and aggregation of expert opinion.

The use of expert opinion to construct prior distributions of Weibull parameters has been explored by authors in the past (Singpurwalla, 1988; Coolen, Mertens, & Newby, 1990; Gutierrez-Pulido, Aguirre-Torres, & Christen, 2005). However, such methods have relied on experts to provide estimates about the values of unobservable quantities such as the Weibull shape parameter, which can be a difficult task for experts. The method presented in this paper requires experts to provide estimates on time to failure, which is an observable quantity and thus easier for the experts to estimate. Time to failure estimates are then used to obtain prior distributions for Weibull parameters.

We begin by providing a summary of the theoretical background in Section 2.2. A detailed description of the methodology is provided in Section 2.3. Finally, we demonstrate the utility of the proposed methodology using a case study based on actual experience with natural gas compression and transmission infrastructure (Section 2.4).

2.2 Theoretical Background

2.2.1 Reliability Engineering

The concept of reliability for engineered (physical) assets is best understood by first considering the meaning of quality, which is the set of characteristics of an asset that determines if it meets specifications and in turn determines customer satisfaction. The reliability of an asset is its ability to retain its quality as it ages. Mathematically, the reliability (R) of an asset is defined as the probability that it continues to retain its quality over a given period of time, whilst operating in a given environment (Bentley, 1999). Conversely, the unreliability (F) of an asset is the probability that it fails to meet specifications.

The unreliability of an asset as function of age (t) is given by the cumulative distribution function $F(t)$, representing the probability that the asset fails by age t. The reliability of an asset is given by $R(t) = 1 - F(t)$ and the instantaneous failure rate (also known as the hazard rate) is given by $h(t) = f(t)/R(t)$, where $f(t)$ is the probability density function of time to failure (Tobias & Trindade, 2012). The hazard rate is indicative of the failure mechanism: a decreasing hazard indicates early failure mechanisms such as installation or quality issues; an increasing hazard is typical of end of life or wear-out failures; and a constant hazard is indicative of no significant wear-out or early failure mechanism (Jardine & Tsang, 2013). The age at which an asset fails is known as the lifetime of the asset, and the uncertainty about the lifetime of an asset is represented using mathematical models known as life distributions. One of the most common models is known as the Weibull distribution, defined by the density and distribution functions

$$f(t;\beta,\eta) = \frac{\beta}{\eta}\left(\frac{t}{\eta}\right)^{\beta-1} exp\left[-\left(\frac{t}{\eta}\right)^{\beta}\right] \quad and \quad F(t;\beta,\eta) = 1 - exp\left[-\left(\frac{t}{\eta}\right)^{\beta}\right], \qquad (1)$$

where $\eta > 0$ is the scale parameter and $\beta > 0$ is the shape parameter, and $t \geq 0$ (Tobias & Trindade, 2012). The Weibull distribution has gained widespread use because of its flexibility, allowing it to fit many failure characteristics. When $\beta = 1$, the Weibull distribution exhibits constant hazard. When $\beta < 1$, the Weibull distribution exhibits decreasing hazard. When $\beta > 1$, the Weibull distribution exhibits increasing hazard.

Typically, parameters are estimated using regression methods (Weibull analysis) or the method of maximum likelihood (MLE) (Jardine & Tsang, 2013). Such methods are classical approaches to statistical analysis, and they perform well when sample sizes are high (Tobias & Trindade, 2012). In practice, a sufficient sample is often not available for multiple reasons.

For example, assets may operate in vastly different operating environments or are of different design. This would require stratification, reducing the number of samples in each group of assets. Another possibility is that assets may be highly reliable resulting in limited failures. Or data collection may have been flawed or occurred over a limited duration, resulting in few samples that can be used for statistical analysis. Bayesian statistical inference can be used to fill this gap and can yield more information about the asset life than classical methods if used appropriately (Tobias & Trindade, 2012).

2.2.2 Bayesian Inference in Reliability Analysis

Bayesian updating of an initial hypothesis is performed using Bayes' theorem. The theorem describes how to update a prior belief about a phenomenon or process considering new evidence, and is given by

$$p(\theta|x) = \frac{p(x|\theta)p(\theta)}{p(x)} = \frac{p(x|\theta)p(\theta)}{\int p(x|\theta)p(\theta)\, d\theta}, \qquad (2)$$

where $p(\theta|x)$ is the posterior probability distribution for the set of parameters (θ) describing the process and x is the observed data. The prior distribution $p(\theta)$ reflects the initial state of knowledge about the process before observing any data, whereas the posterior distribution $p(\theta|x)$ shows the updated state of knowledge after new evidence becomes available. These two expressions are linked through a likelihood function $p(x|\theta)$. This function describes the plausibility of the observed data given model parameters θ. Lastly, $p(x)$ is the marginal distribution of the data and is given by $\int_{All\ \theta} p(x|\theta)\ p(\theta)\ d\theta$ (Hamada, Wilson, Reese, & Martz, 2008).

In the literature, the prior is also often referred as a subjective distribution. Some degree of subjectivity may be involved to construct a prior distribution. This subjectivity is often used as a basis for criticism of Bayesian methods. Despite this criticism, the prior distribution is not a shortcoming, rather a key feature of the Bayesian paradigm. The prior distribution offers a flexible and cohesive approach to incorporate different types of information. This property is particularly useful in reliability studies where a significant amount of prior information and tacit knowledge is often available but cannot be incorporated using classical methods of reliability analysis. Prior knowledge may include, but is not limited to, asset condition information, engineering judgement, accelerated life testing, industry failure data on similar assets, and so on. Thus, incorporation of such information through prior distributions helps to make more realistic assumptions as opposed to fully relying on data

alone and assuming no other information is available (Li & Meeker, 2014). Furthermore, the issue of data availability and small sample size in general is highly relevant for reliability studies, especially in the modelling of rare events. In fact, for rare events, one may need to rely more on engineering knowledge and tacit information than on actual scarce incident data (Sridhar, 2018).

To ensure superiority of Bayesian inference, the prior distribution must be rigorously constructed. This may not be crucial for a large sample size (i.e. data overwhelms importance of prior), but for a small sample size a properly specified prior is essential because the choice of prior may have a predominant impact on the posterior (McNeish, 2016). As noted by van de Schoot, et al. (2013): "the smaller the sample size, the bigger the influence of the prior specification and the more can be gained from specifying subjective priors". Thus, for small sample size problems as much advantage can be gained by using Bayesian methods, as much bias can be introduced if the prior is incorrectly specified. To avoid the problem, this paper implements a rigorous elicitation approach to properly construct subjective prior distributions. Details on this approach are discussed in the following section.

2.3 Methodology

This section provides details of the proposed methodology for conducting reliability analysis using Bayesian methods when faced with limited failure data. As discussed previously, Bayesian methods for reliability analysis have a distinct advantage over classical approaches using informative prior distributions for model parameters. The methodology presented in this paper provides a framework for obtaining prior distributions for the Weibull distribution parameters, which are then updated using actual failure data. A flow chart of the methodology is shown in Figure 1.

Emphasis is placed on a Weibull model for asset failure due to a wear out failure mechanism. However, this methodology is flexible and may be extended to other life distributions. The methodology first requires that the failure mechanism be understood to determine if a Weibull wear out model is applicable (Section 2.3.1). Once this is confirmed, AHP is used to aggregate time to failure estimates from multiple experts (Section 2.3.2). The expert estimates are used to obtain prior distributions for the Weibull parameters as described in Section 2.3.3. If failure data is available, a Bayesian update of the priors is conducted using the Metropolis-Hastings (MH) MCMC algorithm as discussed in Section 2.3.4. Recommended posterior checks are discussed in Section 2.3.5 to evaluate model fit.

In presenting this methodology, we refer to three key roles in the prior elicitation, Bayesian inference and decision-making process (Bedford, Quigley, & Walls, 2006):

- **Decision-maker:** person responsible for making the final decision (e.g. proactive replacement of assets) and must be informed about relevant uncertainties by experts and available data.
- **Experts:** persons who are subject matter experts with respect to the problem (i.e. asset reliability) of interest.
- **Analyst:** person responsible for selecting experts, eliciting their opinion with respect to the problem, and performing reliability analysis with available data.

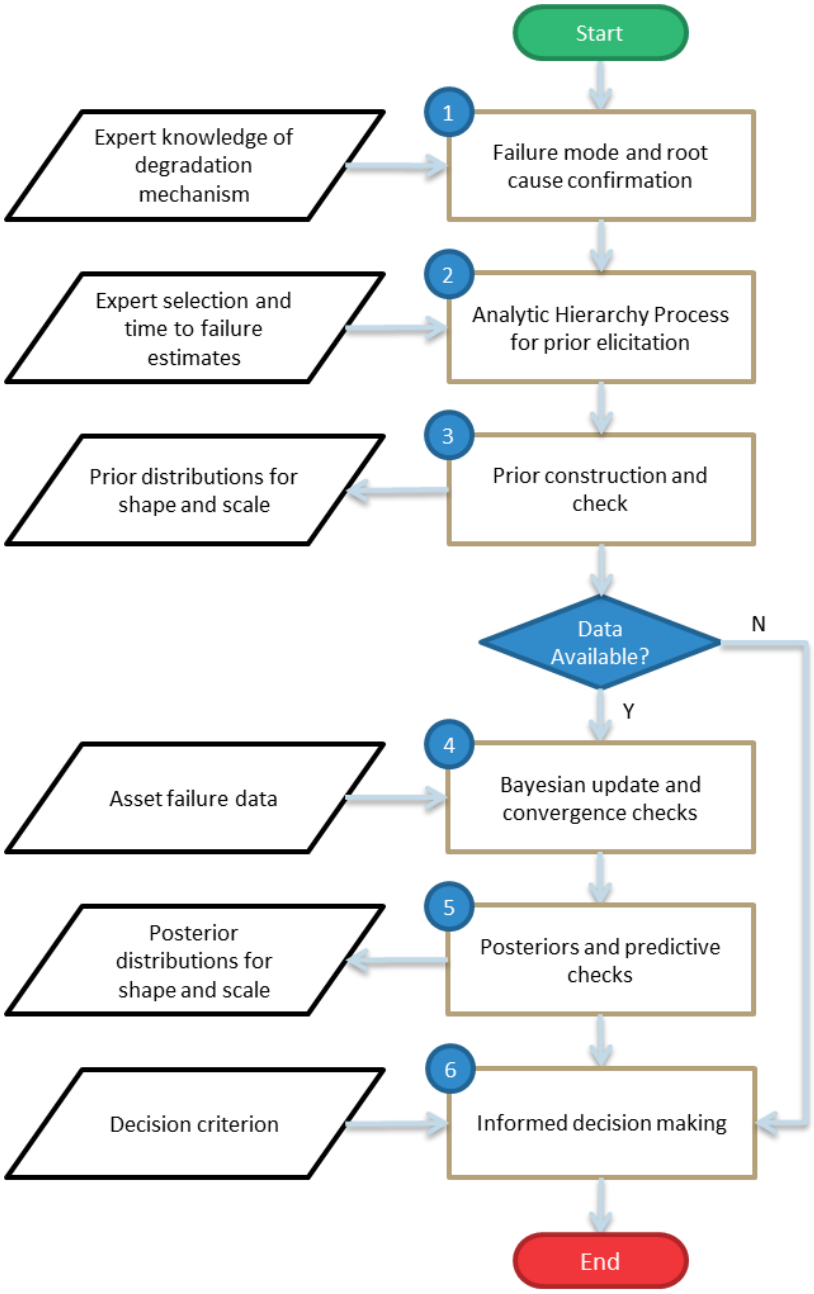

Figure 1. Decision-Making Flow Chart

2.3.1 Failure Mechanism

To fully characterize a failure mechanism, it is necessary to define the failure mode as well as the root cause. This concept is perhaps best explained with an illustrative example. Consider a manually operated ball valve in a chemical process facility. A critical failure mode of this type of asset may be internal leakage. One root cause of this failure mode may be wearing of the seals due to repeated cycling (open/close) of the valve, and a different root cause may be an overturning of the valve resulting in a misalignment between the valve stem and the ball. In the first case, the time to failure may be modelled using a Weibull distribution with $\beta > 1$. In the second case, the failure is due to a random event that is not age dependent and may be modelled using a Weibull distribution with $\beta = 1$.

As highlighted with the above example, in order to ensure that estimates provided by experts are consistent with the failure mechanism to be modelled, the failure mode and root cause must be established before applying the proposed methodology. Furthermore, the failure mechanism must be communicated to all experts before eliciting their opinion, with the aim towards managing cognitive biases (Quigley, Bedford, & Walls, 2008). It has been proposed that qualitative structuring of the model is equally important to quantitative assessment to ensure proper parameterization of the reliability model (Bedford, Quigley, & Walls, 2006). If the failure mechanism is confirmed to exhibit a wear out pattern, the time to failure can be modelled using a Weibull distribution with $\beta > 1$, and in turn one with a non-zero mode. This characteristic, as explained in Section 2.3.3, is used to obtain the prior distributions for the Weibull shape and scale.

2.3.2 Expert Elicitation

Expert knowledge and engineering judgement are essential components in understanding and estimating reliability of assets. Such information represents subjective knowledge which is encoded in the form of meaningful mathematical statements (i.e. eliciting) (Evans, 1989). This sub-section presents a methodology for eliciting subjective information about asset time to failure that is then summarized in the form of informative prior distributions for the Weibull model parameters. Construction of the informative prior is a challenge, but if performed properly, it can significantly improve inference, especially in the case of a small sample of actual asset failures. AHP is used to aggregate expert estimates in an objective and structured manner.

AHP is a multi-criteria decision-making methodology that has been extensively studied and widely used in many industries (Saaty, 1980). The objective of AHP is to provide decision-

makers with a structured method of evaluating alternative solutions against decision criteria. Alternatives can be potential capital projects, candidates for hire, equipment purchase options, etc. Decision criteria are factors that are of importance in the selection of an alternative. For example, cost, functional performance criteria, lead time, etc. The aim then is to obtain relative ranking of the solution alternatives based on how well they meet the decision criteria to help select the best alternative. AHP has been used to objectively select students for admission to graduate business school programs (Saaty & Vargas, 2012), as well as for recruitment of sales personnel (Duben & Ricks, 2015). Similarly, in this application, AHP is used to objectively select experts and then aggregate their input regarding prior information about the Weibull parameters.

We implement the AHP method with a single level in the decision hierarchy and three criteria: years of experience, number of observed failures, and level of training with respect to maintenance/operation of the asset in question. However, the methodology may be extended to any number of levels and criteria. The analyst may choose to define the AHP criteria differently depending on the problem at hand. For example, number of observed failures can refer to only observations of the exact type of asset being analysed or may be defined to include an expert's observations of failure of similar assets. The important part is ensuring consistency in definition when performing pairwise comparison of the decision criteria and when evaluating each expert against the criteria.

The analyst, perhaps through collaboration with the decision-maker, must first select (by pairwise comparison) the relative importance of each of the decision criteria. Saaty's numeric scale is recommended (Saaty, 1980) to quantify the relative importance (Table 1). The relative importance must be evaluated based on the analyst's judgment about how much each criterion will contribute to the validity of asset time to failure estimates provided by an expert. For example, if it is known that the failure mechanism in question has historically been managed through regular inspection/maintenance then the expert's relevant training may receive high importance. Conversely, if the asset is highly reliable then the analyst may wish to put more importance on observed failures. After completing the pairwise comparison, the AHP consistency check must be performed to ensure consistency in the importance ratings.

Table 1. AHP Numeric Scale with Linguistic Interpretation

Intensity of Importance	Definition	Explanation
1	Equal importance	Two factors contribute equally to the objective.
3	Somewhat more important	Experience and judgement slightly favour one over the other.
5	Much more important	Experience and judgement strongly favour one over the other.
7	Very much more important	Experience and judgement very strongly favour one over the other. Its importance is demonstrated in practice.
9	Absolutely more important	The evidence favouring one over the other is of the highest possible validity.
2,4,6,8	Intermediate values	When compromise is needed.

It must be noted that for Bayesian inference to be valid, observed failures in the expert selection context must be independent of the recorded failure data to be used in Bayesian updating (Section 2.3.4). In other words, the expert must be instructed to form his/her opinion based on his/her personal knowledge of past, and likely unrecorded, failures. If the analyst judges that the expert's opinion is being influenced by the failure data to be used for Bayesian updating, then it is recommended that the expert be removed from the selection process or given a low score when evaluated against this criterion.

The next step requires that the analyst score the relative degree to which each expert meets the requirements of each decision criterion. It is recommended that Saaty's 1 to 9 numeric scale be used, and the analyst give a score of 9 to the expert that best meets a given criterion. All other experts are then ranked relative to the best expert. Note that rankings are done within each decision criterion, independent of an expert's ranking in another criterion. The AHP calculation is then performed by constructing the comparison matrices, calculating criteria weights, priority vectors of experts within each decision criterion, and finally the overall weighting of each expert (Saaty & Vargas, 2012). The calculated weights are used in two different ways: to create a shortlist of experts from whom to elicit time to failure estimates, and to aggregate expert estimates of asset time to failure for prior construction.

Before eliciting expert estimates and aggregating their input, the analyst must take precautions to minimize the impact of cognitive biases. Behavioural psychology studies have shown that experts who were asked to directly evaluate a probability number of a certain event fail to provide an adequate estimate (Tversky & Kahneman, 1982). This is confirmed by Bedford and Cooke (2001) who emphasize that an expert is unlikely to provide a reliable subjective judgment of an unobservable quantity. Furthermore, expert estimates are significantly influenced by a variety of biases that human judgment is inherently subjected to (Tversky & Kahneman, 1982). To name a few: group bias, authority bias, anchoring bias and over confidence (e.g. Dunning-Kruger effect) are biases that can drastically affect the elicitation process (Johnson, Tomlinson, Hawker, Granton, & Feldman, 2010). Therefore, to ensure quality of subjective probabilities (i.e. informative priors), not only is a structured procedure necessary for proper expert elicitation, but an efficient approach to minimize impacts of biases is also required. We propose the following method for eliciting expert estimates:

- Avoid eliciting estimates in a group and opt for individual interviews instead. The aim is to eliminate authority bias and group bias. If time/resource restrictions put a limit on the number of interviews that can be conducted, select the top experts as ranked by the AHP methodology proposed.
- Ensure that the expert is fully aware of the failure mechanism being examined and that there is minimal ambiguity or room for interpretation (see Section 2.3.1).
- Minimize the effect of anchoring bias and overconfidence by involving multiple experts, whose opinions are aggregated using the weights derived from the AHP methodology proposed.
- Ask the expert for directly observable quantities such as the median or mode of the asset times to failure rather than percentiles, means or variances. Suggested questions for modelling wear out failures using the Weibull distribution are discussed in Section 2.3.3.

2.3.3 Prior Construction

A method for construction of prior distributions for the Weibull parameters is discussed in this section. The objectives are two-fold: capture the expert's uncertainty about the observable quantities and construct priors using expert estimates of observable quantities. A Weibull distribution used to model time to failure due to a wear out mechanism exhibits a non-zero mode. This characteristic was used by Lad and Kulkarni (2010) to obtain Weibull

parameters from expert estimates of time to failure. The mode (T_{mode}) of the time to failure distribution is an observable quantity and can be interpreted as the age at which an asset typically fails or is most likely to fail. Lad and Kulkarni (2010) suggest obtaining a second observable quantity; the maximum survival age of the asset (T_{max}) defined as the 99th percentile of the Weibull time to failure distribution. The expert may be prompted by asking for the age of the longest surviving asset. An example Weibull distribution with $T_{mode} = 20$ and $T_{max} = 70$ is shown in Figure 2. Note that in this section we do not specify units for the time to failure since the analysis would proceed the same way regardless of the units. Units maybe hours, cycles, days, weeks, years, etc.

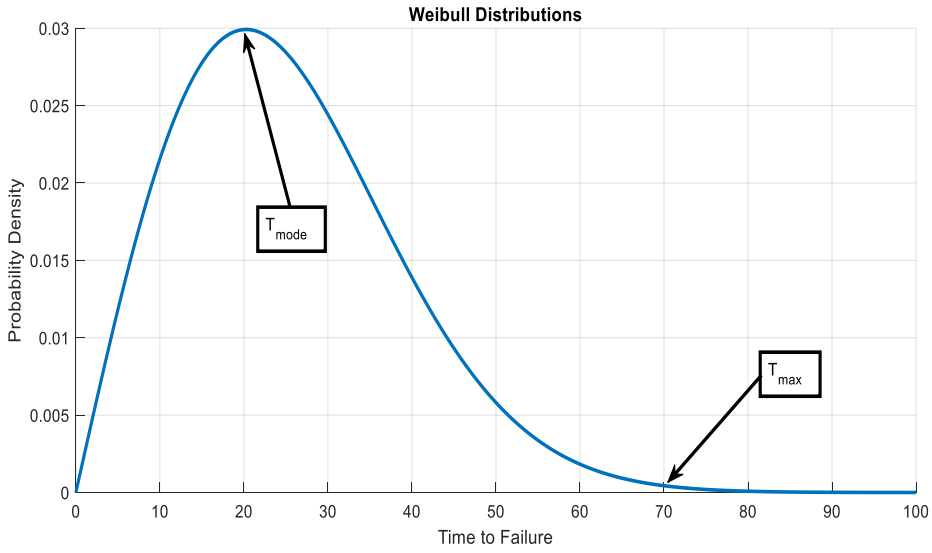

Figure 2. Example Weibull Distribution

To capture the expert's uncertainty about T_{mode} and T_{max} we suggest prompting him/her for a lower bound (T_{mode}^{LB} and T_{max}^{LB}), best estimate (T_{mode}^{BE} and T_{max}^{BE}) and upper bound (T_{mode}^{UB} and T_{max}^{UB}). Estimates should be elicited from multiple experts and a weighted average of each quantity ($\bar{T}_{mode}$ and $\bar{T}_{max}$) calculated using the weights obtained via AHP as described in Section 2.3.2 and illustrated with an example in Section 2.4. The aggregated expert estimates are used to construct Modified Beta-PERT distributions for $\bar{T}_{mode}$ and $\bar{T}_{max}$. Such distributions are ideally suited to model uncertainty based on expert opinion because of the convenient parameterization relying on four parameters: a minimum (a), mode (m), maximum (b) and a weighting factor (γ) for the mode (Vose, 2008). The pdf of the modified Beta-PERT is given by

$$f(x) = \frac{1}{B(\alpha_1, \alpha_2)} \frac{(x-a)^{\alpha_1 - 1}(b-x)^{\alpha_2 - 1}}{(b-a)^{\alpha_1 + \alpha_2 - 1}}, \qquad (3)$$

where $B(\alpha_1, \alpha_2)$ is the beta function, $\alpha_1 = 1 + \gamma\left(\frac{m-a}{b-a}\right)$, $\alpha_2 = 1 + \gamma\left(\frac{b-m}{b-a}\right)$, and $a \leq m \leq b$. The support of the density function (where it is non-zero) is $[a, b]$.

We obtain a Beta-PERT distribution for $\bar{T}_{mode}$ by setting $a = \bar{T}^{LB}_{mode}$, $b = \bar{T}^{UB}_{mode}$ and $m = \bar{T}^{BE}_{mode}$. The standard Beta-PERT distribution uses $\gamma = 4$, though higher or lower values may be used to modify the curve, where lower values have the effect of flattening the curve and higher values make it peakier (Vose, 2008). A distribution for $\bar{T}_{max}$ is similarly obtained. Example distributions are shown in Figure 3, where $\bar{T}^{LB}_{mode} = 10$, $\bar{T}^{UB}_{mode} = 30$, $\bar{T}^{BE}_{mode} = 20$, $\bar{T}^{LB}_{max} = 40$, $\bar{T}^{UB}_{max} = 80$ and $\bar{T}^{BE}_{max} = 70$. The values used to plot Figure 3 have been selected arbitrarily for illustration purposes. In practice the analyst would derive the values as described earlier in this sub-section.

Figure 3 shows the flexibility of the Modified Beta-PERT distribution, where selection of the weighting factor (γ) can change the shape from extremely peaky to uniformly flat. The chart on the left uses the standard value of $\gamma = 4$. In the chart on the right, $\gamma = 0$ is used for $\bar{T}_{mode}$ and $\gamma = 8$ is used for $\bar{T}_{max}$. While the introduction of this factor is a source of subjectivity, it is nevertheless a useful feature because it allows the analyst to adjust the distribution precision based on his/her judgment of the quality (i.e. accuracy) of the expert input on an absolute basis. In contrast, the AHP weights provide a measure of quality based on relative weight of experts to each other.

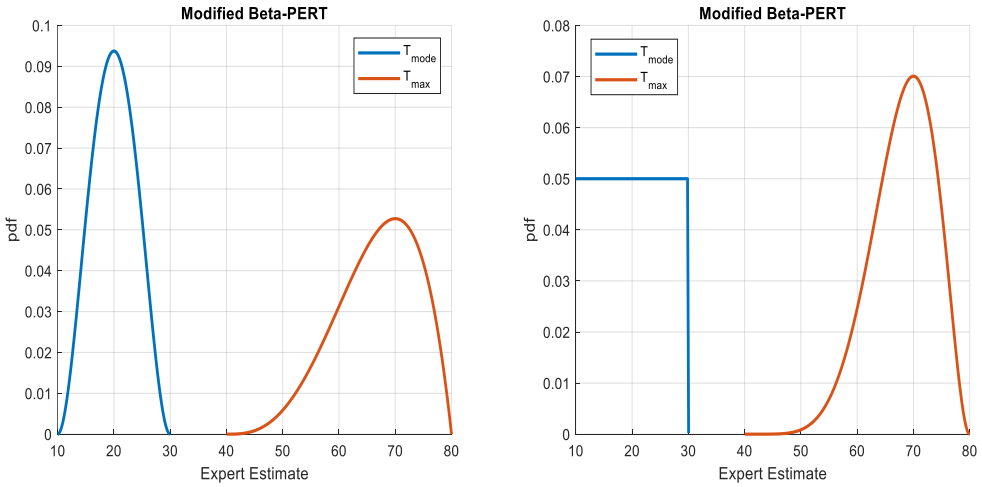

Figure 3. Example Modified Beta-PERT distributions for $\bar{T}_{mode}$ and $\bar{T}_{max}$

Once distributions for $\bar{T}_{mode}$ and $\bar{T}_{max}$ have been constructed, an algorithm is used to generate distributions for the Weibull parameters (β and η). The algorithm randomly samples a value of $\bar{T}_{\text{mode}}$ and $\bar{T}_{max}$ from the Beta-PERT distributions of each and then calculates the Weibull parameters for the pair of samples. The Weibull parameters are

calculated by solving equations for $\bar{T}_{mode}$ and $\bar{T}_{max}$ simultaneously as proposed by Lad and Kulkarni (2010). The maxima of the Weibull pdf can be found by simple differentiation of $f(t)$ with respect to t (see Equation 1) and is given by

$$\bar{T}_{mode} = \eta \left[\frac{\beta - 1}{\beta}\right]^{\frac{1}{\beta}}. \tag{4}$$

An expression for $\bar{T}_{max}$ is found by setting the Weibull CDF ($F(t)$) equal to 0.99 and re-arranging to give

$$\bar{T}_{max} = \eta \left[ln\left(\frac{1}{1 - 0.99}\right)\right]^{\frac{1}{\beta}}. \tag{5}$$

Equation 4 and 5 can be solved for η and β. We generate sample data for each Weibull parameter in this manner and proceed to fit gamma distributions to the sample data (Figure 4). The parameterization of the gamma distribution commonly used in Bayesian statistics is used:

$$f(x) = \frac{\left(\frac{\sigma^2}{\mu}\right)^{\frac{\mu^2}{\sigma^2}} exp\left(\frac{\mu x}{\sigma^2}\right) x^{\frac{\mu^2}{\sigma^2}-1}}{\Gamma\left(\frac{\mu^2}{\sigma^2}\right)}, \tag{6}$$

where μ is the mean and σ^2 is the variance (Lambert, 2018). Figure 4 shows examples of priors constructed by sampling $\bar{T}_{mode}$ and $\bar{T}_{max}$ from the distributions shown in the left-hand chart in Figure 3. Testing with different Beta-PERT distributions for $\bar{T}_{mode}$ and $\bar{T}_{max}$ shows that the gamma distribution provides acceptable fits for sample data of Weibull shape and scale generated using the algorithm described in this sub-section. Moreover, it has the appropriate support since both $\beta > 0$ and $\eta > 0$. The informative priors constructed using the method described in this sub-section are used to perform Bayesian inference with actual failure data as described in Section 2.3.4.

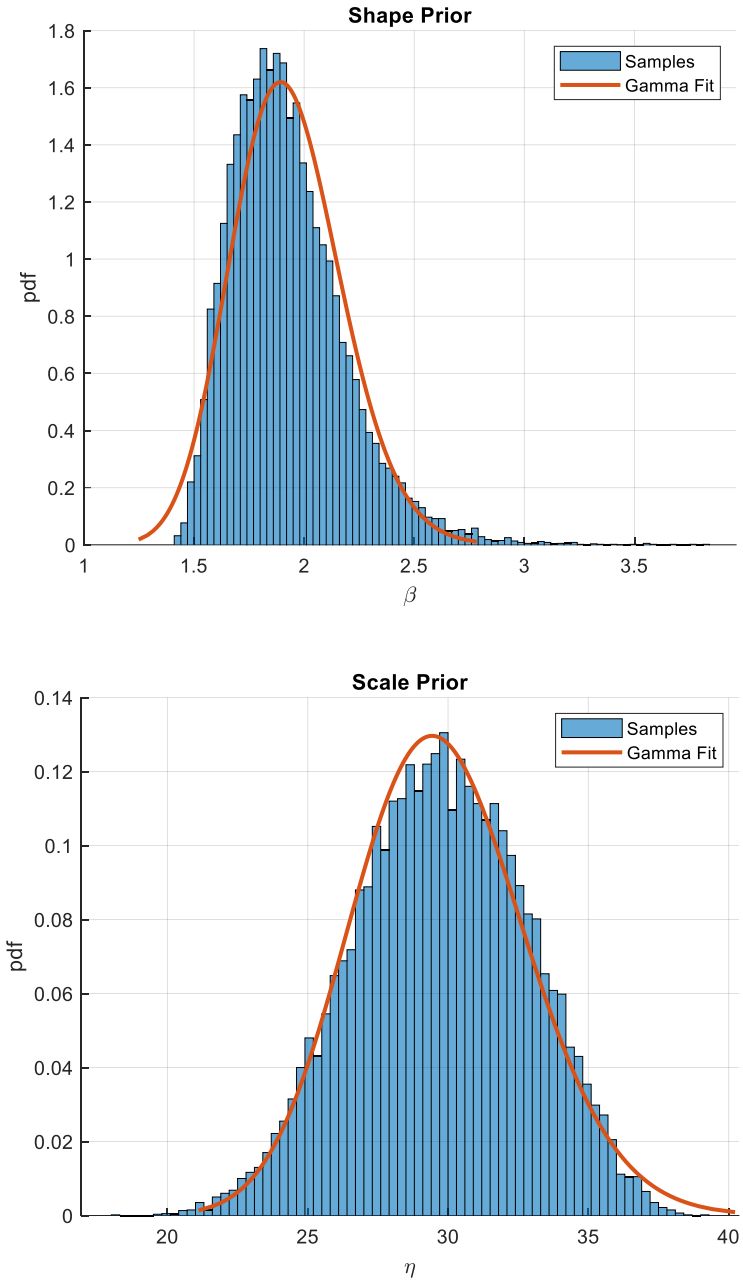

Figure 4. Gamma fit for Weibull parameter samples

2.3.4 Bayesian Update

This sub-section provides a detailed description of the Bayesian updating algorithm implemented for the methodology presented in this paper. The likelihood function ($p(x|\theta)$) is discussed (see Equation 2). We then discuss the numerical method employed to solve Equation 2 for parameters of the Weibull distribution. This is followed by a brief discussion on convergence criteria for the implemented numerical algorithm.

Under the Bayesian paradigm, observed data (e.g. failures) is incorporated in the analysis through the likelihood function. It is not uncommon for failure data to have observational

constraints, and omitting such constraints may introduce significant sampling bias (Emura & Shiu, 2014; Hong, Meeker, & McCalley, 2009). In reliability studies, the most frequently encountered observational constraints are Left Truncation (LT), Right Censoring (RC), or a combination of both (LTRC). The LT constraint occurs when failures may have been excluded from the sample because some of the assets potentially failed before observations were started to be recorded. The RC constraint occurs when an asset is still in service when observations end or if an asset is removed for a reason other than failure. Consequently, if asset data is limited by LT as well as RC constraints simultaneously such data is called LTRC. Let x represent the set of T observed times to failure (i.e. $x \in t_i$), then the likelihood function, accounting for LTRC data, proposed by Mitra (2012):

$$p(x|\theta) = \prod_{i=1}^{T} \{f(t_i;\theta)\}^{\delta_i \nu_i} \times \{1 - F(t_i;\theta)\}^{(1-\delta_i)\nu_i} \times \left\{\frac{f(t_i;\theta)}{1 - F(\tau_i;\theta)}\right\}^{\delta_i(1-\nu_i)} \times \left\{\frac{1 - F(t_i;\theta)}{1 - F(\tau_i;\theta)}\right\}^{(1-\delta_i)(1-\nu_i)} \quad (7)$$

where $f(t_i;\theta)$ and $F(t_i;\theta)$ denote the pdf and CDF (see Equation 1) of a single observation of time to failure t_i; τ_i represents truncation time; ν_i is an indicator function for LT cases; δ_i is an indicator functions for RC cases. The truncation time is the difference between the age at failure or censoring and the age when observations were started to be recorded. The likelihood function can be easily extended to account for other types of observational constraints such as interval-censoring, right truncation and so on (Mitra, 2012).

The outcome of Bayesian updating is the posterior distribution ($p(\theta|x)$), which is nothing else but the normalized product of the prior and likelihood, where the normalizing constant is $p(x)$ (see Equation 2). For many cases, including for Weibull likelihood, there is no analytical solution for the integral needed to obtain $p(x)$. Numerical methods must be employed to address this problem. In this study, we use the MH MCMC sampling algorithm to solve Equation 2. The pseudocode of this algorithm is provided below, whereas detailed discussion of this approach can be found in (Chib & Greenberg, 1995).

MH MCMC Algorithm:

1. Start:
    a. Set $m = 1$
2. Initialize Markov Chain:
    a. Set $n = 1$
    b. Generate an initial value of parameter(s) θ_n
3. Propose Next Step:
    a. Generate a proposal θ_{n+1} from jumping distribution $J(\theta_{n+1}|\theta_n)$
    b. Calculate acceptance ratio $r = \min\left(1, \frac{p(\theta_{n+1})}{p(\theta_n)} \frac{p(x|\theta_{n+1})}{p(x|\theta_n)} \frac{J(\theta_n|\theta_{n+1})}{J(\theta_{n+1}|\theta_n)}\right)$
4. Accept or Reject:
    a. Generate a uniform random number $u \in [0,1]$
    b. If $r \geq u$ accept the new state θ_{n+1}
    c. If $r < u$ reject the new state and copy the previous state $\theta_{n+1} = \theta_n$
5. Increment Markov Chain:
    a. Set $n = n + 1$
    b. Go back to Step 3 or if maximum iterations (N) for chain reached go to Step 6
6. End of Chain:
    a. Set $m = m + 1$
    b. Go back to Step 2 or end simulation if maximum number of chains (M) reached

Running the MH MCMC sampler for multiple chains and enough iterations for each chain numerically recreates the posterior distribution that is used in Bayesian inference. To ensure convergence of this numerical method, we apply the Gelman-Rubin convergence criterion, which compares local chain variance with global variance (Gelman & Rubin, 1992). If the difference is insignificant, then MH MCMC sampler has reached the stationary posterior distribution. The Gelman-Rubin convergence criterion is given by

$$W = \frac{1}{M}\sum_{m=1}^{M} s_m^2 \; ; \; B = \frac{N}{M-1}\sum_{m=1}^{M}(\bar{\theta}_m - \bar{\theta})^2 \; ; \; \hat{R} = \sqrt{\frac{W + \frac{1}{N}(B - W)}{W}} \qquad (8)$$

where W is the within chain variance calculated from the sample variance $s_m^2 = (1/N - 1)\sum_{n=1}^{N}(\theta_{nm} - \bar{\theta}_m)^2$ of chain m. θ_{nm} is the nth sample of the mth chain and $\bar{\theta}_m$ is the mean of the mth chain. B is the between chain variability and $\bar{\theta}$ is the overall sample mean. $\hat{R}$ is

the Gelman-Rubin convergence criterion that tends towards 1 as the simulation converges. Generally, a $\hat{R} < 1.1$ is required for convergence (Lambert, 2018).

2.3.5 Posterior Check

In this section we discuss methods to check the posterior distributions for η and β. We also demonstrate a visual check for the influence of the priors and likelihoods using prior-likelihood-posterior (PLP) plots. Informative priors (see example in Figure 4) are used for Bayesian updating. Likelihoods were calculated using sample data simulated from a Weibull distribution with known parameters ($\eta = 50$ and $\beta = 3$). Parameters were arbitrarily selected for illustration purposes. The use of selected posterior checks is demonstrated through a case study in Section 2.4.

Contribution of the priors and likelihoods to the posteriors can be examined visually using PLP plots. The analyst can use PLP plots to examine the degree to which the posterior is based on expert estimates versus actual data. Figure 5 shows the PLP plot with Bayesian updating performed using 10 samples generated from a Weibull distribution with $\eta = 50$ and $\beta = 3$. In the top chart (shape parameter), the limited sample size results in a wide likelihood function. As a result, the posterior is strongly influenced by the prior. In the bottom chart (scale parameter), the prior and likelihood have similar variance, resulting in a posterior that lies halfway between the two. The PLP plot in Figure 6 shows the influence of increasing sample size, whereby the posterior shifts much closer to the maximum likelihood value. In Figure 7, one can see that priors with higher variance as compared to Figure 5 and Figure 6 result in increased influence of the likelihoods, even if the likelihoods are wide.

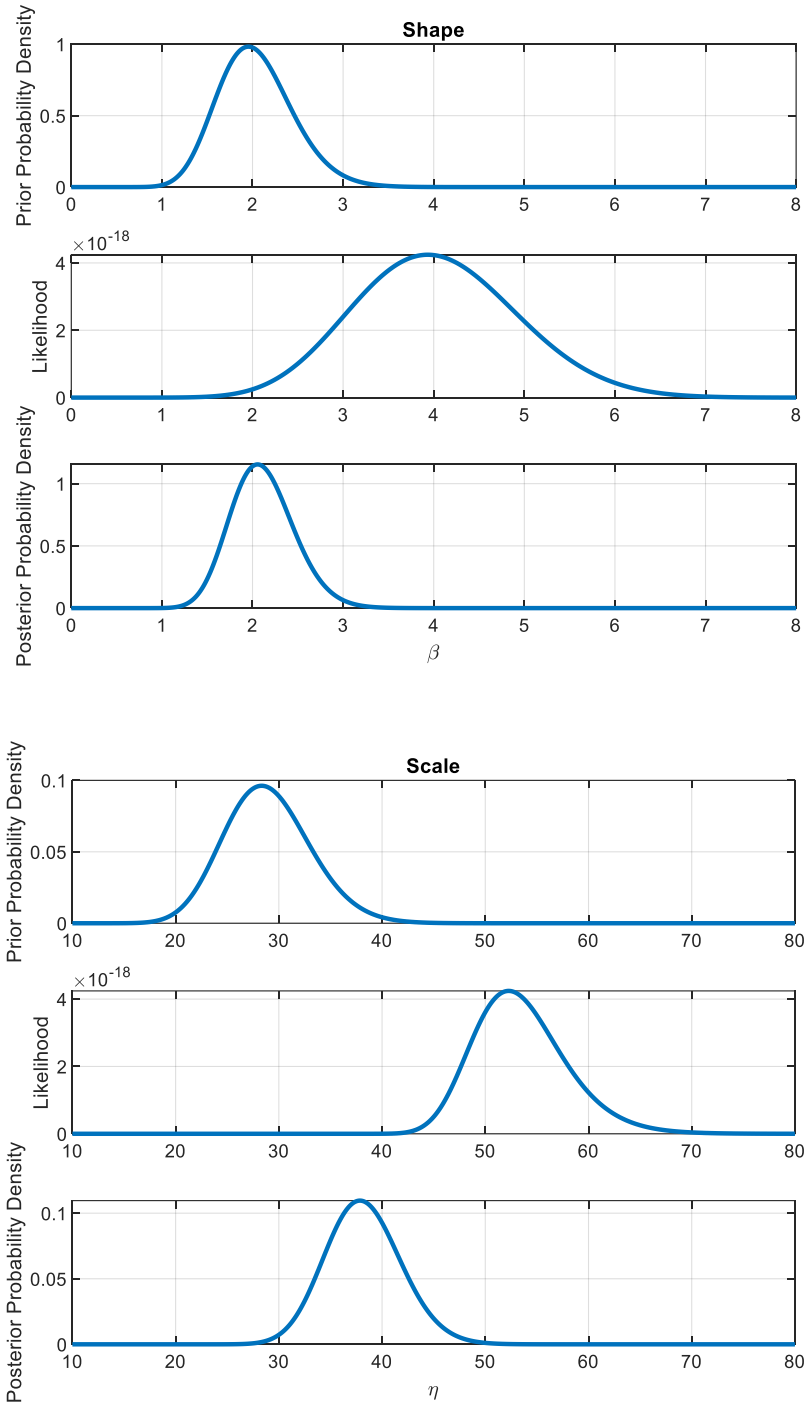

Figure 5. PLP Plot for Weibull Parameters – 10 samples

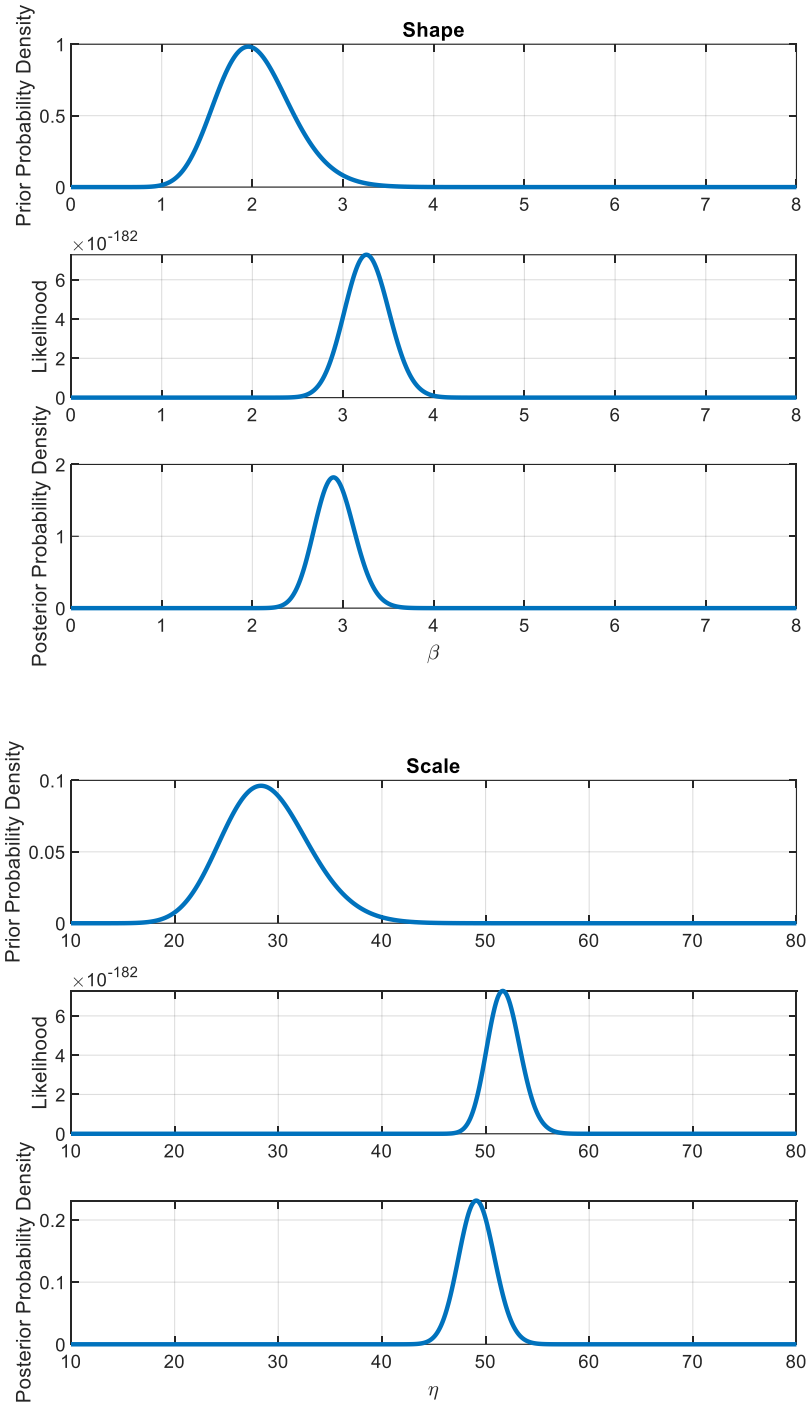

Figure 6. PLP Plot for Weibull Parameters – 100 samples

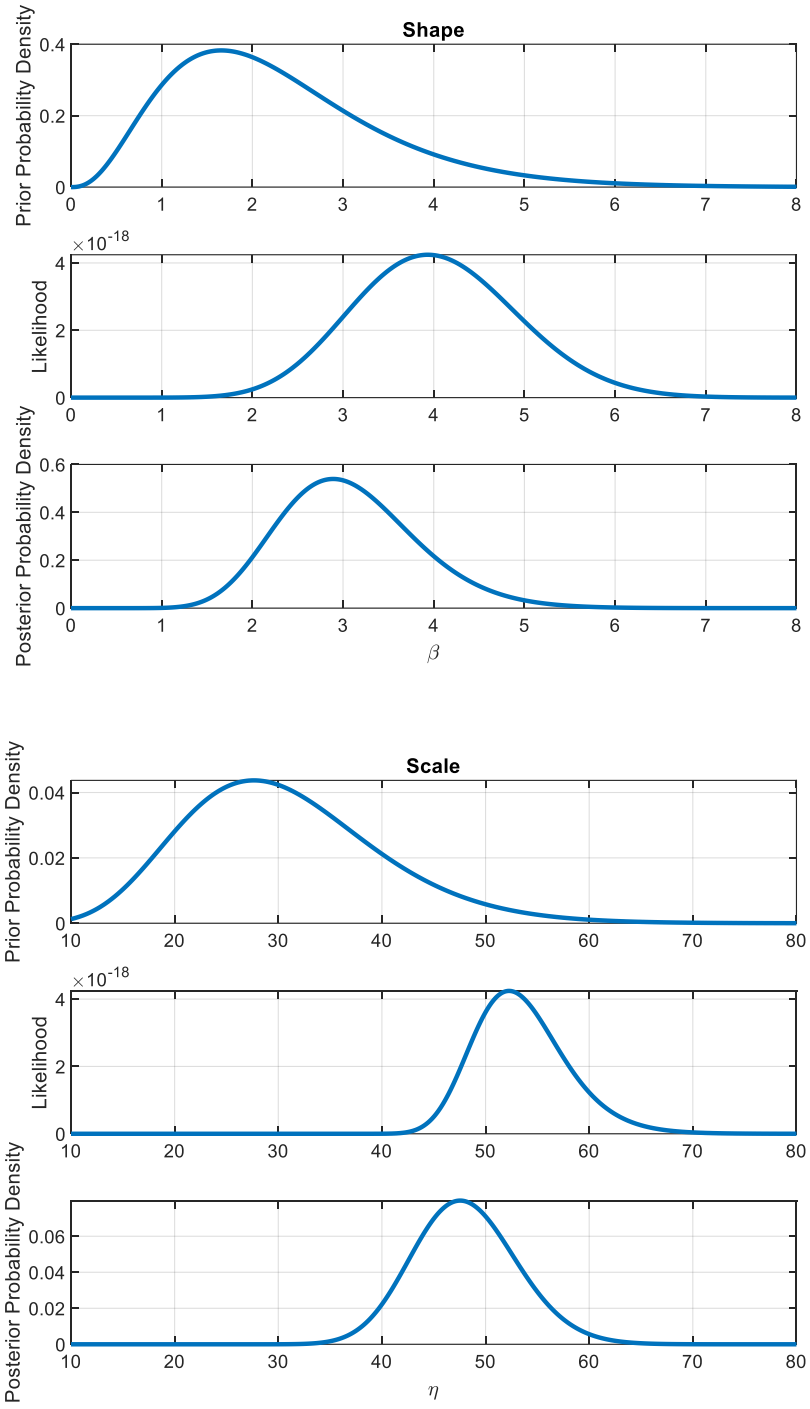

Figure 7. PLP Plot for Weibull Parameters – 10 samples and priors with high variance

In addition to PLP plots, the analyst may wish to examine parameter uncertainty using credible intervals, whereby an $X\%$ credible interval represents the probability that the parameter value lies within the parameter range. We summarize the posterior distribution uncertainty using the central posterior density (CPD) intervals defined as $X\% = (1 - \alpha) \times 100\%$. It is a range of parameter values for which the posterior distribution probability above and below the endpoints is given by $(\alpha/2) \times 100\%$ (Hamada, Wilson, Reese, & Martz, 2008). For example, for a 95% CPD interval, $\alpha = 0.05$.

The posterior predictive distribution is checked by comparing the median CDF and prediction intervals with the empirical distribution function (EDF) as shown in Figure 8. The EDF is the product limit estimator proposed by Lynden-Bell (1971). The median CDF is calculated using the median values of the Weibull parameters (η and β). Two commonly used test statistics for goodness-of-fit based on the EDF include the Kolmogorov-Smirnov (KS) test, and the Anderson-Darling (AD) test. The AD test is particularly useful for testing EDF departure from the CDF in the tails of the distribution. Both tests are extensively used in reliability analysis (Tobias & Trindade, 2012).

A visual check of the fitted EDF can be done by comparing where it lies relative to the prediction interval (PI) as shown in Figure 8. Prediction intervals are calculated by sampling from the posterior distributions of the Weibull parameters and generating a CDF curve for each pair of samples. The $X\% = (1 - \alpha) \times 100\%$ prediction intervals are calculated by considering the set of CDF curves generated and determining the CDF values at the α and $1 - \alpha$ percentiles for each time to failure. For example, for a 95% PI, $\alpha = 0.05$.

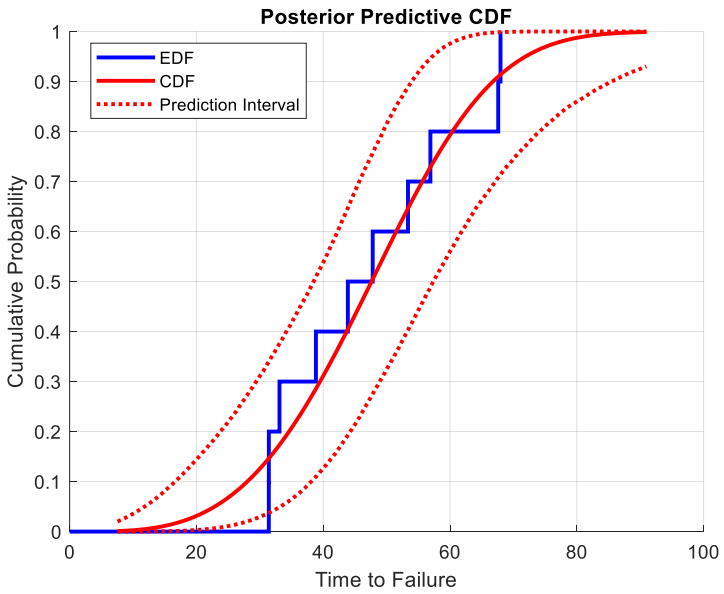

Figure 8. Example Posterior Predictive Check with 95% PI

2.4 Case Study

The utility of the proposed methodology is demonstrated using a case study based on actual experience with assets used in natural gas compression and transmission infrastructure. For confidentiality purposes, the actual data is not presented, rather a simulated data set is used as described in Section 2.4.1. We examine three cases in this study: inference with no prior information, inference with weakly informative prior information, and inference with prior information elicited from experts. The cases are described in detail in Section 2.4.2 and inference results are presented in Section 2.4.3.

2.4.1 Simulated Data

A data set that mimics the actual data is created by simulating the installation and failure of 100 similar assets. The assets were installed in the period between 1955 and 1990. As such, we simulate installation years using a discrete uniform distribution sampling between the installation year range. Random times to failure are generated from a Weibull distribution with parameters $\eta = 30$ and $\beta = 3$. We simulate limited recording of failure data by defining the observation period from 1987 to 2015. Assets installed prior to 1987 are considered truncated samples and assets failing after 2015 are considered suspensions (censored samples). Truncation results in 80 out of the 100 installed assets being considered in the sample for inference (20 having failed at a time before data was recorded). Histograms of the simulated failures and suspensions are plotted with the simulated population pdf in Figure 9. The complete simulated failure data set is provided in the supplementary materials (Chapter 7). A subset of 10 samples is also provided in the supplementary materials. The subset is used to demonstrate inference with limited samples.

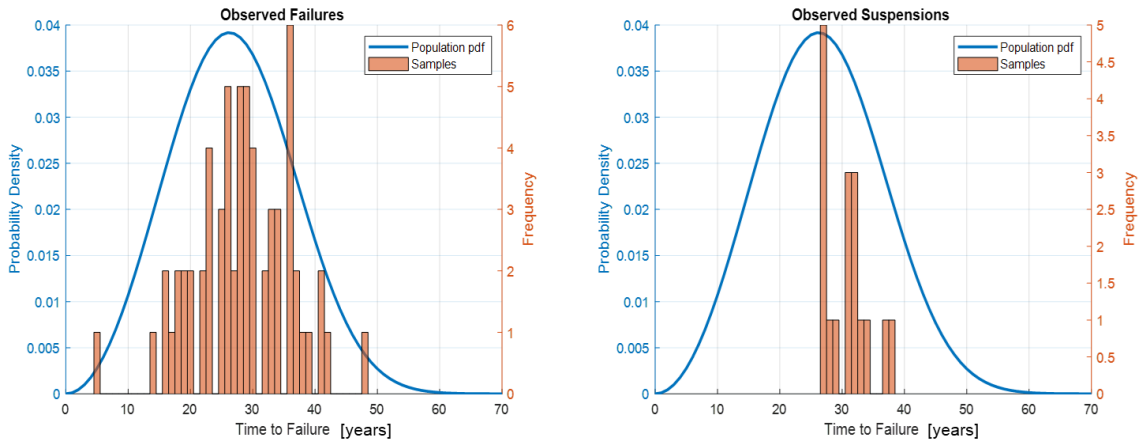

Figure 9. Simulated Data for Case Study with Weibull population pdf parameters $\eta = 30$ and $\beta = 3$

2.4.2 Prior Information Cases

In this section we demonstrate the utility of prior information using three case examples. Case 1 demonstrates Bayesian inference using non-informative priors, which is essentially the same as classical inference (e.g. MLE). Case 2 uses weakly informative priors derived from highly uncertain estimates of times to failure. We demonstrate that even weakly informative priors improve the parameter estimates as compared to Case 1. Finally, we demonstrate the power of expert elicited priors in Case 3.

2.4.2.1 Case 1: Non-Informative Priors

In the first case, Bayesian inference with non-informative priors means that the results will be entirely based on the observed data. This is the Bayesian analogue to classical inference. We define non-informative priors as Gamma distributions with mean of 1 and standard deviation of 100, as proposed by Kundu and Mitra (2016). The choice of hyperparameters creates a very flat distribution that is essentially non-informative.

2.4.2.2 Case 2: Weakly Informative Priors

In the second case, to demonstrate the power of priors, we construct informative prior distributions using weak prior information. Weak prior information is given by a $\bar{T}_{mode}$ that is uniformly distributed between 0 and 40, and $\bar{T}_{max}$ that is uniformly distributed between 50 and 100. The choice of uniform distributions and wide ranges (40 and 50 years) is meant to mimic minimal knowledge (high uncertainty) about the asset time to failure. Prior distributions for Weibull shape and scale are generated using the method described in Section 2.3.3 and shown in Figure 10. As will be discussed in Section 2.4.3, even weakly informative priors can greatly improve inference results as compared to inference with non-informative priors.

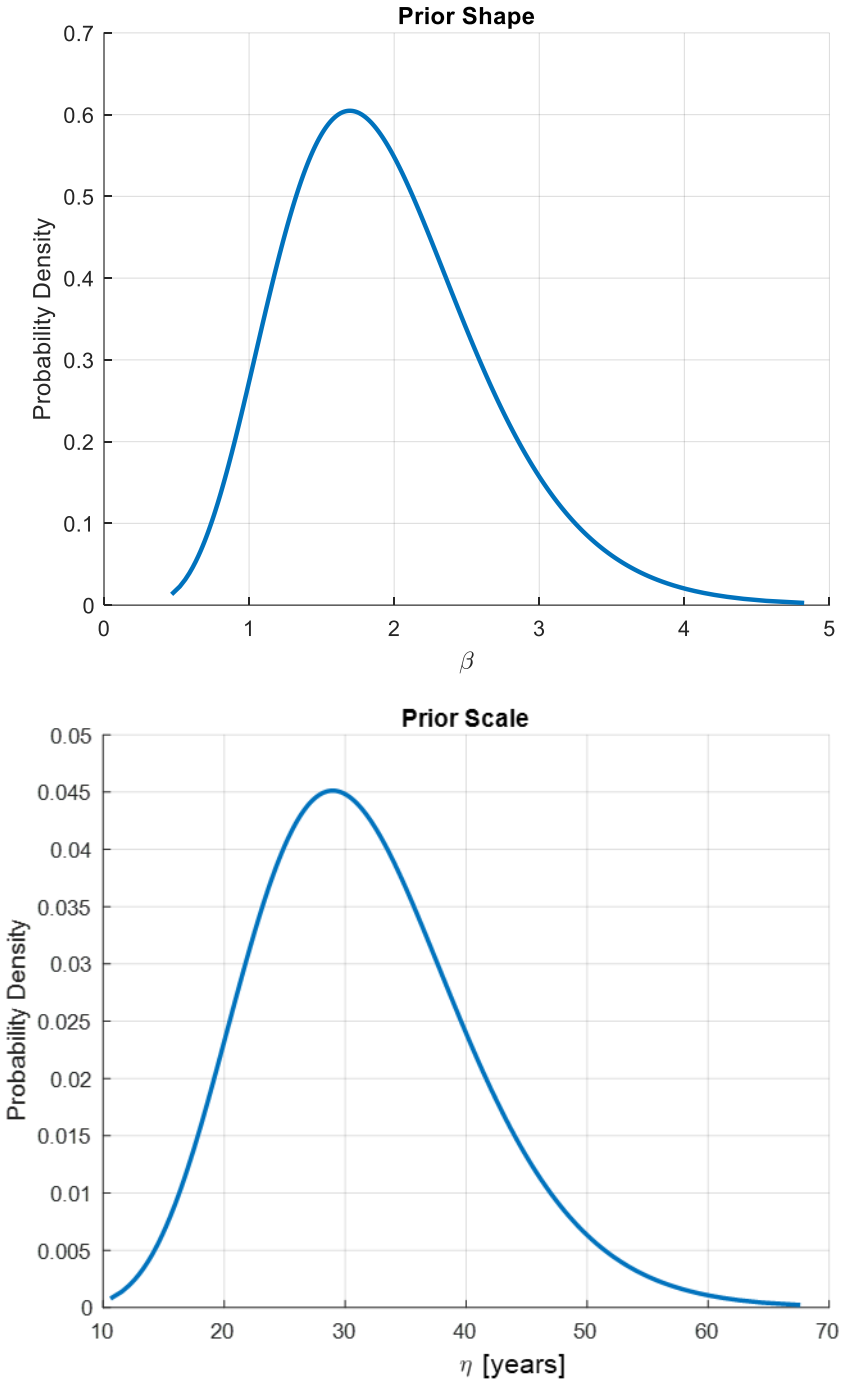

Figure 10. Prior Distributions Based on Weak Prior Information

2.4.2.3 Case 3: Expert Elicited Priors

Since weakly informative priors can greatly improve the inference results, we expect that priors obtained from experts will improve inference results further and is modelled appropriately in the third case. Experts are selected and their opinion about asset time to failure is elicited using the methodology described in Section 2.3.2. Informative priors are constructed based on time to failure estimates elicited from experts as described in Section 2.3.3.

Before eliciting expert estimates, we obtain an understanding of the failure mechanism and use that understanding to determine the importance of each expert selection criteria; years of experience, number of observed failures, and level of training with respect to maintenance/operation of the asset in question (see Section 2.3.2). We know that much of the data is missing because of truncation (i.e. failures occurred before data was recorded). We also know that the degradation cause isn't well understood and that, while in service, the condition of the assets cannot be monitored directly through inspections. The asset is only examined when a removal occurs. As such, we put highest importance on past observations that experts may have had. Given that similar assets are used throughout the natural gas infrastructure, we put strong importance on years of (relevant) experience as we expect that experts with more experience will be able to draw upon knowledge of similar assets that they have observed in operation. It is expected that formal training will not improve an expert's estimate of time to failure because the scientific foundation with respect to the degradation mechanism is limited. As such, it is given the least importance.

Performing pairwise comparison using the rationale described above and the scale presented in Table 1 we evaluate 'Observed Failures' as having an importance of 3 relative to 'Years of Experience', and an importance of 9 relative to 'Relevant Training'. Being consistent with the previous pairwise comparison, 'Years of Experience' is given a relative importance of 5 against 'Relevant Training'. The suggested importance rankings are used to fill in the AHP criteria comparison matrix shown in Table 2. Once criteria importance is assigned, we rank each expert (on a relative scale) against each AHP criteria. The rankings shown in column 2-4 of Table 3, combined with the importance ratings in Table 2, are used to calculate a weighting factor (Table 3, column 5). More experts were considered originally but did not score highly in the categories of "Observed Failures" and Years of Experience", and so had a low relative rank. As such they were excluded from consideration and final weights as shown in Table 3 were calculated for the top four experts. The final weights are applied to the time to failure estimates provided by each expert. Time to failure estimates shown in Table 4 are aggregated using a simple weighted average based on the weights in Table 3. The weighted average results for $\bar{T}_{mode}$ and $\bar{T}_{max}$ are shown in Table 5. Expert rankings and their estimates have been masked but are based on experience gained through actual interviews with experts with respect to natural gas infrastructure.

Table 2. AHP Criteria Comparison Matrix

Comparison Matrix	Years of Experience	Observed Failures	Relevant Training
Years of Experience	1	1/3	5
Observed Failures	3	1	9
Relevant Training	1/5	1/9	1

Table 3. Expert Ratings and Weights

Expert	Years of Experience	Observed Failures	Relevant Training	Weight
Expert 1	9	7	1	50.05%
Expert 2	9	5	1	24.63%
Expert 3	5	5	5	17.42%
Expert 4	1	1	9	7.90%

Table 4. Expert Estimates for Time to Failure

Expert	Time to Failure Estimates					
	Mode			Maximum		
	Lower Bound	Best Estimate	Upper Bound	Lower Bound	Best Estimate	Upper Bound
Expert 1	10	20	30	40	50	60
Expert 2	20	30	40	50	60	70
Expert 3	15	20	25	35	40	45
Expert 4	0	20	40	50	75	100

Table 5. Aggregated Time to Failure Estimates

Estimate	Lower Bound	Best Estimate	Upper Bound
$\bar{T}_{mode}$	12.5	22.5	32.4
$\bar{T}_{max}$	42.4	52.7	63.0

Modified Beta-PERT distributions constructed based on the data in Table 5 are shown in Figure 11. The distribution for $\bar{T}_{mode}$ is given a $\gamma = 4$. The distribution for $\bar{T}_{max}$ is given a $\gamma = 0$. The choice, a subjective interpretation by the analyst, was based on the experts' feedback that maximum life is difficult to estimate and so their estimates are highly uncertain. Prior distributions generated from the expert input are shown in Figure 12.

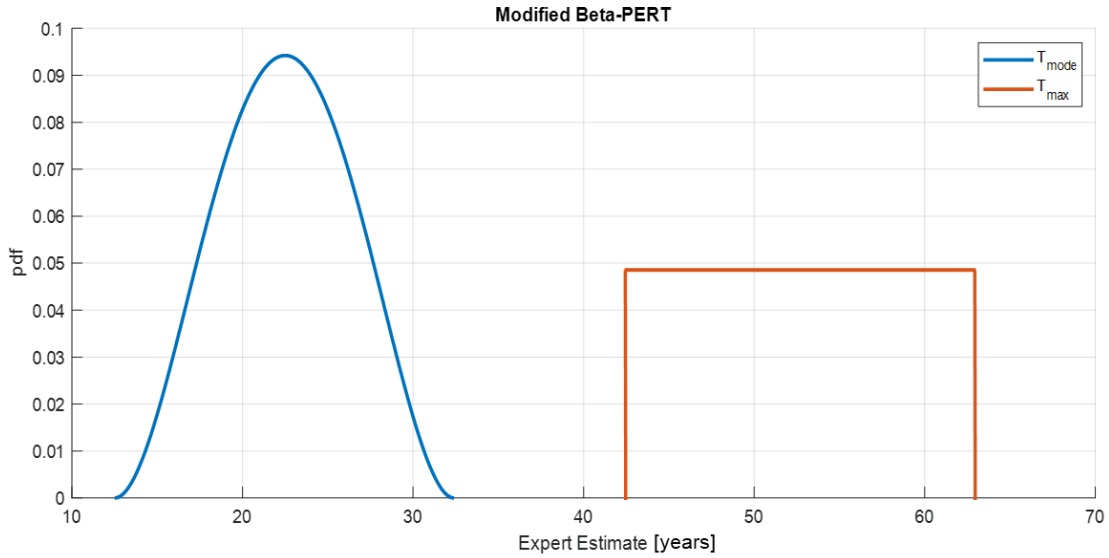

Figure 11. Estimated Modified Beta-PERT distributions for $\overline{T}_{mode}$ and $\overline{T}_{max}$

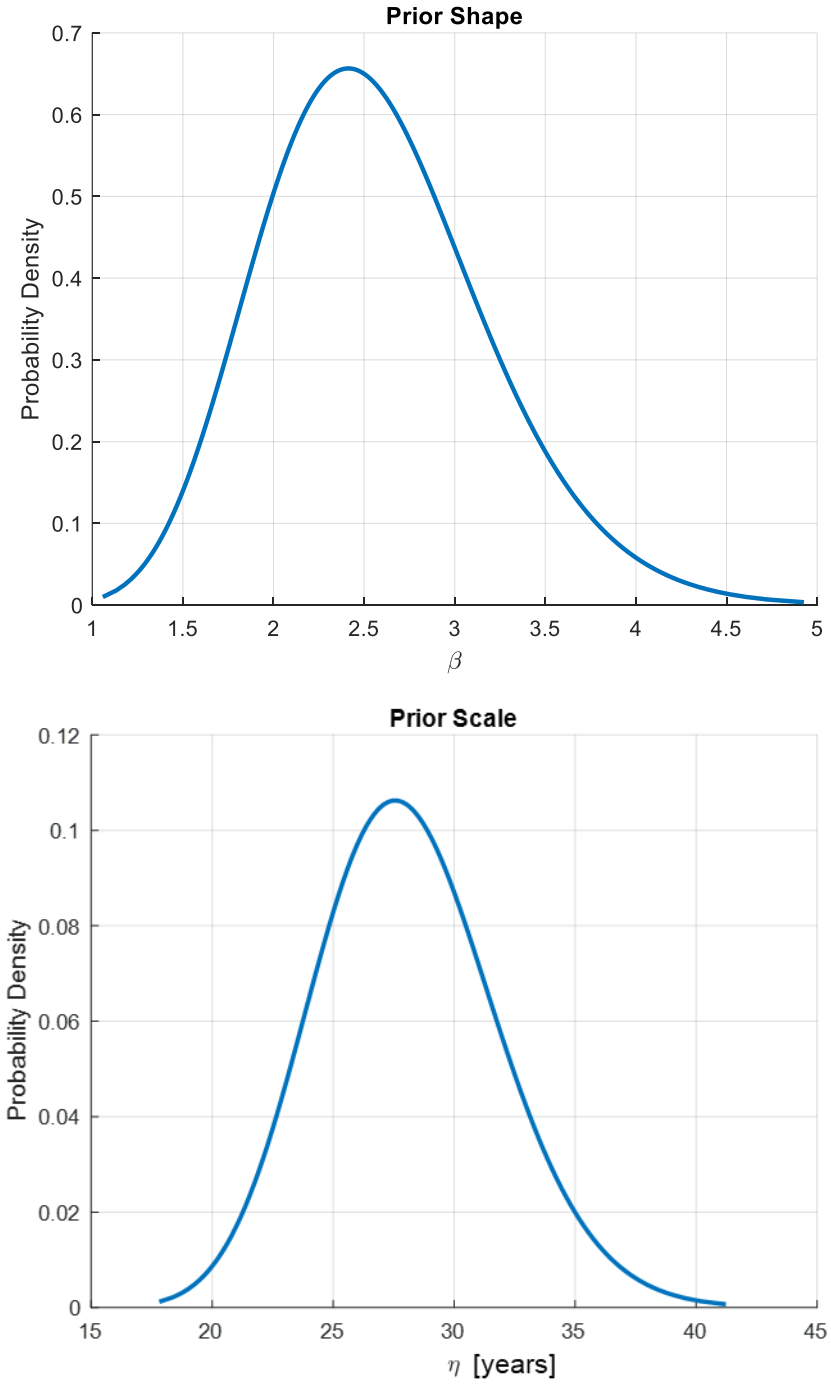

Figure 12. Prior Distributions Based on Expert Estimates

2.4.3 Results and Discussion

Bayesian inference is performed for each case using MH MCMC as described in Section 2.3.4. We perform inference using a 10-sample data set provided in the supplementary materials (Chapter 7). The resultant Weibull parameter estimates are summarized in Table 6 for each case of prior information.

Table 6. Bayesian Inference Results – 10 Samples

Case	Non-Informative Priors	Weakly Informative Priors	Expert Elicited Priors
Shape			
Prior Median	0	1.864	2.495
Posterior Median with 95% CPD Interval	9.676 [3.236,21.67]	2.648 [1.378,4.532]	2.846 [1.817,4.474]
Scale [years]			
Prior Median	0	30.81	27.91
Posterior Median with 95% CPD Interval	36.41 [31.11,42.28]	38.73 [28.56,51.08]	32.5 [27.55,39.06]

As a point of reference, consider that the resultant parameters using MLE and the limited (10-sample) data set are $\beta = 12.79$ and $\eta = 35.11$. We see that there is little difference between the MLE results and MH MCMC with non-informative priors (Table 6). This is consistent with the findings of McNeish (2016), and underscores the importance of informative priors. With weakly informative priors, the MH MCMC estimate of the Weibull shape parameter is improved as evidenced by the more accurate median estimate and increased precision. However, the estimate of the Weibull scale parameter becomes more uncertain (increased 95% CPD interval), reflecting the uncertainty in the prior information. With expert elicited priors MH MCMC produces superior results for both Weibull parameters. Not only are the estimated parameters more accurate, the precision is increased significantly as compared to the other two cases as shown by the 95% CPD intervals.

Visually comparing (Figure 13) the predictive distributions resulting from each method of inference, one can see the potential for ill-informed decision-making when faced with limited samples and no prior information. However, even with weak prior information, the difference between the true population life distribution and the inferred distribution can be greatly reduced. Calculating the Kullback-Leibler (KL) divergence between the inferred distribution and the population distribution serves as a means of examining the information lost by the inferred predictive distributions as compared to the population life distribution

(Bauckhage, 2013). A KL divergence of 0 is the ideal case (i.e. no information loss). KL values for all the cases are summarized in Table 7, showing significant improvement using expert elicited priors as compared to other means.

Table 7. KL Divergence for Inference Cases

Case	KL Divergence
MLE	6.25
MH MCMC with Non-Informative Priors	2.22
MH MCMC with Weakly Informative Priors	0.22
MH MCMC with Expert Elicited Priors	0.031

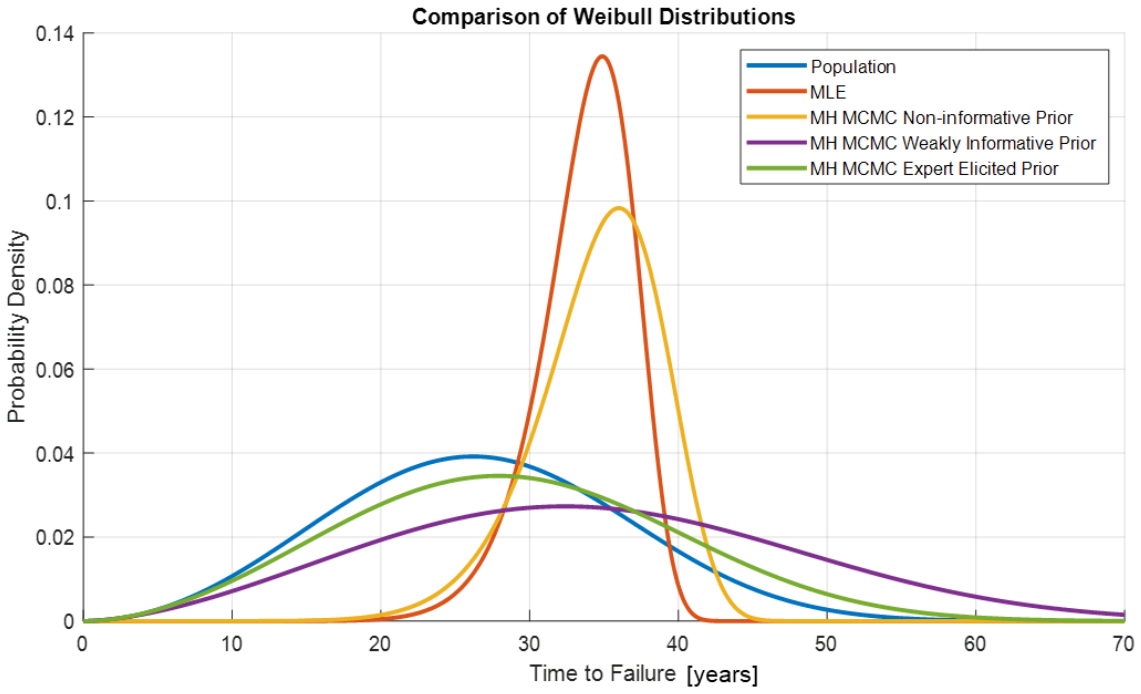

Figure 13. Posterior Predictive Comparison

Table 8 shows the results of Bayesian inference for each prior information case and with 80 samples. As expected, the results improve (more accurate and precise) with increasing sample size. Moreover, the difference between MH MCMC results and MLE results ($\beta = 3.773$ and $\eta = 31.84$) is almost impercetible.

Table 8. Bayesian Inference Results – 80 Samples

Case	Non-Informative Priors	Weakly Informative Priors	Expert Elicited Priors
Shape			
Prior Median	0	1.864	2.495
Posterior Median with 95% CPD Interval	3.677 [2.906,4.574]	3.390 [2.694,4.197]	3.385 [2.716,4.156]
Scale [years]			
Prior Median	0	30.81	27.91
Posterior Median with 95% CPD Interval	31.78 [29.53,34.15]	31.55 [29.16,34.08]	31.29 [29.04,33.65]

The influence of data versus prior information can be visually examined using the PLP plots in Figure 14 and Figure 15. As sample sizes increase, the likelihood becomes more precise, causing the posterior distribution to be more influenced by the data. Examining chart for the shape parameter in Figure 14 we see that with a small sample size the shape parameter value is predominantly based on prior information, underscoring the importance of good prior information.

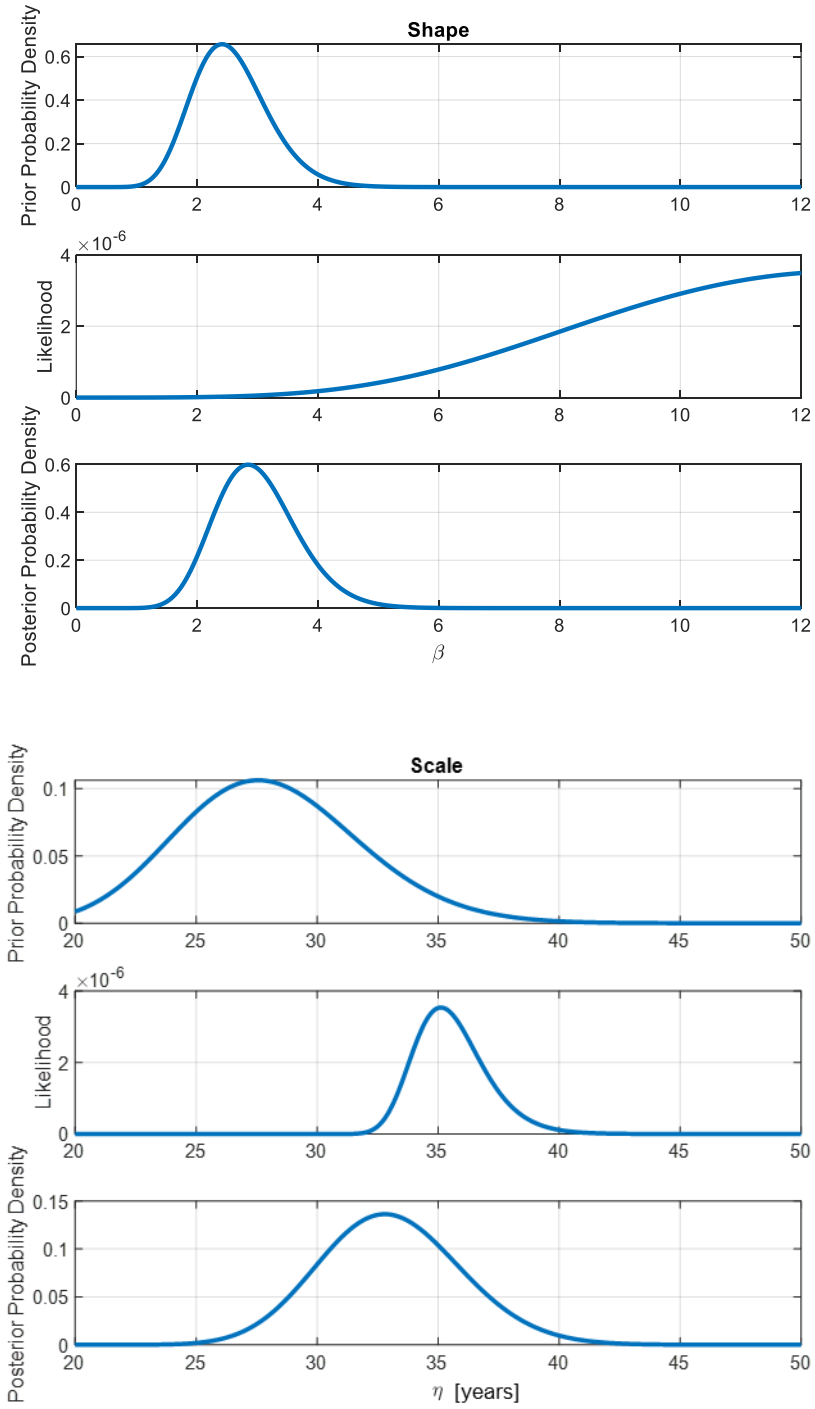

Figure 14. PLP Plot for Inference with 10 Samples and Expert Elicited Priors

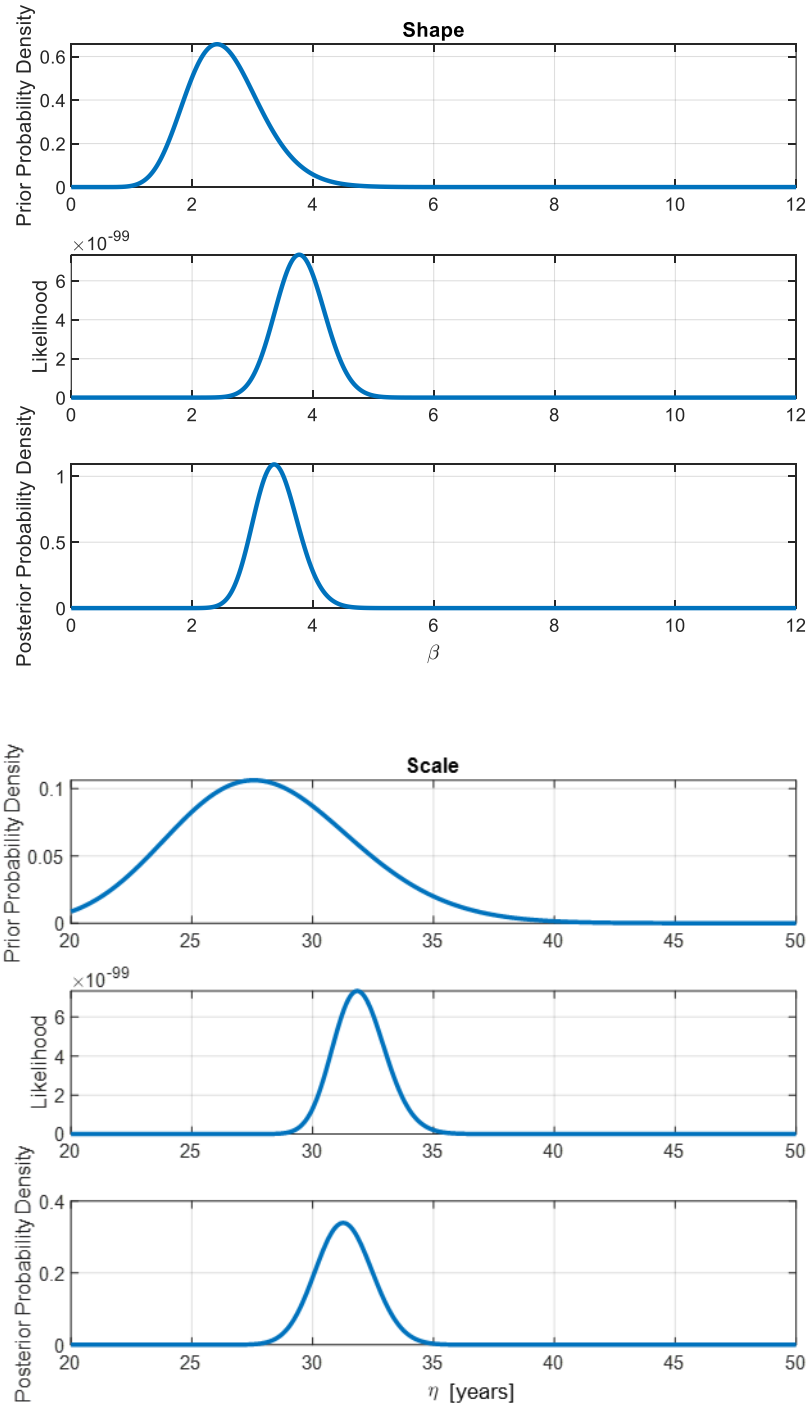

Figure 15. PLP Plot for Inference with 80 Samples and Expert Elicited Priors

We have demonstrated (see Table 6) that with limited data both MLE and MH MCMC (using non-informative priors) produce inadequate results. On the other hand, with a large sample size, the results are virtually identical (see Table 8). The power of prior information is demonstrated using both weakly informative priors and expert elicited priors. Even weakly informative priors improve (i.e. increase accuracy and precision of posteriors) inference

results over MLE and MH MCMC with non-informative priors. Further improvement is achieved by using expert elicited priors. By eliciting expert opinion about asset time to failure we can consider knowledge and experience of asset failures (not captured in failure data) through the prior distributions, and augment that knowledge with failure data.

2.5 Conclusions

This paper presents a methodology to address limited and incomplete data when attempting to perform statistical inference on the time to failure of physical assets. Under the Bayesian paradigm, expert knowledge about asset life is encoded in prior distributions for Weibull parameters. As is shown in this work, incorporation of such knowledge may be of crucial importance for proper decision-making under uncertainty. AHP is used as a framework for rigorously selecting experts and aggregating their knowledge to construct informative priors. MH MCMC is used to perform Bayesian updating of the prior distributions using actual failure data. We utilize a flexible likelihood function to account for missing or incomplete data (truncation and censoring). Such data issues can occur due to poor data collection practices. As is demonstrated, the result is more accurate estimation of model parameters as well as better precision (reduced uncertainty) of the parameters. The usefulness of the methodology for improved decision-making is illustrated using a case study.

Ultimately the results of reliability analysis of assets must be used for decisions regarding design, maintenance and replacement. There are significant costs involved in all such decisions and the decision-maker must be confident in the course of action. As has been illustrated, when dealing with limited, incomplete and missing data, classical methods such as MLE produce inadequate results with a high level of uncertainty. This uncertainty, coupled with the significant capital or operating expenditures at stake, essentially prohibits the decision-maker from properly deciding on a course of action. The methodology presented provides an elegant and powerful way of addressing uncertainty by allowing the analyst to take into consideration all types of available information.

While in this paper we have focused on incorporating expert opinion for the construction of priors, the methodology is flexible and can be easily extended to other sources of information. Such information can include accelerated life tests, analogous data from similar assets, physics of failure computer simulations, etc. AHP may be used as a means of weighting and aggregating the information from such sources. Future work will explore the suggested approach for extending the methodology.

3 Risk Analysis of an Underground Gas Storage Facility using a Physics-based System Performance Model and Monte Carlo Simulation

ABSTRACT

Engineered systems consist of many interconnected assets that work together to perform a system level function. As such, to obtain a complete view of operational reliability risk associated with potential asset failures, a system level analysis is necessary. This paper presents a quantitative risk analysis model to study operational reliability risk of an underground gas storage (UGS) facility. The model combines a thermo-hydraulic performance model for a gas storage facility consisting of a gathering system, compression system and transmission system with a Monte Carlo simulation of potential disruption events. The disruption events can impact the availability of one or more critical assets within the gas storage facility, which in turn affect the gas flow capability. The flow capability is compared against externally derived gas flow demand patterns to determine if shortfalls in supply can occur. The proposed model is highly configurable and can be used to quantitatively assess operational reliability risk in a UGS facility. The integrated physics model implicitly accounts for changes in system performance resulting from disruption events. As such, many combinations of system configurations, system states and disruption events can be analyzed within a single modelling framework.

3.1 Introduction

The demand for natural gas has been growing every year since 2009 at a compound rate of 2.6%. In 2017, production hit a record high of 3,768 billion cubic metres (IEA, 2018). Inevitably this will put a greater strain on the natural gas supply chain, meaning the consequence of failure of critical elements of the supply chain will be higher than before. The physical natural gas supply chain consists of three sectors: upstream, midstream, and downstream (InQvis, Inc., 2011). The upstream sector is focused on drilling and exploration for natural gas. The sector starts at the wellheads, where natural gas is produced, and ends at the delivery point for processing facilities. The midstream sector is primarily focused on processing the gas received from the upstream sector. Raw gas is processed to remove heavier hydrocarbons and other impurities (e.g. sulfur, water). The processed gas is kept in storage facilities for the downstream sector. The downstream sector consists of three parts: transmission, for moving gas over long distances via pipelines; storage, for providing a buffer for market fluctuations; and distribution, for moving gas from transmission lines or storage facilities to the end consumer.

Storage facilities serve a crucial role in the natural gas supply chain; managing the imbalances that occur between supply and demand. Fluctuations can come on the production side as well as the demand side (Plaat, 2009). Underground gas storage (UGS) facilities consist of large underground reservoirs for temporarily holding gas. Reservoirs can be depleted oil and gas fields, aquifers, salt caverns and other underground spaces such as abandoned mines (Plaat, 2009). Compression equipment is used to inject or withdraw gas from the underground caverns as needed. The compression power requirements for injecting or withdrawing gas depend on the inventory levels in the storage caverns. When inventory levels are high, power needs for withdrawal is low and power needs for injection is high. The opposite occurs when inventory levels are low (InQvis, Inc., 2011).

As the world's demand for natural gas increases, the need to manage risk in the natural gas supply chain becomes imperative. In order to manage risk, gas infrastructure operators will require tools and methods to identify, analyse and evaluate risk in the natural gas supply chain. As described earlier, a UGS facility serves a critical role in managing the supply and demand imbalances. This paper aims to present a model for quantitatively analysing operational reliability risk for a UGS facility. A physics-based UGS facility performance model is combined with a Monte Carlo simulation of potential disruption events that can

cause all or parts of the system to be unavailable. The model allows for quantitative risk analysis of a UGS facility withdrawal and injection capability.

3.1.1 Existing Models

This section presents a review of risk assessment models for the natural gas supply chain in the current academic literature. There is a significant concern of safety risk resulting from loss of containment (LoC) of natural gas, and subsequent fires and explosions. As such, much of the risk literature for the natural gas supply chain consists of analysis of loss of containment events. Since the objective of this paper is to model operational reliability of a UGS facility, this review focuses on models that capture loss of production (LoP) risk in the natural gas supply chain. A summary table of the models reviewed is provided below (Table 9). Review of the existing literature shows a lack of quantitative risk models for UGS facilities. Emphasis for risk modelling appears to be on gas distribution and transmission pipelines and networks. Monte Carlo simulation appears to be favoured by researchers, presumably due to the complex interaction of components of a natural gas supply chain.

Table 9. Summary of Current Natural Gas Supply Chain Risk Models

#	Source	Risk Category		Supply Chain Segment		
		LoC	LoP	Trans.	Storage	Dist.
1	von Lanzenauer, James and Wright (1992)		X		X	
2	von Lanzenauer, James and Wright (1995)		X	X***		
3	Yang, et al. (2013)	X	X		X*	
4	Praks, Kopustinskas and Masera (2015)		X	X		
5	Tran, et al. (2018)		X	X		
6	Aouam, Rardin and Abrache (2010)		X			X**
7	Fodstad, Midthun and Tomasgard (2015)		X	X		
8	Han and Weng (2010)	X	X			X

*Limited to underground storage caverns. Did not model entire system.

**Modeled supply risk based on aggregate demand in the network. Did not model the network.

***Transmission capacity modeled as constraint only.

Von Lanzenauer et al. (1992; 1995) developed a quantitative risk model for capacity planning of a natural gas storage facility and transmission system. The model focuses on demand side risk resulting from temperature variability modelled as a zero order Markov Chain. The storage system is modelled as two storage pools of varying deliverability and a compression system. The transmission system is modelled as a set of parallel pipelines. The performance of the system is modelled in a computer program called GASUS, which is a pipeline system gas hydraulics simulator. The model was used to calculate the probability of unmet demand.

Yang, et al. (2013) developed a fault tree analysis model for studying risk related to hydrocarbon storage caverns. The model focuses on salt rock caverns and considers three types of events: oil and gas leakage, ground subsidence, and cavern failure. The factors that can lead to each type of event are modelled in a fault tree structure. However, the basic events in the fault tree are not assigned probabilities. The fault tree model is used to study the relative importance of each of the basic events based on the minimal cut sets. In terms of consequence, the model considers economic, environmental and loss of life impacts resulting from storage cavern failure. The relative importance of each of the impact categories is evaluated using the analytic hierarchy process for each of the event types.

Praks, Kopustinskas and Masera (2015) developed a Monte Carlo simulation model for a gas transmission network to study reliability of supply problems using graph theory. The nodes in the graph represent sources (e.g. production wells), compressor stations, and sinks (e.g. distribution networks) for natural gas. The arcs represent pipelines connecting each of the nodes. The model solves the maximum flow problem in graph theory. The physics of gas pipeline hydraulics is not modelled. A failure model (probability of reduced or no capacity) for nodes and arcs is implemented and the overall reliability of supply in the network is calculated using Monte Carlo simulation. A similar approach was taken by Tran, et al. (2018) to develop a Monte Carlo simulation model to assess the risk of compressor failures on gas transmission network capacity.

Aouam, Rardin and Abrache (2010) developed a stochastic optimization model for natural gas procurement for a distribution network. The objective of the model is to minimize the cost of gas procurement while also minimizing risk of unmet demand. Fodstad, Midthun and Tomasgard (2015) developed a simulation model to analyse the use of interruptible transportation services in a natural gas transmission system. The model attempts to maximize profit (i.e. utilization of capacity) while minimizing risk (i.e. unmet demand). The capacity

booking dynamics between the pipeline operator and customers is modelled using an agent-based modelling paradigm. Both models focus on external source of risk (demand fluctuations).

Han and Weng (2010) developed a quantitative risk assessment model for a gas distribution network that considers risk of loss of containment from pipes. The model does not consider the transmission and storage segments of the natural gas supply chain. Both loss of life consequence and the economic impact of a loss of gas pressure in the pipe resulting from the loss of containment is evaluated. It is assumed that the economic output of an industrial gas consumer is directly proportional to the pressure in the distribution pipe delivering the gas. As such, a reduction in pressure due to a loss of containment is correlated to an economic impact.

Review of the literature on risk modelling in the natural gas supply chain shows an emphasis on external threats such as fluctuations in demand. Reliability of the natural gas infrastructure is considered in some models, but the emphasis is on transmission and distribution networks. UGS facilities and their performance have not been analysed in the risk context. Furthermore, integration of physics-based system performance models with disruption event (system failures, external threats) models is seldom done, as concluded in a recent literature review of critical infrastructure resilience modelling (Wang, et al., 2019). Of the 30 models reviewed, one used a physics-based approach, and none studied UGS facility operations. The aim of this paper is to bridge these gaps in the current literature.

3.2 Methodology

3.2.1 Model Overview

This section provides an overview of the UGS facility operational reliability risk model. It consists of a physics model for UGS system performance, integrated with a Monte Carlo simulation of potential disruption events. The simulation model has been implemented in MATLAB r2018a, chosen because it has excellent algorithms for root finding (needed for solving physics equations) and sampling (needed for Monte Carlo simulation).

The objective of the simulation model is to quantify the magnitude and probability of potential shortfalls in supply from an underground gas storage facility that consists of several critical sub-systems (assets): storage reservoirs, meter stations (MS), reservoir pipelines, compressors and transmission pipelines. A schematic representation of a UGS facility is shown in Figure 16. For withdrawal, gas flows from the underground storage reservoirs, into

the compression system (if needed) and finally into the transmission system for transport to the custody transfer point. For injection, gas is supplied to the transmission system, flows through the compression system (if needed) and finally into the reservoirs for storage.

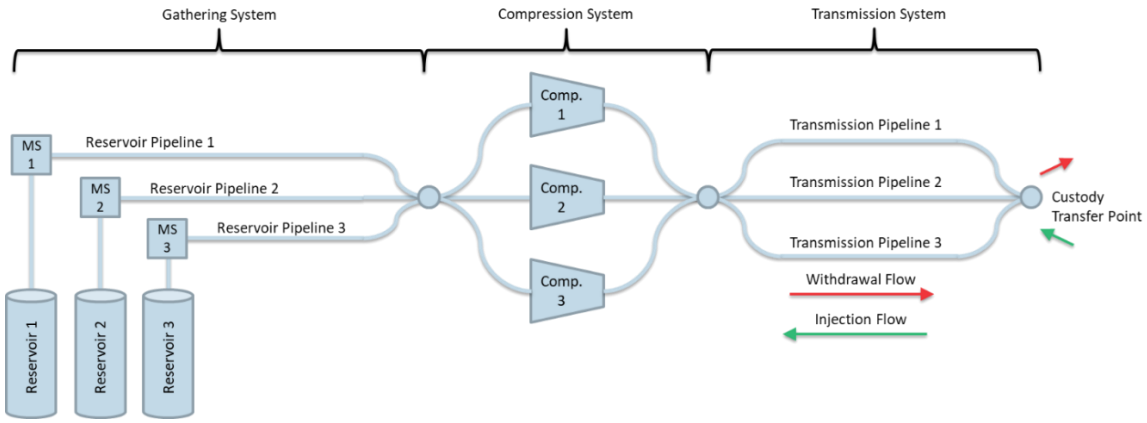

Figure 16. UGS Facility Schematic

The simulation models random occurrence of disruption events that can cause one or more of the critical assets in the UGS facility to be unavailable, and evaluates the impact on the system performance, measured as a mismatch in required gas flow and system flow capacity. This is achieved via two interacting sub-models: a thermo-hydraulic performance model (TPM) and a disruption event model (DEM).

The TPM takes an input of a daily gas injection/withdrawal flow requirement and calculates the flow capability of the UGS facility based on inventory levels and availability of critical assets. It must be configured with gas material properties, performance characteristics of critical assets and pre-determined priorities for asset utilization. The TPM is described in detail in Section 3.2.2. The DEM predicts the occurrence of disruption events and the availability of critical assets. It requires inputs for the probability of disruption events, the time to recover from each event and inputs for how each disruption event affects asset availability. The DEM reports on available assets based on what events have occurred, and remaining recovery time for each event. The DEM is described in detail in Section 3.2.3.

The two sub-models are combined in a Monte Carlo simulation as shown in Figure 17. The simulation program takes in a set of demand time series each of length D days. The demand time series is the daily net gas flow requirement (either injection or withdrawal) for the UGS facility. For each iteration of the simulation, a demand time series is randomly selected from the set (Step 1). The simulation then steps through each day (d) of the time series and sends the total daily flow requirement to the TPM (Step 2). The TPM simulates the gas flow for the

day in increments of Δt hours (Step 3), based on which the asset utilization is determined, and reservoir inventory levels are updated (Step 4). At each time step, the DEM predicts the occurrence of disruption events that can cause critical assets of the UGS facility to be unavailable (Step 5). Based on the results of Step 4, the DEM updates the availability of critical assets for the next time step (Step 6). Once the simulation has completed all time steps for a day, the mismatch (if any) between required flow and system flow capacity is calculated (Step 7). Only shortfalls are of concern (system flow less than required flow).

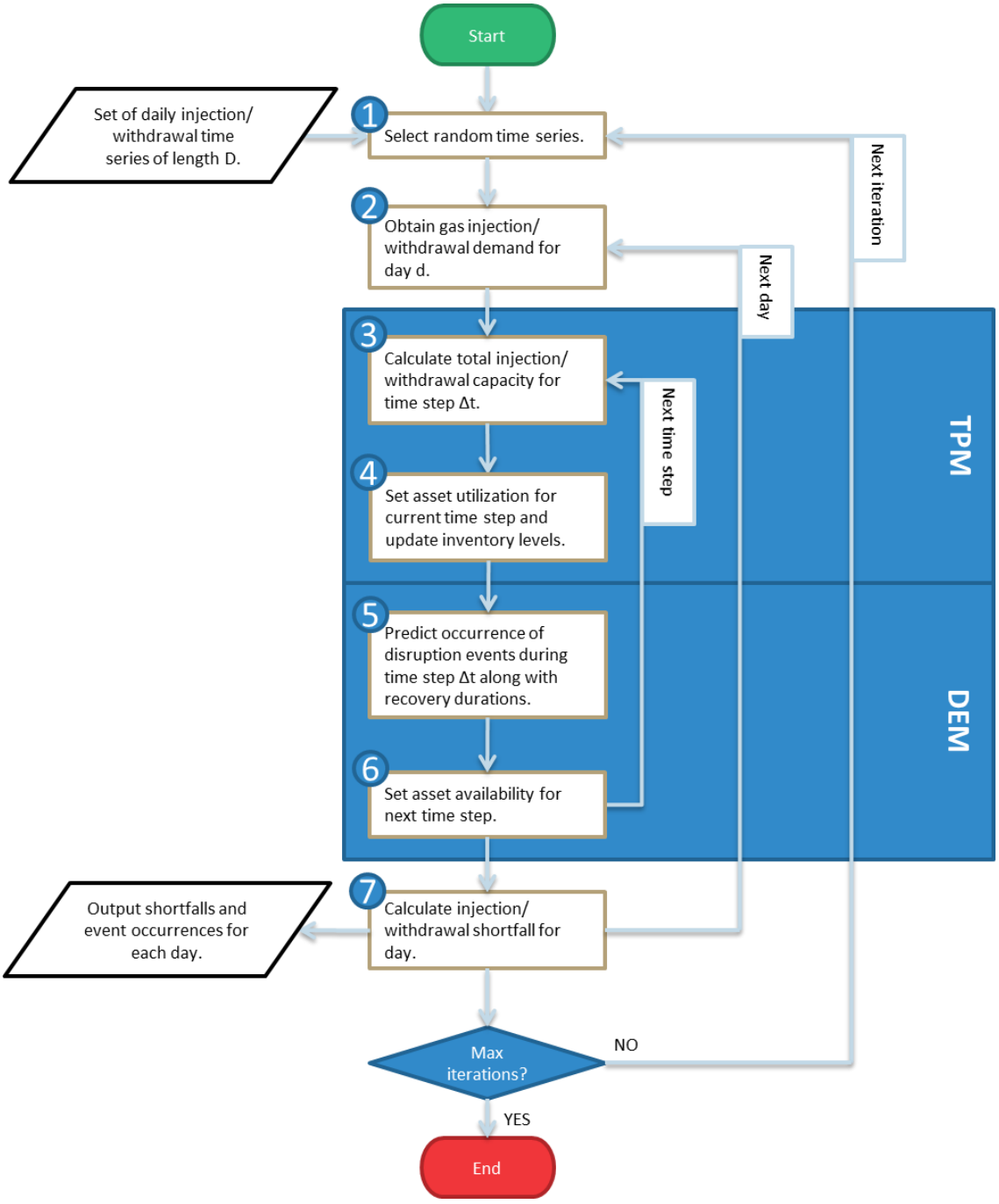

Figure 17. Monte Carlo Simulation Flow Chart

3.2.2 Thermo-hydraulic Performance Model

The TPM is designed to calculate the flow capacity of a storage system that consists of underground gas reservoirs and their pipelines (gathering system), a compressor station consisting of compressors in single stage or double stage configuration (compression system), and a transmission pipeline corridor consisting of parallel pipelines (transmission system). A schematic of the flow model is shown in Figure 16. It is possible for the gathering system to bypass the compression system and flow directly to the transmission system. This is known as free flow. The TPM makes use of a sign convention where withdrawal flow is positive and injection flow is negative.

The TPM requires an input for net gas withdrawal or injection demand (Q_d) for the day. It then outputs a gas flow capacity for each time step based on asset availability. The TPM is not a transient gas hydraulics model, rather an approach referred to as succession of steady states is used. It has been shown that gas systems reach steady state flow rates within hours (Modisette & Modisette, 2001). As such, a succession of steady states model is deemed sufficient for the operational risk analysis, where the aim is to determine daily gas supply shortfalls. The remainder of this section discusses the details of the solution methods used to solve for the gas flow capacity.

3.2.2.1 Equation of State

At the heart of any process simulation involving fluids is an equation of state. In this model the Peng-Robinson equation of state (PR-EOS) is used. It was developed at the University of Alberta specifically for application with light hydrocarbons. It provides the appropriate balance between accuracy and simplicity necessary for simulation (Peng & Robinson, 1976). The form of the PR-EOS used in the TPM is

$$P = \frac{RT}{v-b} - \frac{a(T)}{v(v+b)+b(v-b)}, \qquad (9)$$

where P is the fluid absolute pressure, R is the universal gas constant, T is the fluid temperature, v is the fluid molar volume, and $a(T)$ and b are derived from critical fluid properties as described by Peng and Robinson (1976). The compressibility factor (z) as calculated from the PR-EOS is

$$z^3 - (1-B)z^2 + (A - 3B^2 - 2B)z - (AB - B^2 - B^3) = 0\,, \qquad (10)$$

where the constants are given by $A = aP/R^2T^2$ and $B = bP/RT$. The largest of the real roots of the above equation give the compressibility factor for the vapour phase of the fluid.

3.2.2.2 Thermodynamic Properties

In order to calculate compressed flow, it is necessary to obtain thermodynamic properties such as specific heat (c_p and c_v), enthalpy (h) and entropy (s). The real gas thermodynamic properties are calculated by summing the ideal gas properties with an appropriate departure function derived from the PR-EOS. The ideal gas property functions and coefficients were adopted from a NASA Glenn report for the Chemical Equilibrium with Applications computer program (McBride, Zehe, & Gordon, 2002). In order to obtain the real gas thermodynamic properties departure functions derived from the PR-EOS must be used. The departure functions for specific heats at constant pressure and constant volume are $c_p^{dep} = c_v^{dep} + T\frac{\partial v}{\partial T}\frac{\partial P}{\partial T} - R$ and $c_v^{dep} = \frac{Ta''}{b\sqrt{8}} ln\left[\frac{z+B(1+\sqrt{2})}{z+B(1-\sqrt{2})}\right]$, respectively. The departure function for enthalpy is

$$h^{dep} = RT(z-1) + \frac{Ta' - a}{2\sqrt{2}b} ln\left[\frac{z + B(1+\sqrt{2})}{z + B(1-\sqrt{2})}\right], \quad (11)$$

and the departure function for entropy is

$$s^{dep} = Rln(z-B) + \frac{a'}{2\sqrt{2}b} ln\left[\frac{z + B(1+\sqrt{2})}{z + B(1-\sqrt{2})}\right] \quad (12)$$

where a, b, B, z, $\frac{\partial v}{\partial T}$ and $\frac{\partial P}{\partial T}$ are calculated from the PR-EOS (Equation 9 and 10). The derivation of the departure functions from the PR-EOS is provided by Sandler (1999).

3.2.2.3 Solution Method

This section describes the solution method used in the TPM to determine UGS system flow capacity. A flow chart of the TPM solution process is shown in Figure 18. The TPM takes an input for the demand flow (Q_d) and the required pressure (P_d) at the custody transfer point (Figure 16). It then calculates the flow (Q_{ts}) through the transmission system (Step 1) as described in Section 3.2.2.3.1. In Step 2, the TPM attempts to find free flow capacity (Q_{ff}) of the gathering system, bypassing the compression system (Section 3.2.2.3.3). In Step 3, considering only reservoirs that cannot be free flowed, the TPM finds compressed flow capacity of the system (Q_{cf}) as described in Section 3.2.2.3.2 and 3.2.2.3.3. In Step 4, the TPM balances the flow out of the storage reservoirs with the total demand flow. If $|Q_d| \leq |Q_{ff} + Q_{cf}|$ then the system can flow more gas than is required. The TPM therefore throttles flow into/out of each reservoir based on a predetermined priority as described in

Section 3.2.2.3.4. If $|Q_d| > |Q_{ff} + Q_{cf}|$ then the TPM reports a shortfall in gas flow (Step 5). The procedure described above correspond to Steps 3, 4 and 7 in Figure 17.

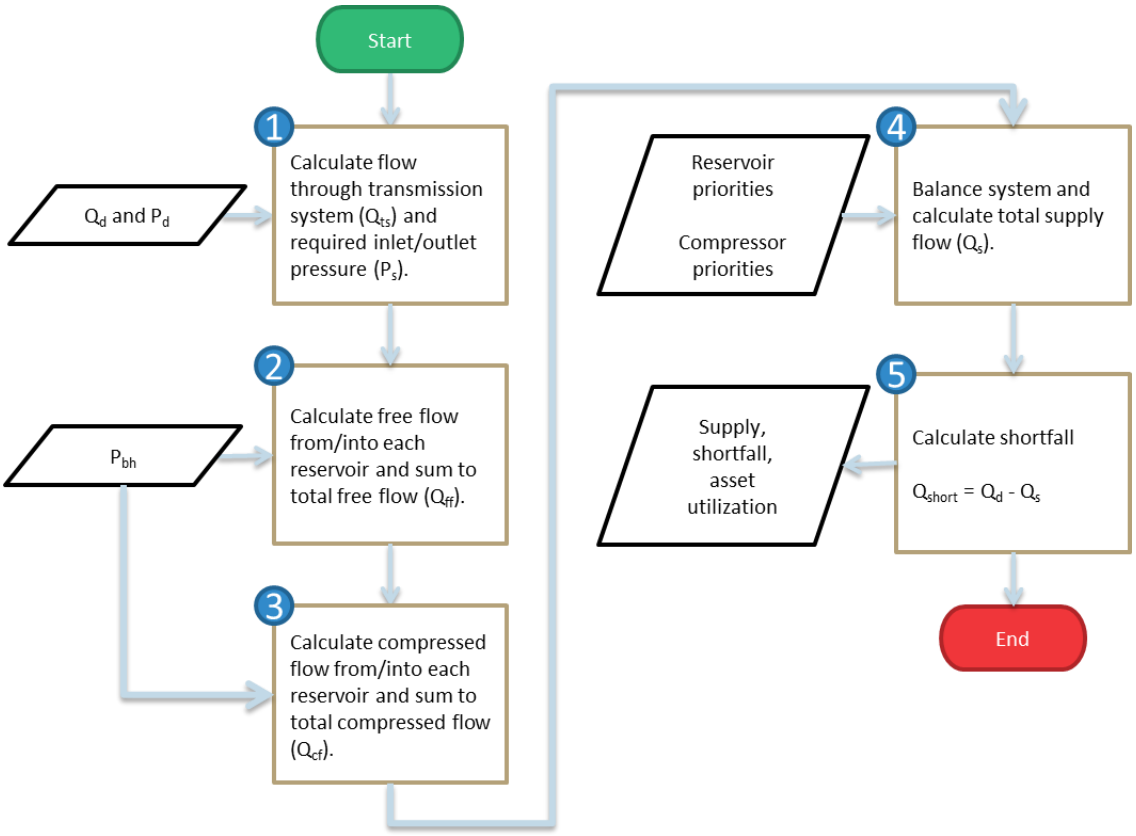

Figure 18. TPM Solution Flow Chart

3.2.2.3.1 Transmission System

Flow through a pipeline is calculated using the Weymouth equation (Menon, 2005). It is commonly used for high pressure, high flow rate, and large diameter gas gathering and transport systems. The equation assumes isothermal flow. In units of standard cubic metres per day (SCMD), the equation is

$$Q = 0.010667 \times \eta \times \left[\frac{P_1^2 - P_2^2}{SG \times T_f \times L \times z}\right]^{0.5} \times D^{2.667}, \qquad (13)$$

where η is the pipeline efficiency, P_1 is the pipeline inlet pressure [kPa], P_2 is the pipeline outlet pressure [kPa], SG is the specific gravity of the gas, T_f is the flowing temperature [K], L is the pipeline length [km], z is the gas compressibility factor as given by Equation 10, and D is the pipe diameter [mm].

The transmission system can be configured to have any number of parallel pipelines. A configuration with three parallel lines is shown in Figure 19. The user must specify four properties for each pipeline in the system: length, inner diameter, efficiency and maximum operating pressure. The transmission system pipelines are restricted to sharing common inlet (P_s) and outlet (P_d) pressures. When configuring the TPM, the user must specify a P_d, which is the required pressure at the delivery (withdrawal) or supply (injection) point. P_d is one boundary condition for the overall system, the other being reservoir pressures, discussed in Section 3.2.2.3.3. Lastly, the user must specify the flowing temperature.

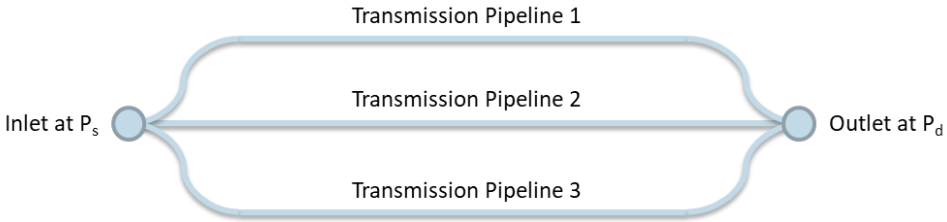

Figure 19. Transmission System Schematic

For a given demand flow (Q_d), the TPM attempts to find a P_s (within defined bounds) that meets the flow requirement. During withdrawal flow (positive Q_d) the lower bound for P_s is equal to P_d, and an upper bound equal to the lowest of the maximum operating pressure of the pipelines in the system. For injection flow (negative Q_d) the lower bound is atmospheric pressure and the upper bound is P_d. The total flow through the system (Q_s) is the sum of the flow through each pipeline. If the TPM can't find a solution that meets the flow requirement, it defaults to the maximum possible flow. This solution corresponds to Step 1 in Figure 18.

3.2.2.3.2 Compression System

Flow through a compressor is calculated from the thermodynamic relations of a compression process (Cengel & Boles, 2006). The ideal rate of work (power) based on an isentropic compression process, which is given by $\dot{W}^* = \dot{m}(h^*_{out} - h_{in})$, must be calculated. The compressor efficiency is used to determine the actual rate of work as $\dot{W} = \dot{W}^*/\eta$, where $\dot{m}$ is the compressor flow rate, h_{in} is the enthalpy of the gas at inlet conditions, h^*_{out} is the enthalpy of the gas at outlet conditions for isentropic compression, and η is the overall efficiency. The actual enthalpy at outlet conditions can be calculated as $h_{out} = \dot{W}/\dot{m} + h_{in}$. The TPM calculates compressor flow capacity for a given inlet condition (P_{in},T_{in}), a desired outlet pressure (P_{out}) and available power ($\dot{W}$) using the above relationships and the thermodynamic equations described in Section 3.2.2.2. The user must specify four properties for each compressor in the system: rated power, rated pressure, maximum pressure ratio and

overall efficiency, which is a product of the adiabatic, mechanical, and volumetric efficiencies. The total flow through a compressor unit is calculated by balancing the power of the unit with the rate of work needed to pressurize the gas from inlet to outlet pressure. The compressor is limited by the rated pressure and pressure ratio. If the required outlet pressure exceeds the rated pressure or the required pressure lift (P_{out}/P_{in}) is greater than the maximum pressure ratio, then the TPM defaults to zero flow.

The compression system can be configured in two different ways: single stage compression (Figure 20) or double stage compression with units grouped into two parallel banks that are in series (Figure 21). The compression units are restricted to sharing common inlet (P_{in}) and outlet (P_{out}) pressures as shown in Figure 20. In the double stage configuration, P_{mid} is the common outlet for the first stage and common inlet to the second stage of compression. The TPM attempts to solve for flow through the parallel configuration provided the required pressure lift is less than or equal to the lowest pressure ratio limit of the compression units in the system. Otherwise the TPM attempts to solve for flow through the double stage configuration (provided it has been defined). If no double stage configuration exists, then the TPM assumes the flow requirement can't be met. For the double stage configuration, the required pressure lift must be less than or equal to the product of the pressure ratio limits of each stage of compression. The TPM defaults to obtaining the maximum pressure lift through the stage with the highest amount of available power. The remainder of the pressure lift is achieved through the stage with less power.

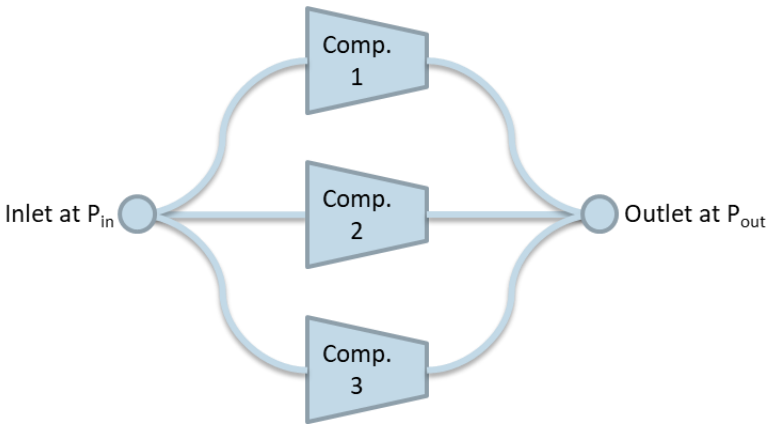

Figure 20. Compression System Schematic (Single Stage Compression)

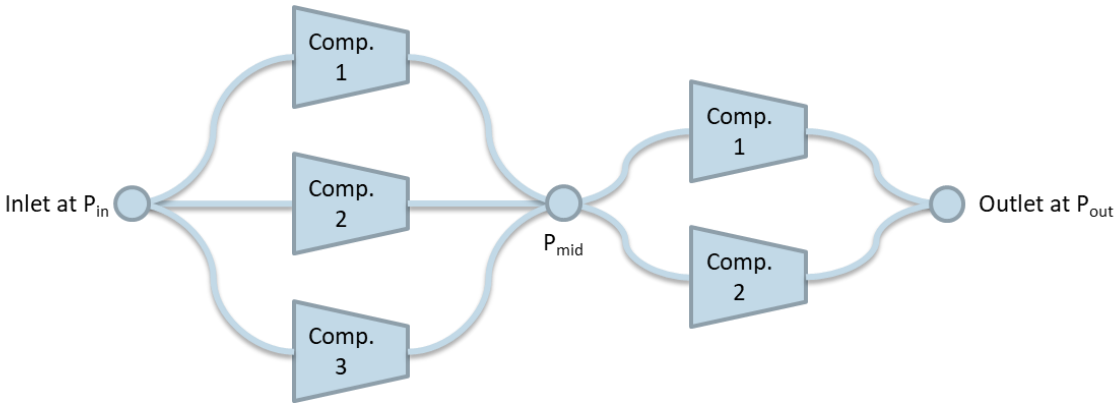

Figure 21. Compression System Schematic (Double Stage Compression)

For withdrawal flow (positive Q_s) the TPM solves for flow through the compression system if there are reservoirs that cannot supply gas at pressures higher than the required inlet (P_s) to the transmission system (reservoirs cannot free flow). P_{out} is set to P_s. The TPM then attempts to balance the flow through the compression system with the flow out of the gathering system by searching for a P_{in} between atmospheric and P_{out}. For injection flow (negative Q_s) the TPM solves for flow through the compression system if there are reservoirs that cannot receive gas at pressures at the supply pressure from the transmission system (P_s). In other words, free flowing gas into the reservoirs is not possible. P_{in} is set to P_s. The TPM then attempts to balance the flow through the compression system with the flow into the gathering system by searching for a P_{out} between P_s and the lowest maximum operating pressure of the reservoirs requiring compressed flow. The total flow through the compression system (Q_{cf}) is limited by the available power and the required outlet pressure (P_{out}). The solution described above corresponds to Step 3 in Figure 18.

3.2.2.3.3 Gathering System

The gathering system configuration can consist of any number of parallel groups of reservoirs and reservoir pipelines. The TPM calculates flow from a storage reservoir using the equation described below (Guo & Ghalambor, 2005)

$$Q = C\left[{P_2}^2 - {P_1}^2\right]^n, \tag{14}$$

where P_2 is the high-pressure point and P_1 is the low-pressure point. C and n are the empirically derived flow constant and flow exponent, respectively. When withdrawing from a reservoir, the low pressure point is the pressure at the inlet to the reservoir pipeline, measured at the reservoir meter station (P_{ms}), while the high pressure point is the reservoir pressure, often referred to as the bottom hole pressure (P_{bh}). During injection the high pressure and low-pressure points are reversed. Flow from a reservoir is calculated by

balancing the total flow through the wells of the reservoir (Equation 14) with the flow through the reservoir pipeline linked to the reservoir. Flow through the reservoir pipeline is calculated using Equation 13. The reservoir pipelines share a common outlet/inlet for withdrawal/injection flow that is the inlet/outlet of the compression system (compressed flow) or inlet/outlet of the transmission system (free flow). A schematic representation of the gathering system is shown in Figure 22. Refer to Figure 16 for the overall system schematic.

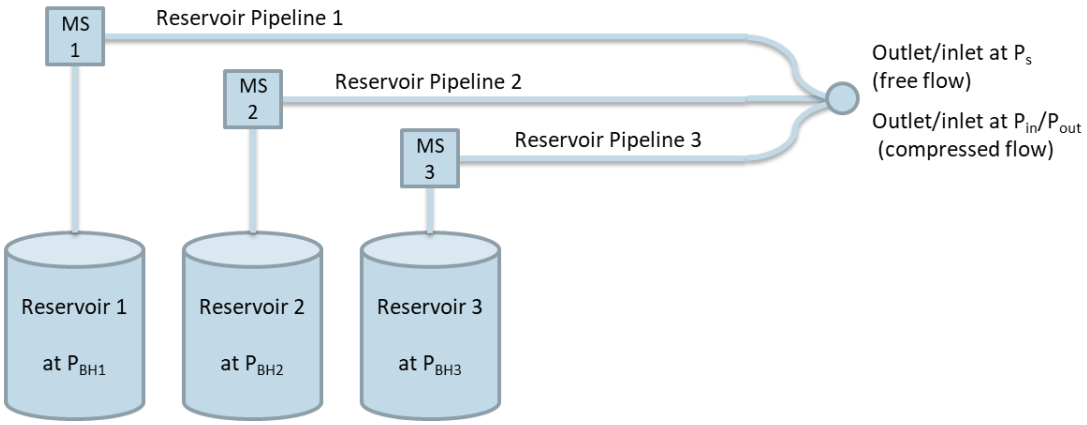

Figure 22. Gathering System Schematic

Reservoir flow is throttled by controlling the meter station pressure (P_{ms}). The P_{ms} pressure must always be between the pipeline outlet/inlet pressure and the bottom hole pressure. During withdrawal, P_{ms} is restricted by the draw down limit. Draw down is calculated as

$$r = \frac{P_{bh} - P_{ms}}{P_{bh}}. \tag{15}$$

The draw down limit is a user specified value between 0 and 1 and is meant to place a restriction on the flow velocity through the reservoir wells. The TPM restricts the meter station pressure based on the draw down limit. The reservoir pressure changes with the gas inventory level in the reservoir. The relationship between reservoir pressure and gas in place (inventory) is calculated based on a mass balance using the equation

$$\frac{P_{bh}}{z} = \frac{I}{K_{reservoir}}, \tag{16}$$

where P_{bh} is the reservoir pressure, z is the compressibility factor (Equation 10), I is the inventory (mass or standard volume of gas) and $K_{reservoir}$ is an empirically derived constant (Wang & Economides, 2009). Pressure and inventory measurements show that a linear relationship is appropriate as $P_{bh}/z \propto I$. As such, the gas in place at the reservoir's

maximum operating pressure must be known and specified by the user to calculate the constant, $K_{reservoir}$.

As shown in Figure 22, the gathering system can be configured to have multiple reservoirs and pipelines operating in parallel. To configure the gathering system the user must specify seven properties for each reservoir and four properties for each reservoir pipeline. For each reservoir in the system the necessary properties are cushion pressure, maximum operating pressure, gas in place at maximum pressure, the reservoir temperature, flow constant, flow exponent and draw down ratio (see Equation 15). The available inventory, also known as the working gas, is the difference in gas in place at maximum operating pressure and cushion pressure, calculated using Equation 16. For each reservoir pipeline in the system the necessary properties are length, inner diameter, efficiency and maximum operating pressure, like the pipelines in the transmission system.

The TPM first attempts to determine the amount of free flow that is possible (Step 2 in Figure 18). Free flow occurs when gas flows directly from the gathering system (for withdrawal flow) into the transmission system, bypassing the compression system. Free flow can be achieved when reservoir pressures (P_{bh}) are high, making it possible for the gathering system outlet pressure to equal P_s. For injection flow, free flow occurs when gas flows directly from the transmission system into the gathering system reservoirs, bypassing the compression system. Free flow on injection can be achieved when reservoir pressures (P_{bh}) are low, making it possible for the gathering system inlet pressure to equal P_s. The total amount of free flow gas (Q_{ff}) is the total free flow out of or into each available reservoir. Any reservoirs that cannot be free flowed are connected to the compression system.

3.2.2.3.4 Flow Balancing

The final step the TPM takes is balancing the total supply flow ($Q_s = Q_{ff} + Q_{cf}$) with the demand flow (Q_d). Flow balancing is done based on the user specified reservoir priority, which is the pre-determined order in which the reservoirs will be drawn down or filled. The prioritization is flexible; allowing reservoirs to be drawn down or filled in tandem (same priority) or sequentially (different priority). The TPM incrementally sums the flow out of/into each reservoir in order of priority until the demand flow is met. If the remaining unmet demand is less than the total supply flow from the reservoir priority group, the flow out of/into each reservoir is throttled based on the remaining unmet demand flow. In addition to the flow balancing, the TPM also sets the compressor utilization based on the final compressed flow required (after balancing flows for the reservoirs). The power required to

achieve the pressure lift for the adjusted compressor flow is calculated, and compressor units are utilized until the power requirement is met. Units are utilized based on a pre-determined user-specified priority and unit availability. The above procedure refers to Step 4 in Figure 18. Finally, any unmet demand is the shortfall (Q_{short}), referring to Step 5 in Figure 18.

3.2.3 Disruption Event Model

The DEM is a Monte Carlo simulation that models the random occurrence of events that can disrupt UGS facility operation. The impact of disruption events is modelled by UGS facility assets (pipelines, reservoirs, compressors) being unavailable for the duration of the disruption event. The TPM may only utilize available assets to calculate system performance at each time step of the simulation as described in Section 3.2.1 (Figure 17). The DEM's function is to evaluate the occurrence of (and recovery from) multiple disruption events during each simulation time step (Δt), and to update the availability of UGS facility assets for use by the TPM. Figure 23 is a schematic representation of what a hypothetical disruption event occurrence and recovery may look like from a system performance perspective. Multiple disruption events can occur at the same time and their cumulative effect on system performance can be calculated by the TPM.

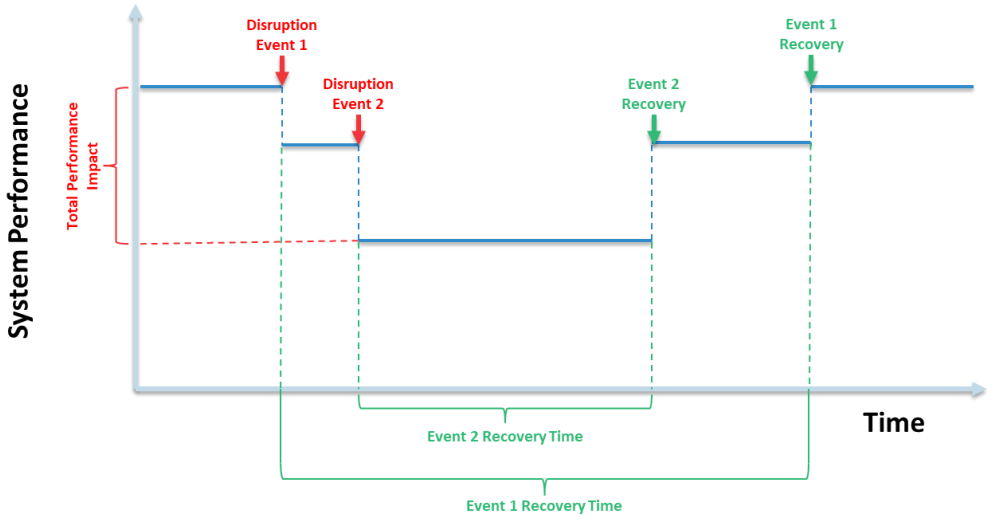

Figure 23. Timeline of Disruption Event Occurrence and Recovery

The DEM requires an input for the duration of the time step (Δt) being used by the TPM and a binary indicator for whether an asset is in use during the time step. For events that have not occurred, the DEM evaluates the potential occurrence of the event during the current time step. For events that have already occurred, the DEM evaluates whether recovery is completed during the current time step. Based on the evaluations, the DEM reports available

assets to the TPM for use in the next simulation time step. The remainder of this section discusses the details of the solution methods used to solve for occurrence probability, recovery time and impact of disruption events.

3.2.3.1 Event Occurrence

For each potential disruption event to be evaluated by the DEM the user must specify a probabilistic model for the occurrence of the event. The user must specify the following properties: time at risk, probability of occurrence model (discussed below), starting event clock and event clock units. All models in the DEM assume that the event occurrences are time dependent.

The time at risk parameter defines whether an event occurs according to calendar time or the time during which a specific asset is in use. For example, an event such as a corrosion leak on a pipeline is dependent on calendar time, whereas an event such as compressor bearing failure is dependent on usage time (sometimes referred to as the mission time). If an event time at risk parameter is set to usage time, the DEM solver will only consider the event occurrence during a time step in which the related asset is in use as determined by the TPM solver. If the user specifies an event time at risk as usage time, then an additional input specifying which asset's usage time to consider must also be defined.

The user can select from pre-programmed models for the probability of event occurrence. If the event occurrence times are independent and identically distributed (iid) then the user can specify distributions for the occurrence times as exponential or Weibull. The iid assumption holds when modelling failure of assets that are non-repairable (i.e. replaced with a brand new one upon failure) or repairable assets for which the repair action restores it to as good as new (Tobias & Trindade, 2012). If the events are not iid, then the user can specify occurrences as following a non-homogeneous Poisson process (NHPP) with either a power law or log linear intensity function. NHPPs are often used to model failure of repairable assets that undergo minimal repair. In other words, the asset is restored to the condition it was in just before the failure occurred (Louit, Pascual, & Jardine, 2009). Note, that while the above discussion provides examples for asset related failure events, external threats such as inclement weather, third party damage, terrorism/vandalism, etc. can also be modelled using the pre-programmed probability models. One such example would be modelling of rare events using a Poisson distribution, for which the time to event occurrence would follow an Exponential distribution (Falk, Husler, & Reiss, 2011).

The DEM simulates event occurrences for each time step (Δt) in the simulation (see Figure 17). The conditional probability of occurrence (Pr_{event}) for each event is calculated based on the current value of the event clock (T_{ec}) and the event occurrence window (ΔT_{ec}). If the time at risk for the event is based on calendar time, then $\Delta T_{ec} = \Delta t$ always. If it is based on usage time then $\Delta T_{ec} = \Delta t$ if the associated asset is in use according to the TPM solver, and zero otherwise. For iid event occurrence times, the conditional probability of event occurrence is given by

$$Pr_{event} = \frac{F(T_{ec} + \Delta T_{ec}) - F(T_{ec})}{1 - F(T_{ec})}, \tag{17}$$

where $F(t)$ is the appropriate cumulative distribution function. For event occurrences that follow a Poisson process, the conditional probability of event occurrence is given by

$$Pr_{event} = 1 - e^{-\int_{T_{ec}}^{T_{ec}+\Delta T_{ec}} \lambda(x)dx}, \tag{18}$$

where $\lambda(x)$ is the intensity function of the Poisson process. For each event, the DEM generates a uniform random number (U) between zero and one, and an event occurs if $U \leq Pr_{event}$.

3.2.3.2 Recovery Time

For each event, the user must define two distributions for the recovery time. The first is a distribution for the time between event occurrence and the start of any recovery action. This is referred to as the recovery lag time. The second is a distribution for the active recovery time, during which recovery work is being done. The DEM determines the total recovery time from a disruption event as the sum of the two randomly sampled recovery times ($T_{recovery} = T_{lag} + T_{active}$). The DEM then begins counting down the recovery clock with each TPM simulation time step, and any impact (Section 3.2.3.3) is assumed to be active until the recovery clock reaches zero. Each of the recovery times can be modelled using the following distributions: uniform, triangular, exponential, generalized Pareto and Weibull.

3.2.3.3 Solution Method

To configure the DEM, the user must provide a list of events (referred to henceforth as the event list), each defined by a model of the probability of occurrence (Section 3.2.3.1) and a model for the recovery time if the event occurs (Section 3.2.3.2). The DEM solution logic is shown in Figure 24. The logic is evaluated for each event in the event list to generate the $\overline{F}$ vector. $\overline{F}$ is an $m \times 1$ column vector representing event occurrence, where the i^{th} element in

$\overline{F}$ is equal to one if the i^{th} event in the event list is active and zero otherwise. An active event is one that has occurred and recovery from the event is not complete. The user must also define a matrix ($\overline{B}$) that defines which assets should be made unavailable if an event occurs. $\overline{B}$ is an $m \times n$ matrix where m is the number of events in the event list and n is the number of critical assets in the TPM (reservoirs, compressors, and pipelines). The user must configure the impact matrix by entering a value of one for $\overline{B}_{ij}$ if the i^{th} event occurring results in the j^{th} asset being unavailable. A value of zero is entered if there is no relation between event i occurrence and asset j availability. The availability of a critical asset is calculated as

$$\overline{A} = \sim \left(\overline{B}^{T} \times \bar{F}\right), \tag{19}$$

where $\overline{A}$ is an $n \times 1$ column vector representing asset availability. The j^{th} element of $\overline{A}$ is equal to one if the asset is available and zero if it is not.

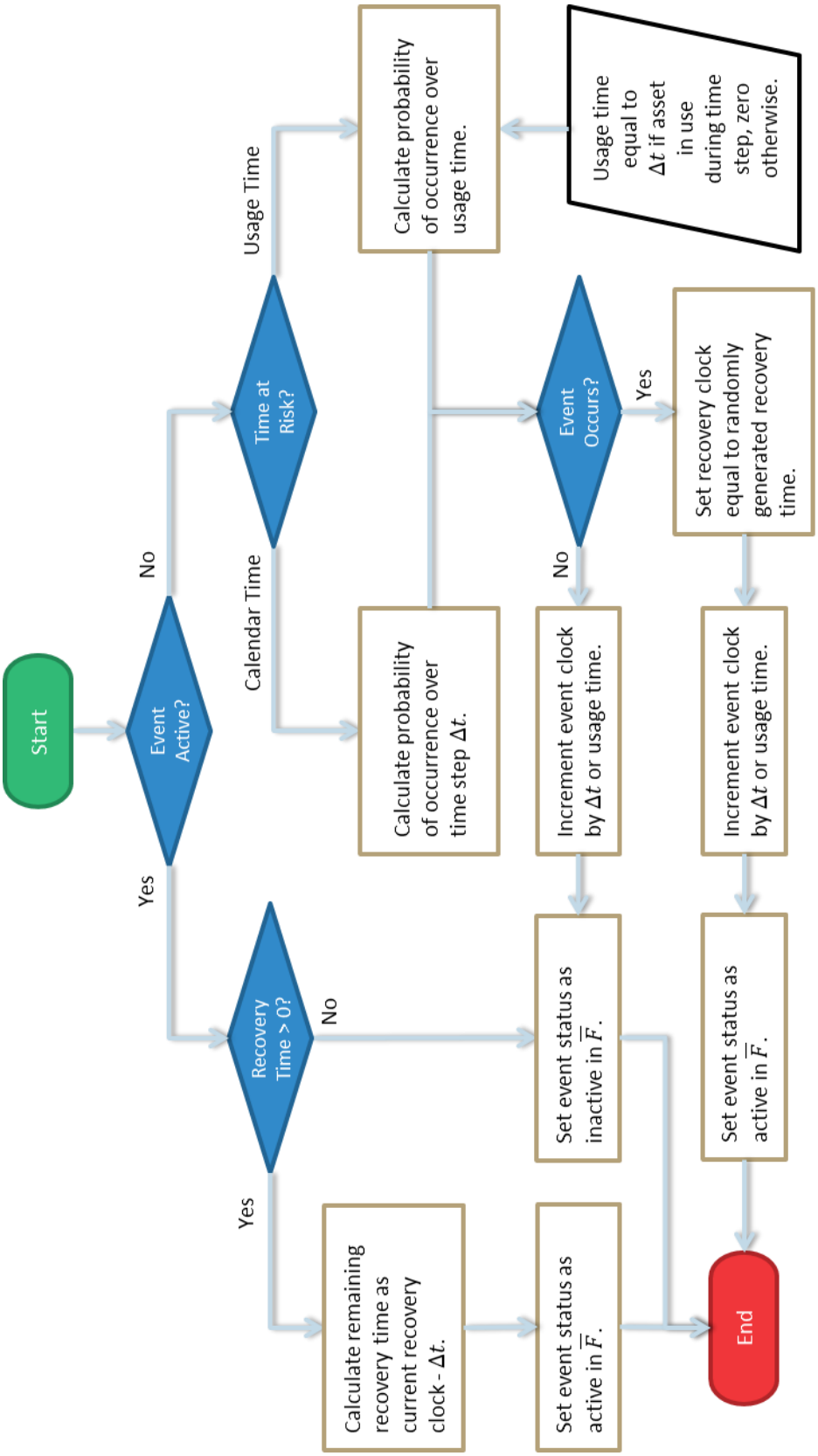

Figure 24. DEM Solution Flow Chart

3.3 Results & Discussion

3.3.1 Model Setup

The model presented in this paper is applied to a hypothetical UGS facility. The hypothetical facility has been based on an actual facility in operation today. However, for confidentiality purposes the system has been modified. As shown in Figure 25, the storage facility consists of four reservoirs or storage fields (SFs); A through D. The storage fields connect to a compressor station that has three compression units. The compressors can be in parallel or double staged configuration (Figure 26). Double staging on withdrawal requires one of the units designed for low suction pressures (designated as LP) to operate on the first stage, with the base load unit (designated MP) on the second stage. The high discharge pressure unit (designated HP) is not used in this configuration. Double staging on injection requires the HP unit to operate on the second stage, with the MP unit on the first stage. The LP unit is not used in this configuration. The TPM decides which configuration to use based on the required suction and discharge pressures. The transmission system consists of three parallel pipelines as shown in Figure 25. More details of the configuration of the storage system used in this analysis are summarized in the supplementary materials (Chapter 7).

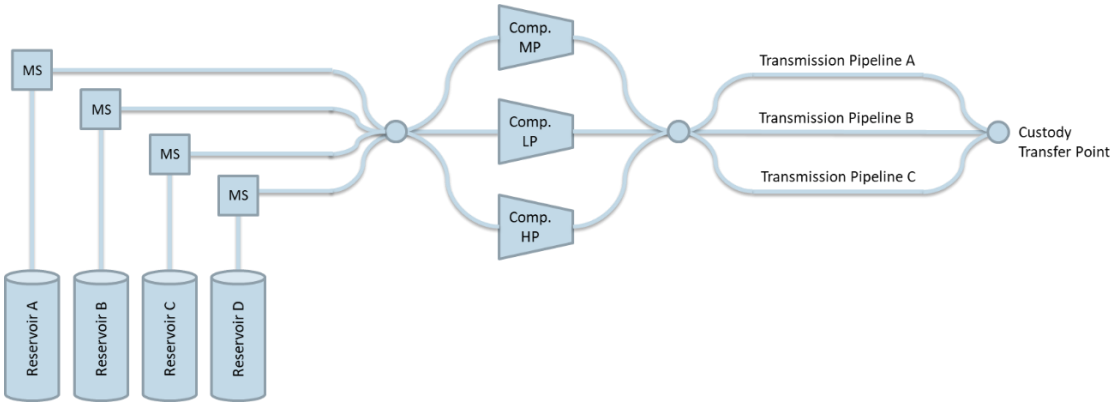

Figure 25. Hypothetical UGS Facility

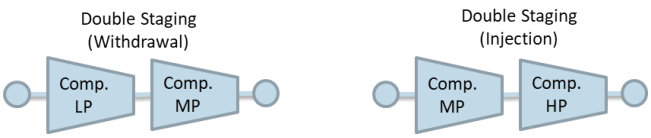

Figure 26. Double Staged Compressor Arrangement

A hypothetical daily gas demand curve is used to test the performance of the system (Figure 27). The flow demand curve is based on the data from an actual storage facility currently in operation. However, for confidentiality purposes the demand curve has been modified whilst maintaining a realistic shape. The demand curve is designed to represent a potential withdrawal and injection pattern when the storage facility is used for seasonal storage. For this type of utilization, gas is withdrawn during the winter months when gas demands (and in turn prices) are high. Gas is injected during the summer months when demand and prices are low. Day 1 of the season represents the start of the summer months when gas is injected (negative flow). Flow demand during injection is relatively steady. Flow demand during withdrawal is impacted by temperature fluctuations and price fluctuations, resulting in a highly variable pattern.

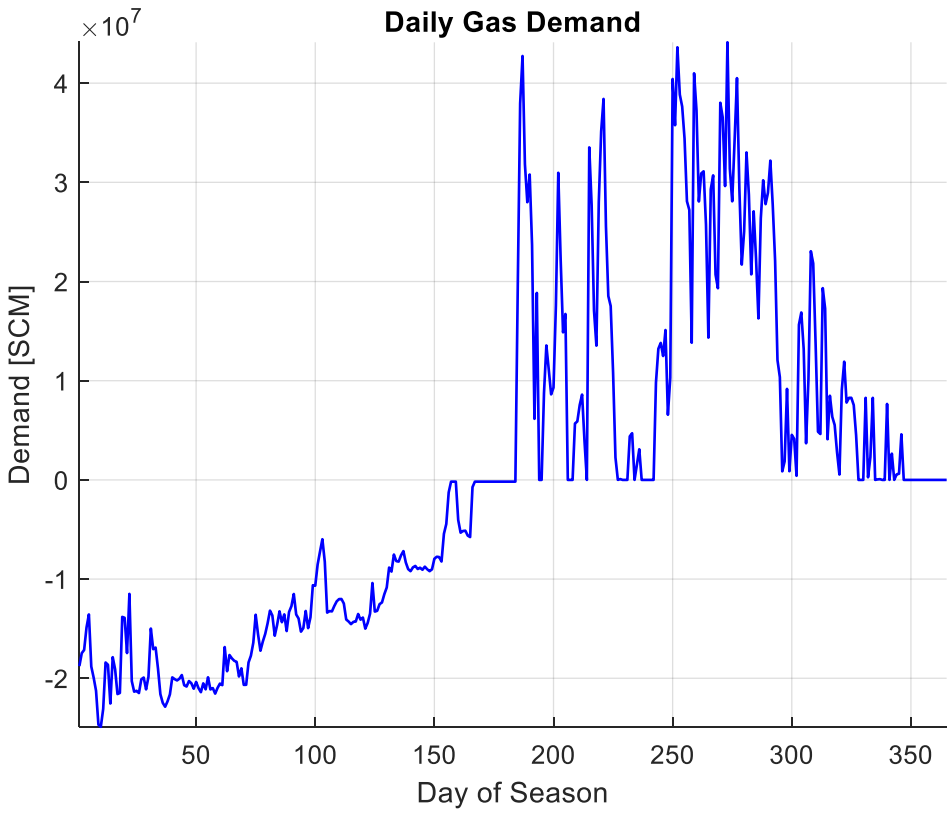

Figure 27. Hypothetical Daily Gas Flow Demand

3.3.2 Scenario Analysis

The effect of disruption events on the gas flow capacity of the storage system is demonstrated using scenario analysis. The scenarios considered are summarized in Table 10. A baseline case with all parts of the UGS facility function is also shown to allow for comparison to the scenarios.

Table 10. Scenario Summary

Scenario Number	Disruption Time and Duration	Unavailable Assets
1	Day 1 to 365	Transmission Pipeline A
2	Day 100 to 160	Reservoir D
3	Day 1 to 80	Reservoir A
4	Day 250 to 310	Compressor MP, LP and HP

Figure 28 shows the results dashboard for the baseline case. The top left chart shows the demand and supply curves superimposed. In the baseline case, all demand spikes are met with the necessary gas supply. The top right chart shows histograms of shortfall events. As expected, none occur for the baseline case since no disruption events are considered. The bottom left chart shows the inventory levels in each of the reservoirs at the end of each day of the season. The simulation begins with injection for the first 184 days of the season. The priority sequence as defined in the model configuration is reflected in chart, with reservoir inventories being filled and depleted in the given order. In this hypothetical case, the priority sequence for injection is SF A, SF B, SF C and finally SF D. The priority sequence specified for withdrawal is SF A first, followed by SF B and SF C in tandem and finally SF D. The bottom right chart shows the compressor flow for each configuration (see Figure 26). The double stage configuration is used on injection when reservoir inventories (pressures) are high. On withdrawal, the double stage configuration is used when reservoir priority group inventories (pressures) are low.

Scenario 1 (Figure 29) models a season long disruption of one of the transmission pipelines. The result is a reduction in the peak flow capacity of the system. Since flow during the injection season occurs at a steady rate, with no high demand days, no shortfalls occur during injection season and the reservoirs are filled. However, the system is unable to meet the highest demand peaks occurring during withdrawal season.

Scenario 2 (Figure 30) and Scenario 3 (Figure 31) model disruption of storage reservoir D (SF D) and A (SF A) operation, respectively. In scenario 2, the disruption occurs late in the injection season and the system is unable to fill reservoir D before withdrawal demand occurs. This results in injection shortfalls as well as withdrawal shortfalls. Scenario 2 illustrates a very useful feature of the model; capturing latent effects of disruption events. The importance of timing of disruptions is illustrated in scenario 3. The disruption occurs

early in the injection season, and the system can fill reservoir A in time before withdrawal demand arrives. As a result, no shortfalls occur.

Scenario 4 (Figure 32) models a disruption of compressor station operation in the middle of withdrawal season. The system can meet some of the flow demand by free-flowing reservoirs. However, peak demands are unmet resulting in shortfalls.

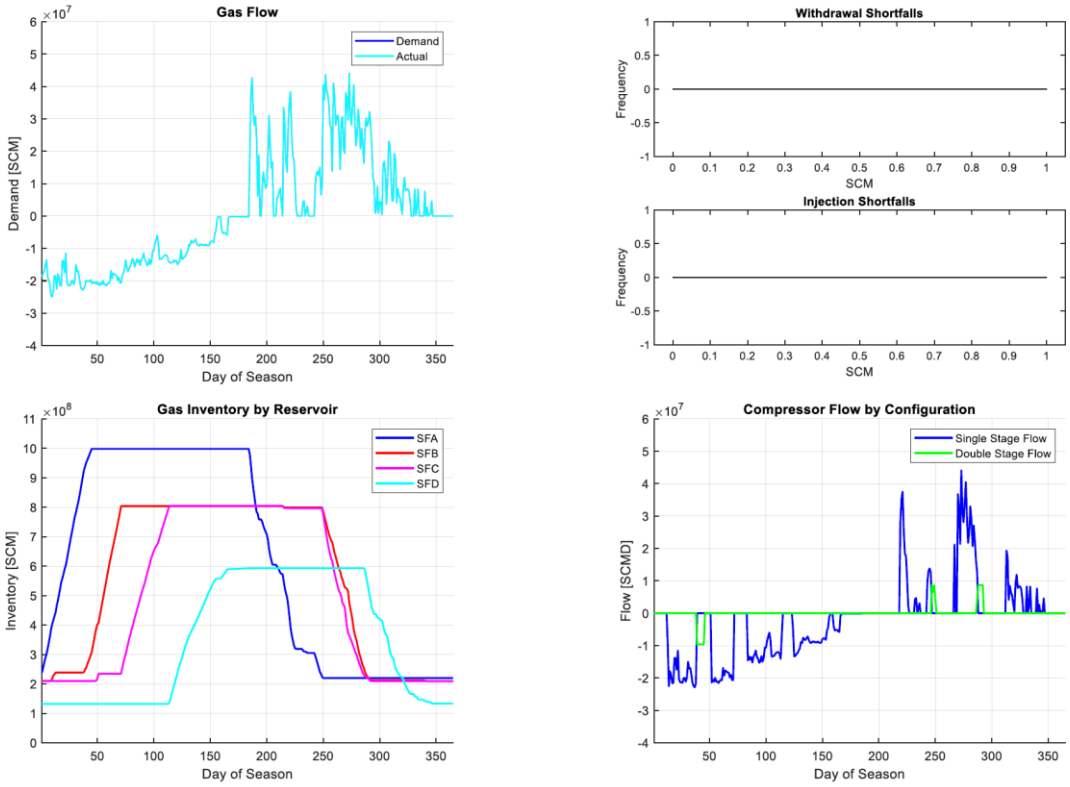

Figure 28. Baseline Results

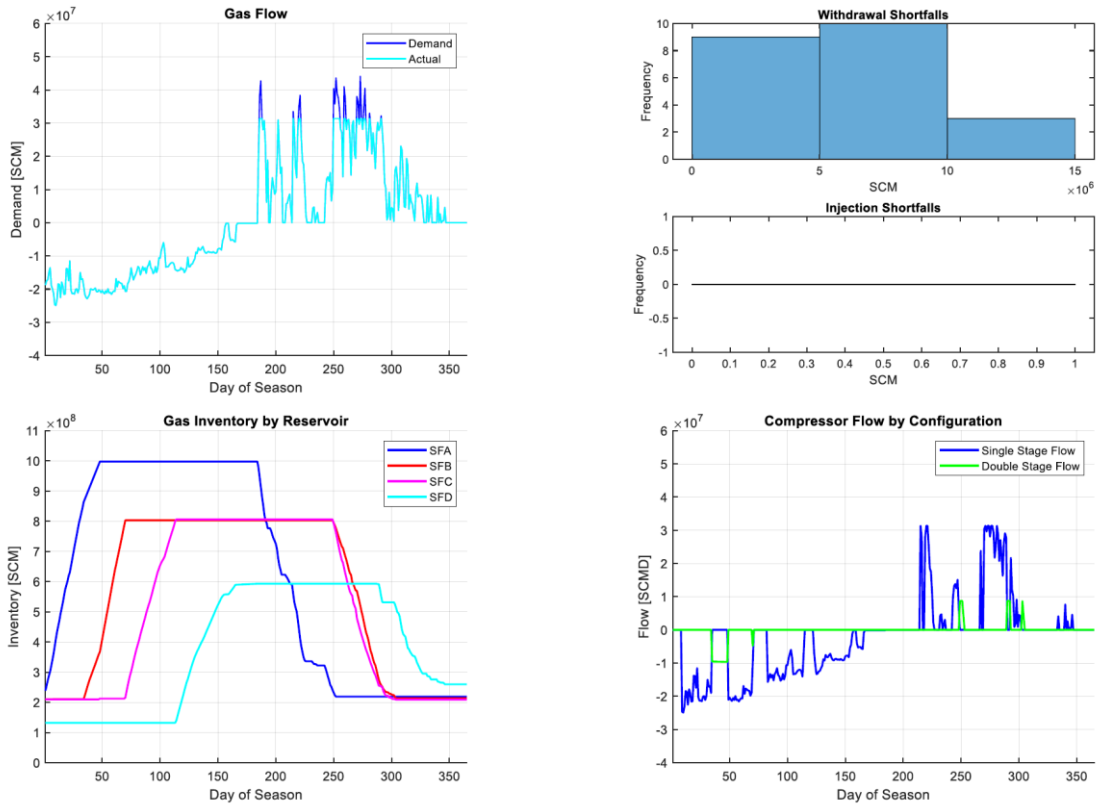

Figure 29. Scenario 1 - Season Long Outage of Transmission Line A

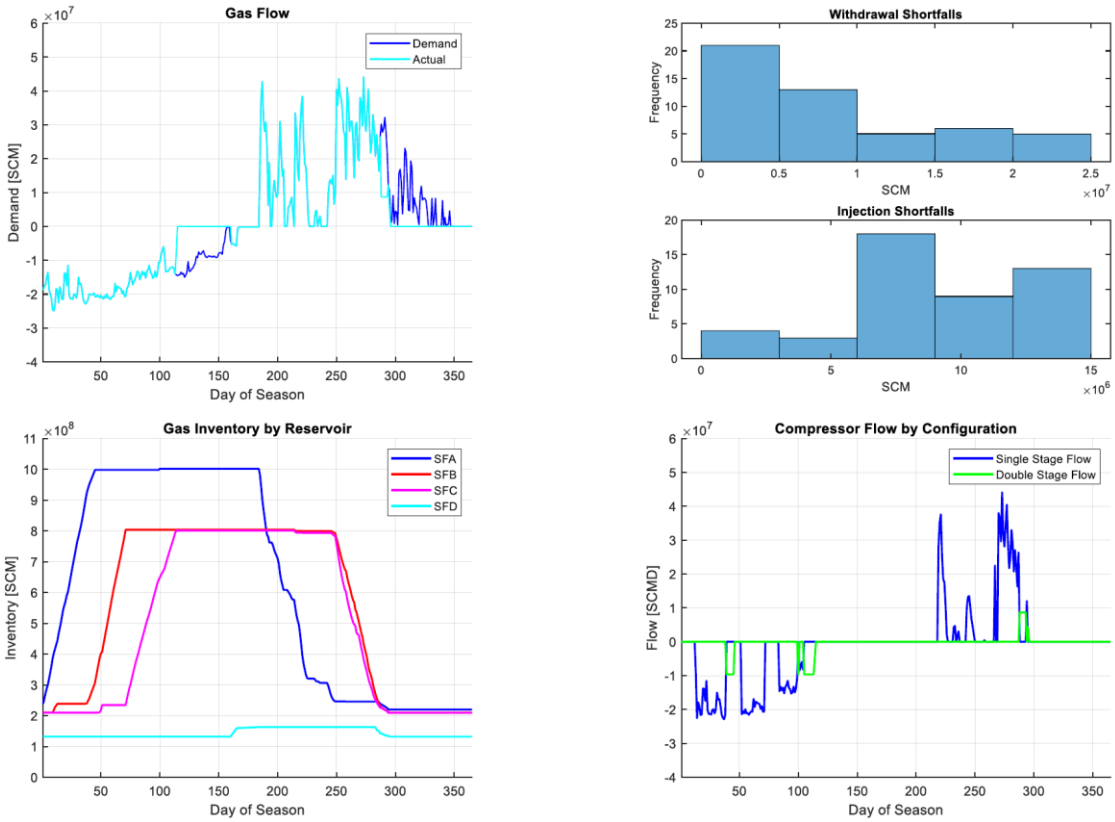

Figure 30. Scenario 2 - Reservoir D Outage from Day 100 to Day 160

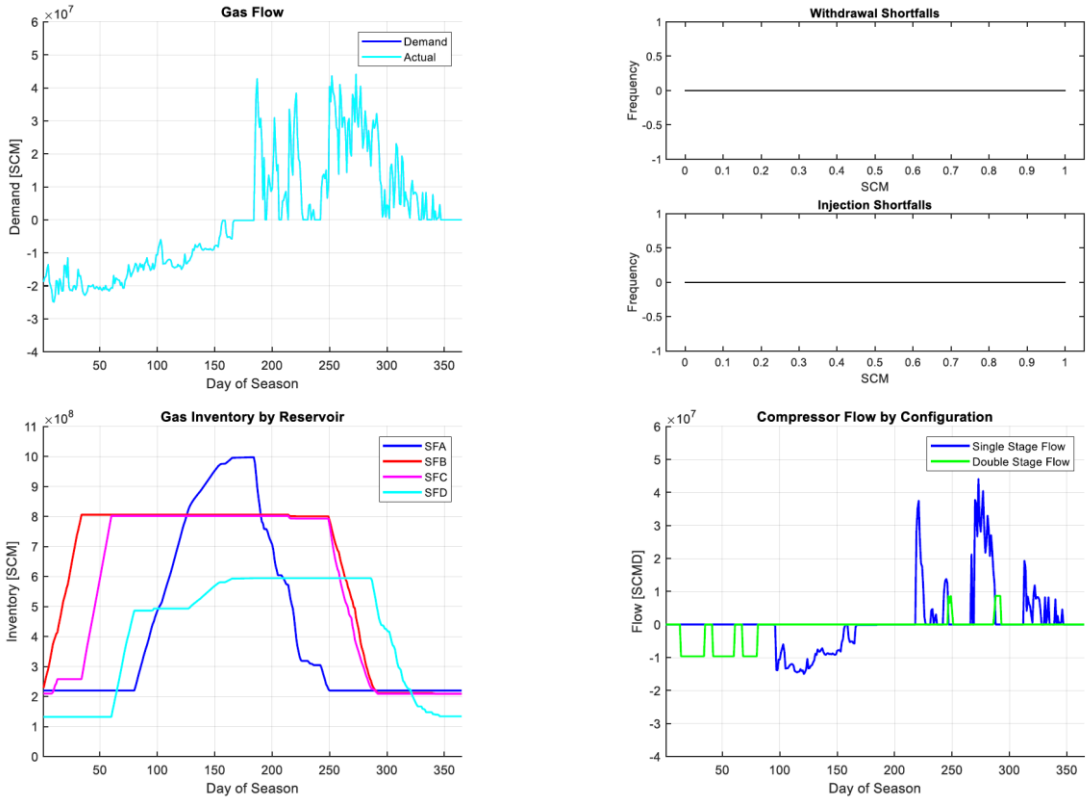

Figure 31. Scenario 3 - Reservoir A Outage from Day 1 to Day 80

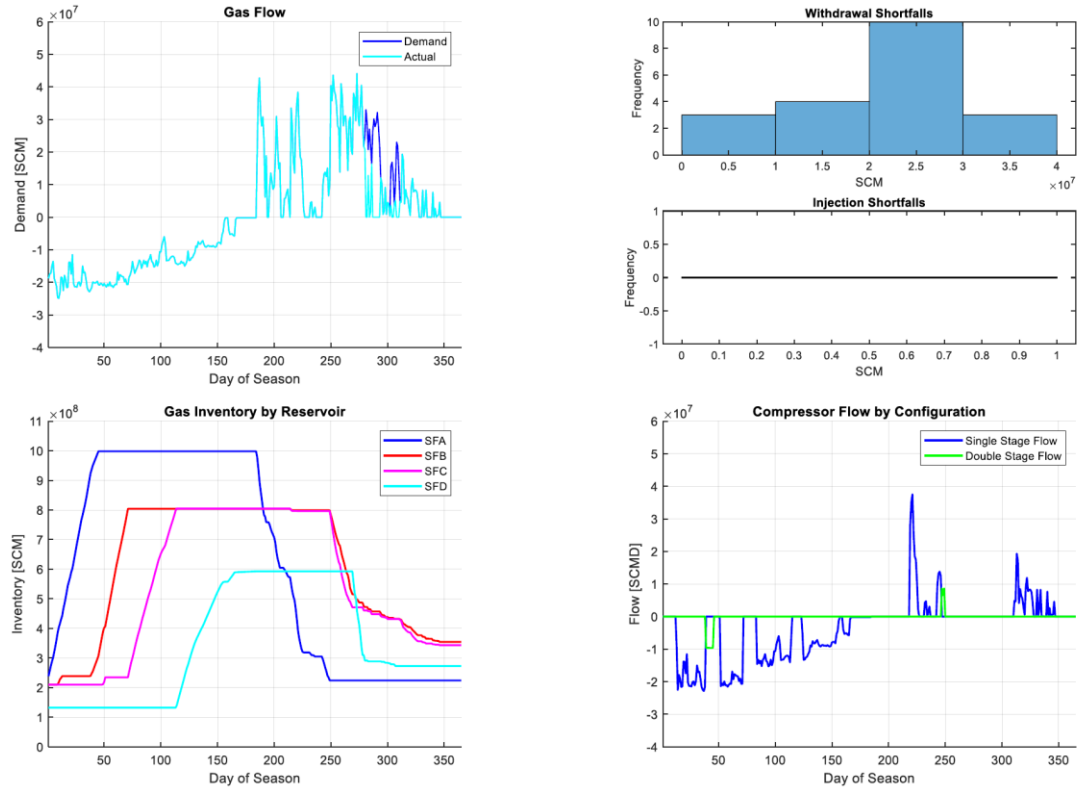

Figure 32. Scenario 4 - Compressor Station Outage from Day 250 to Day 310

3.3.3 Risk Analysis

Integration of the TPM and DEM facilitates quantitative risk analysis of the UGS facility by combining the probability of occurrence of disruption events (DEM) with the impact of such a disruption event (TPM). The risk analysis algorithm follows the Monte Carlo simulation logic shown in Figure 17, where a single iteration consists of withdrawal and injection simulation through the length of the demand time series (Figure 27). The simulation was run for 100, 1000 and 5000 samples. Convergence was confirmed by examining the change in the coefficient of variation of the injection and withdrawal shortfall distributions. A change of less than 5% was used as the convergence criteria. For the hypothetical UGS facility examined here, the model simulation converges at 5000 iterations. The disruption events considered in this analysis include minor and major disruptions of the storage reservoirs, minor and major disruptions of compressor units and major disruptions of transmission pipelines. A summary of the disruption events is provided in Table 11. More details of the configuration of the disruption events considered in this analysis are provided in the supplementary materials (Chapter 7). Whilst the scenarios presented are hypothetical, they have been configured to provide a realistic representation of potential disruption events.

Table 11. Summary of Disruption Events

Disruption Event	Time at Risk	Probability Model	Recovery Duration	Description
Reservoir Meter Station Minor Disruption	Calendar Time	Exponential	Hours	Random equipment failures (e.g. valves, regulators) within the meter station that can be rectified quickly.
Reservoir Meter Station Major Disruption	Calendar Time	Exponential	Days	Loss of containment event within meter station that results in extended outage.
Reservoir Field Valve Failure	Calendar Time	Weibull	Days	Degradation and seizing of field valve that isolates reservoir from compressor station.
Compressor Minor Failures	Usage Time	NHPP	Hours	Minor component failures within compressor unit system that can be rectified quickly.
Compressor Main Bearing Failure	Usage Time	Weibull	Days	Wear out of main bearings that require replacement of the entire main bearing set.
Compressor Cylinder Liner Failure	Usage Time	Weibull	Days	Wear out of compressor cylinder liners requiring extended outage for replacement.
Transmission Pipeline Rupture	Calendar Time	Exponential	Years	Catastrophic loss of containment from transmission pipeline that can result in an extended disruption.

Figure 33 shows the relative frequency histograms of shortfall events during withdrawal and injection. Figure 34 and Figure 35 show the cumulative frequency charts for shortfall events during withdrawal and injection respectively. The y-axis is the cumulative frequency of shortfall events that result in a shortfall of Q (x-axis) or more. Such charts can be used to examine the overall annual risk in the system. During withdrawal the hypothetical system may experience one shortfall every year as high as 3 million SCM. On injection, the system experiences a shortfall of 3 million SCM at a rate of once every two years. Whilst such events may not be a significant risk concern, a more significant shortfall event in excess of 10 million SCM may result in the loss of a contract for a UGS facility operator. Such shortfalls events are predicted to occur at a frequency as high as once every ten years for the hypothetical system analysed. Quantitative risk analysis, as presented in this paper, can be used by UGS facility operators to examine the frequency of major events and design mitigation measures if the risk is deemed unacceptable.

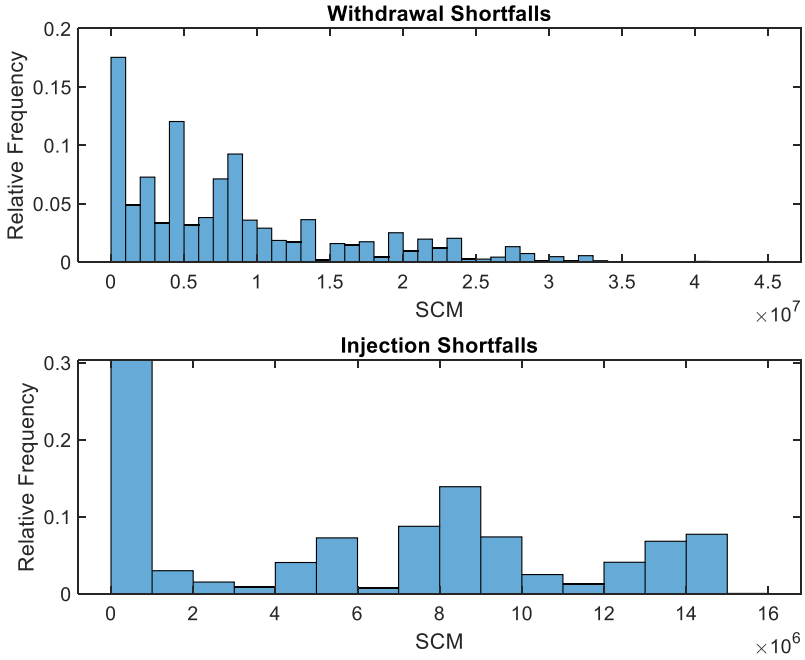

Figure 33. Relative Frequency of Shortfalls

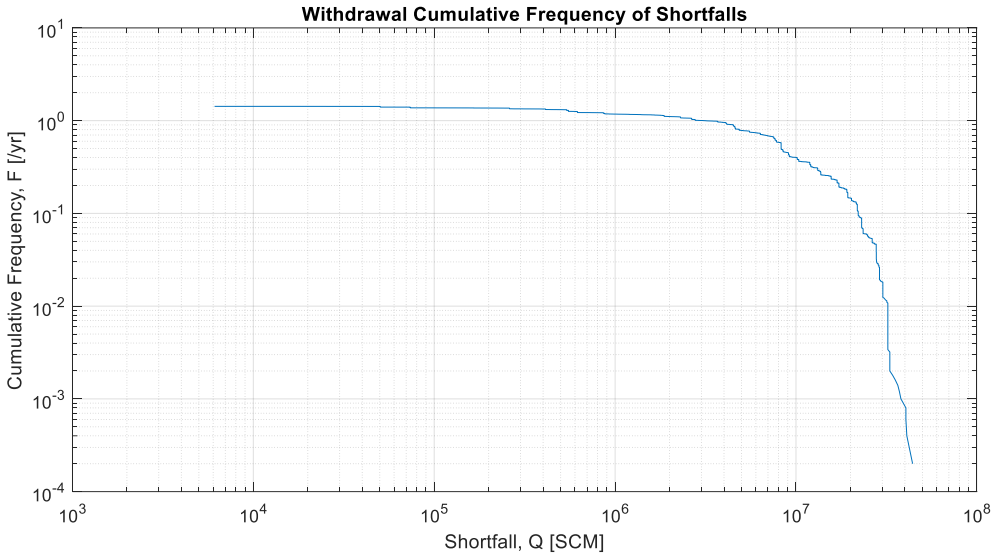

Figure 34. Withdrawal Risk Curve

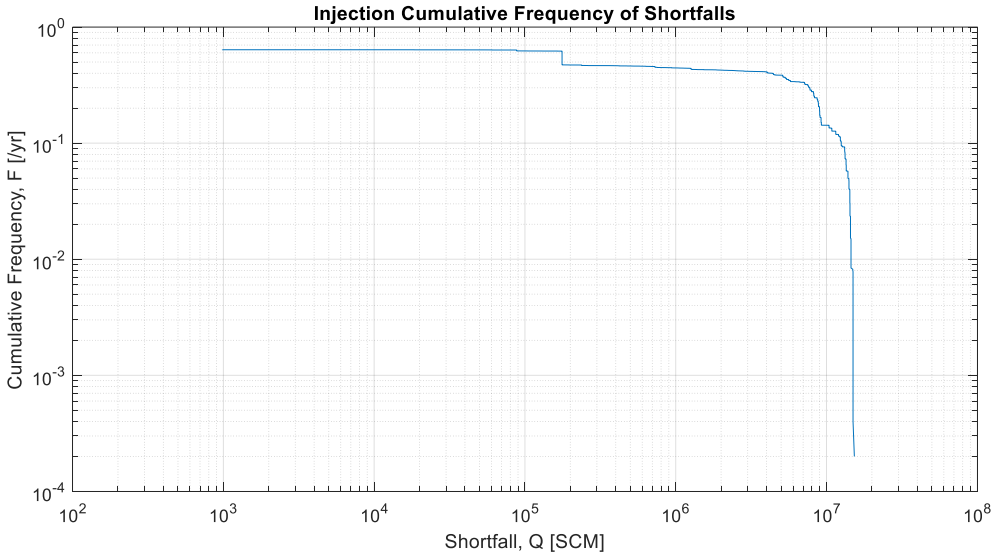

Figure 35. Injection Risk Curve

3.4 Conclusions and Future Work

This paper presents a computer model for quantitatively analysing operational risk in an underground gas storage facility. The model combines a thermo-hydraulic performance model with a Monte Carlo simulation of potential disruption events to quantify risk by severity of gas supply shortfalls and the frequency of such shortfalls. The model is highly configurable and can be applied to typical UGS facilities. Currently the model considers UGS facility assets as having two states only (available or unavailable). Future works will

incorporate intermediate states such as reduced operating capacity. Stand-by redundancy will also be incorporated, particularly for the compression system.

This model can be used to analyse a multitude of potential events that can affect a UGS facility. The integrated physics model means the user does not have to explicitly account for changes in system performance resulting from disruption events. As such, many combinations of asset configurations (performance parameters), system states (inventory levels, asset availability) and disruption events (concurrent events, event timings) can be analysed within a single modelling framework. This paper focuses on the details of the methodology. A simple test case is presented to demonstrate the applicability of the technique.

4 Multi-Criteria Decision-Making Considering Risk and Uncertainty in Physical Asset Management

ABSTRACT

In this work we present a method for risk-informed decision-making in the physical asset management context whereby risk evaluation and cost-benefit analysis are considered in a common framework. The methodology uses quantitative risk measures to prioritize projects based on a combination of risk tolerance criteria, cost-benefit analysis and uncertainty reduction metrics. There is a need in the risk and asset management literature for a unified framework through which quantitative risk can be evaluated against tolerability criteria and trade-off decisions can be made between risk treatment options. The methodology uses quantitative risk measures for loss of life, loss of production and loss of property. A risk matrix is used to classify risk as intolerable, As Low As Reasonably Practicable (ALARP) or broadly tolerable. Risks in the intolerable and ALARP region require risk treatment, and risk treatment options are generated. Risk reduction benefit of the treatment options is quantified, and cost-benefit analysis is performed using discounted cashflow analysis. The Analytic Hierarchy Process is used to derive weights for prioritization criteria based on decision-maker preferences. The weights, along with prioritization criteria for risk reduction, tolerance criteria and project cost, are used to prioritize projects using the Technique for Order Preference by Similarity to Ideal Solution method. The usefulness of the methodology for improved decision-making is illustrated using a numerical example.

4.1 Introduction

In the last decade, the management of physical assets has emerged as a crucial business function for companies operating in asset intensive industries. Furthermore, the complex nature of modern engineered systems has led to the need for physical asset management as a discipline (Hastings, 2015). Complex systems, composed of many interacting and inter-dependent components are increasing the likelihood of extreme, rare and disruptive events (Komljenovic, Gaha, Abdul-Nour, Langheit, & Bourgeois, 2016). As such, it comes as no surprise that the ISO 55000 Asset Management series of standards emphasize the need for risk-informed decisions (ISO, 2014).

Risk assessment in the asset management context requires the identification of what can go wrong (e.g. unexpected asset failures), characterization of the likelihood and consequence of such events, and comparison of the likelihood and consequence against risk tolerability criteria to determine risk treatment options (ISO, 2018). Treatment options give rise to potential asset investments that must be prioritized while taking into consideration several factors (e.g. cost, return on investment, risk tolerability, etc.). In this work we present a framework and methodology for quantitative prioritization of risk-informed asset management projects using multi-criteria decision analysis.

Several methodologies exist in the literature for multi-criteria decision-making (MCDM), sometimes referred to as multi-criteria decision aiding or multi-criteria decision analysis (MCDA). We use the acronym MCDM/A to consider both. A recent review of the application of MCDM/A in risk management has shown a significant increase in publications in this decade (de Almeida, Alencar, Garcez, & Ferreira, 2017). The review revealed that the most promising areas of future research for MCDM/A in the risk context are towards improving the managerial decision-making process. The authors conclude that a multi-dimensional view, taking the decision-maker's preferences into account, is necessary to improve decision-making for complex problems. This conclusion is of importance when consider the application of risk assessments in the asset management context.

A few researchers have proposed frameworks for asset management decisions taking into consideration multiple criteria and decision-maker preferences. Nordgard and Catrinu (2011) applied MCDM/A to select asset management strategies for an electricity distribution system. The method considered a qualitative safety risk criterion as well as maintenance and investment costs as quantitative criteria. Tolerability of safety risk was also considered using a risk matrix. A similar qualitative approach was taken by Lindhe, et al. (2013) for

MCDM/A for water safety measures. Ype Wijnia's PhD thesis, perhaps one of the most comprehensive works considering risk in the asset management context, evaluates risk using a semi-quantitative risk matrix approach (Wijnia, 2016). Quantitative risk measures and how to incorporate them in MCDM/A in the asset management context are not discussed by the above authors. D. E. Nordgard (2012) discussed the potential application of quantitative risk analysis in asset management decisions, drawing connections between the risk management process and the needs of asset management. However, the author does not propose a methodology for risk-informed cost-benefit analysis for the selection of risk treatment options. de Almeida et al (2015) present a quantitative and multi-dimensional risk prioritization approach based on multi-attribute utility theory. However, the method does not integrate cost-benefit analysis in the decision process. Bharadwaj, Silberschmidt and Wintle (2012) integrate quantitative risk analysis with discounted cash flow analysis to optimize asset repair/replace decisions, though they do not incorporate multi-dimensional risk measures or decision-maker preferences. We see a need in MCDM/A literature for risk and asset management, for a unified framework through which quantitative and multi-dimensional risk can be evaluated against tolerability criteria and trade-off decisions can be made between risk treatment options, whilst taking into consideration decision-maker preferences.

In this work we present a method for risk-informed decision-making in the physical asset management context whereby risk evaluation and cost-benefit analysis are considered in a common framework. The methodology uses quantitative risk measures to prioritize projects based on a combination of risk tolerance criteria, cost-benefit analysis and uncertainty reduction metrics. This paper focuses on the details of the methodology. A simple test case is presented to demonstrate the applicability of the technique, which shows logical consistency in the result. The paper is organized as follows: Section 4.2 provides an overview of the theoretical background on risk and risk management. Section 4.3 presents the details of the proposed decision-making framework. In Section 4.4 we apply the proposed methodology to and illustrate its usefulness through a numerical example. Finally, in Section 4.5 we summarize the main findings and discuss potential future work.

4.2 Background

4.2.1 Defining Risk

The word risk has many meanings depending on the context. In the world of finance, risk is defined as the variance in return of an investment (Markowitz, 1952). In the business context, risk is defined as the (negative) variation in performance metrics such as revenue and cost (March & Shapira, 1987). Where public safety is the concern, risk is defined as a measure of the frequency and severity of life-threatening events (CSChE, 2004). The international standard for risk management defines risk as the effect of uncertainty on objectives (ISO, 2018).

Indeed, the discipline of risk analysis has struggled with defining risk. In a talk given at the 1996 Annual Meeting of the Society for Risk Analysis, the famous risk analysis researcher Stan Kaplan said, "The words of risk analysis have been, and continue to be a problem. Many of you here remember that when our Society for Risk Analysis was brand new, one of the first things it did was to establish a committee to define the word 'risk'. This committee laboured for 4 years and then gave up, saying in its final report, that maybe it's better not to define risk. Let each author define it in his own way, only please each should explain clearly what way that is" (Kaplan S. , 1997). Kaplan and Garrick (1981) defined risk by first considering the questions that we attempt to answer through risk analysis:

- What can go wrong (i.e. an undesired event)?
- How likely is it that the event may happen?
- If the event does happen, what are the consequences?

A risk can then be defined as the "set of triplets" denoted by $\langle s_i, p(l_i), p(x_i) \rangle$ where s_i is the i^{th} scenario, for which l_i denotes the likelihood of the scenario occurrence (given as a frequency, say per annum) and x_i the consequence(s) if the i^{th} scenario occurs. Furthermore, since the complete definition of risk requires a measure of the uncertainty about l_i and x_i, the quantities are defined using probability distributions. As such, we use the notation $p(l_i)$ and $p(x_i)$, where $p(\cdot)$ denotes the probability density functions of the quantities.

The risk triplet as defined by Kaplan and Garrick becomes the basis for two of the core elements of risk management: the identification of scenarios (henceforth referred to as undesired events), and the quantification of the likelihood and consequence(s) along with uncertainty about the quantities (i.e. the risk analysis). We adopt the Kaplan and Garrick

definition of risk in this work and demonstrate its usefulness in multi-criteria decision-making under uncertainty for physical asset management.

4.2.2 Risk Management

Risk management is the coordinated set of activities within an organization with the aim towards controlling risk (ISO, 2018). It is a continuous management process by which risk is identified, analysed and evaluated. Risk management also involves decision-making with regards to the implementation of risk treatment (Rausand, 2011). The core elements of risk management as defined in ISO 31000 are shown in Figure 36.

Figure 36. Risk Management Framework

The first step in performing a risk assessment is identifying the undesired events that can cause a negative impact on a part or entirety of a system. This is often called risk or hazard identification. Once undesired events have been identified the next step in risk assessment is determining the likelihood and consequence(s) of these events. The objective of a likelihood analysis is to obtain a measure of the frequency (say per annum) of an undesired event occurring. The objective of a consequence analysis is to obtain a measure of the potential loss incurred as a result of an undesired event (Rausand, 2011).

The final step in a risk assessment is evaluating the risk measure against risk tolerance criteria (Rausand, 2011). A risk matrix is a commonly used method for evaluating risk in an objective way. A risk matrix is used to evaluate the risk of a single scenario and is constructed by defining levels of likelihood along a row (or column) and levels of consequence along a column (or row). Each cell in the matrix, defined by a row-column pair (i.e. a likelihood and consequence pair) has an associated tolerability, which guides a decision

maker by defining the urgency of risk treatment (Cox, 2008). An example risk matrix is shown in Figure 37, with the following categories:

- Intolerable; risk requires immediate treatment
- ALARP; risk must be As Low as Reasonably Practicable (ALARP, further discussed in Section 4.3.1)
- Broadly Tolerable; risk treatment may be undertaken but not required

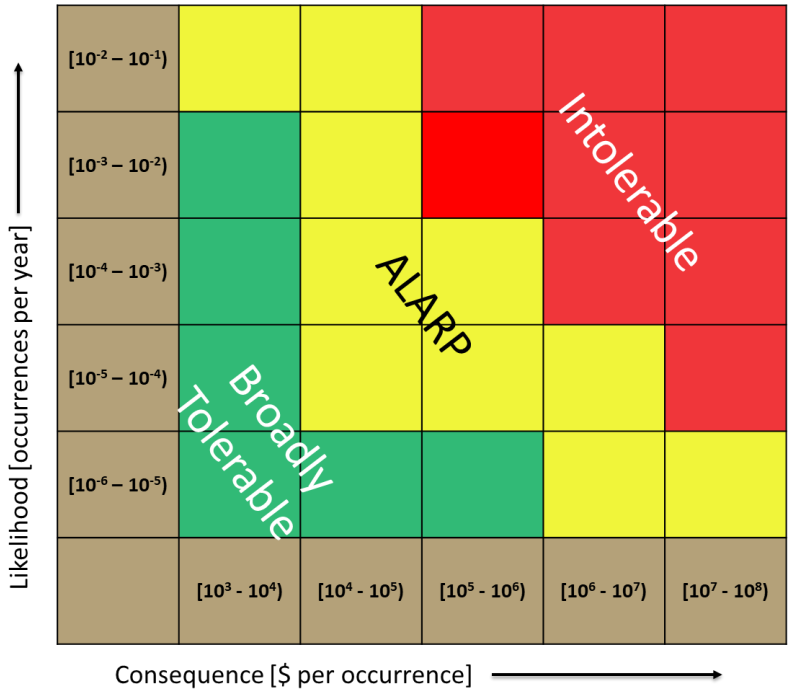

Figure 37. Example Risk Matrix

The results of a risk assessment are used to guide decision-making with respect to risk treatment. Treatment can take many forms (see Figure 36) and treatment options are not necessarily mutually exclusive. Treatment can include reducing the likelihood of the undesired event (prevention), reducing the consequence(s) (mitigation) or sharing the risk through insurance (transfer). Extreme treatments may include avoiding the risk altogether by removing the source of risk (ISO, 2018).

In this work we present a method for evaluating risk taking into consideration the uncertainty in the likelihood and consequence(s), verifying the economic viability of a risk treatment option, and finally prioritizing a portfolio of risk treatment options using multi-criteria decision analysis. The method is illustrated using a numerical example.

4.3 Methodology

This section presents our proposed methodology for risk-informed decision-making for the management of physical assets. The proposed decision-making framework is summarized in the flowchart shown in Figure 1. The first two steps encompass the risk assessment, whereby risk is identified, quantified and evaluated against tolerance criteria (see Section 4.3.1). Risks requiring treatment as determined by the risk tolerance criteria are identified for risk treatment consideration. Section 4.3.2 discusses steps three through five in Figure 1; quantification of risk reduction benefits, cost-benefit analysis of the treatment options, and lastly prioritization of the treatment options using multi-criteria decision analysis.

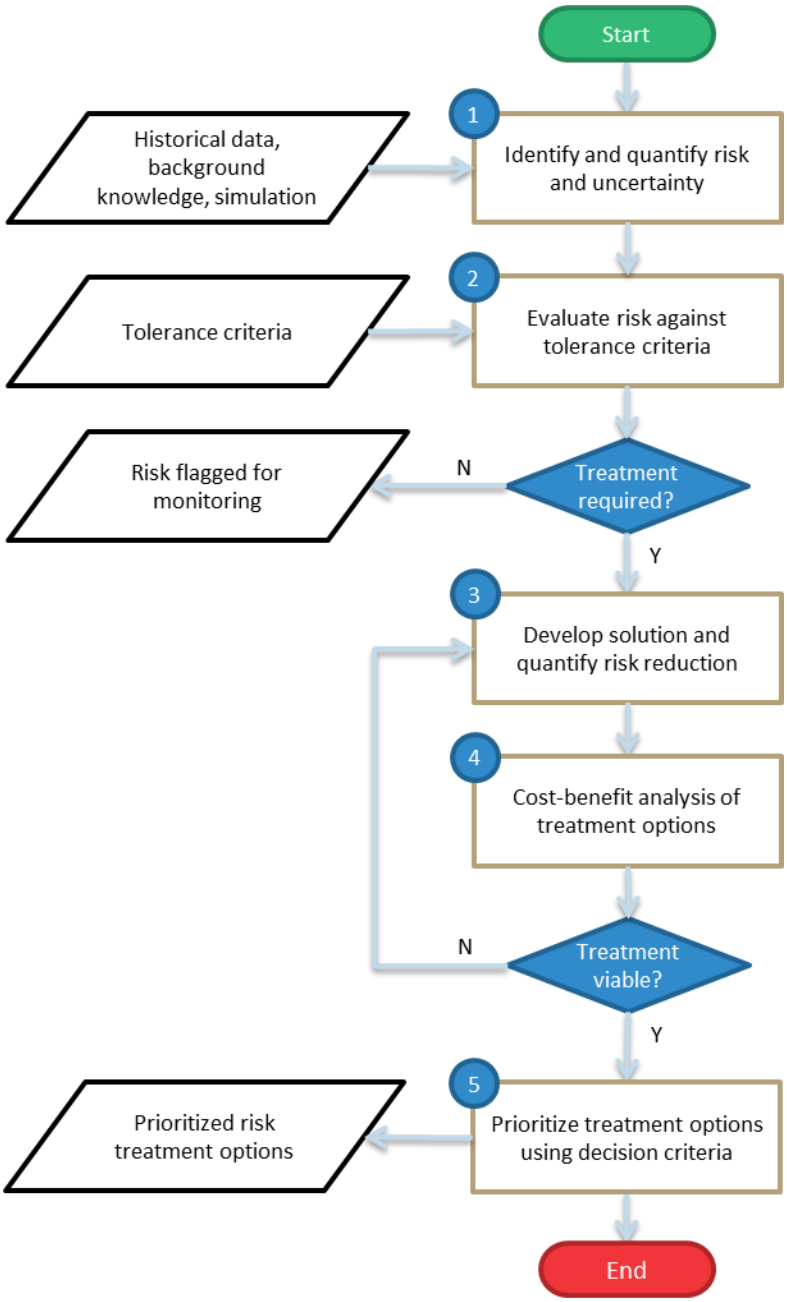

Figure 38. Decision-making Flow Chart

4.3.1 Risk Assessment

4.3.1.1 Identification and Analysis

The risk triplet as defined by Kaplan and Garrick (1981) is often conceptualized using a bowtie analysis, as shown in Figure 39 (Rausand, 2011). The left side of the bowtie represents the likelihood analysis. The objective of the likelihood analysis is to quantify the frequency (per unit time) of the undesired event (e.g. pipe rupture, compressor failure). The quantification considers the frequency with which various threats can present themselves as well as the barriers (vertical bars) in place to prevent those threats from causing the undesired event. The right side of the bowtie represents the consequence analysis, which consists of two parts: outcome analysis and impact analysis. The outcome analysis considers the many ways in which the undesired event can escalate or de-escalate (e.g. gas release leading to fire and explosion). Mitigating measures (vertical bars) designed to protect against certain outcomes are also considered (e.g. emergency shutdown system preventing a gas leak from escalating). The objective is to quantify the likelihood of various outcomes derived from the likelihood of the undesired event. The impact analysis aims to quantify the end consequences of each outcome (e.g. loss of life, production disruption, property damage, etc.). Note that impacts can vary in severity depending on the outcome (as shown in Figure 39).

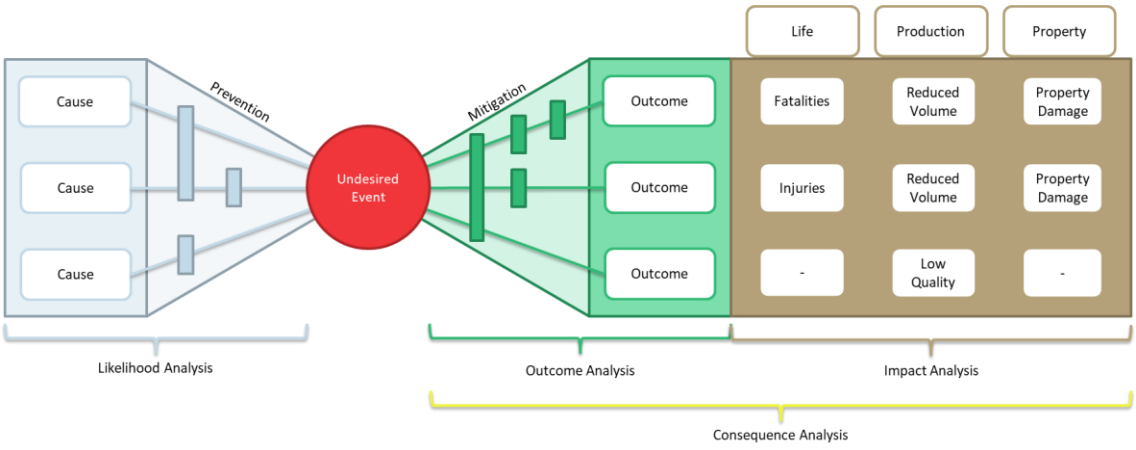

Figure 39. Bowtie Analysis Schematic

Prior to quantifying a given risk, it is useful to conduct a risk identification exercise with stakeholders. Risk identification can be done in numerous ways depending on the context and the type of risk. As such, we do not dedicate much discussion to this topic, instead directing the reader to Marvin Rausand's book for a thorough review of risk identification methods (Rausand, 2011). We focus on the qualitative output from a risk identification exercise necessary to support quantitative risk analysis; identification and interaction of threats and preventive barriers, identification of mitigation measures and potential outcomes

of the undesired event, and the description of potential impacts associated with each outcome. The qualitative output of a risk identification exercise serves as a roadmap for quantitative risk analysis.

Quantitative risk analysis is a complex undertaking, and the methods used can be very context and risk specific. Common methods of likelihood analysis include fault tree analysis, Bayesian belief networks and Petri nets among many others. Such methods are used to model the causal relationship between the undesired event and potential root causes. The outcome analysis (see Figure 39) is almost universally represented (though not always quantified) by means of an event tree analysis. Event tree analysis is used to calculate the frequency of various outcomes after a single initiating event (i.e. the undesired event). The process starts by identifying an initiating event (e.g. gas leak) and its frequency. A sequence of events that can follow the undesired event (e.g. ignition, emergency shutdown failure) are identified and each represents a split in the event tree. This process is repeated until all possible outcomes are identified (Bentley, 1999). Rausand (2011) provides a thorough review of fault trees, event trees and Bayesian networks, as well as other similar techniques. It should be noted that the inputs to fault trees and event trees are often obtained from other context specific analysis techniques. Below are some examples in the context of physical asset management:

- Mechanical integrity failure prediction of assets through corrosion modelling (Nesic, 2007)
- Reliability analysis of complex asset systems through simulation (Rao & Naikan, 2016)
- Estimated maximum loss models for property damage due to fires and explosions (Gustavsson & Shahriari, 2010)
- Resilience modelling of energy infrastructure systems (Wang, et al., 2019)

Regardless of the modelling approach used, the important aspect of any quantitative risk analysis is that it provides a full picture of the risk. The complete picture, as described by Kaplan and Garrick (1981) requires that likelihood and consequence be quantified using probability distributions (see Section 4.2.1). Decades of experience by risk practitioners, applying sophisticated modelling techniques, has demonstrated that risk simply cannot be adequately represented using expected values of likelihoods and consequences (Aven, 2011). Uncertainty is a core component of risk, particularly when assessing rare and extreme events.

We illustrate the Kaplan and Garrick concept of quantitative risk using an example (Figure 40 and Figure 41) discussed below.

Consider a gas leak event in an oil and gas production facility. Quantitative analysis of the likelihood suggests that the frequency of occurrence per annum is 1E-3 (or once per 1000 years). Of course, a gas production facility is not expected to be in operation for anything close to 1000 years. Our frequency estimation is simply a reflection of the rarity of the event. If we were able to run an experiment for a year, with 1000 identical facilities, we could expect that one of them would experience a gas leak event. Since such an experiment is infeasible, the frequency of event occurrence is based on other sources of information (or background knowledge) and may be interpreted as a subjective probability of the event occurring (Aven, 2011). Since this background knowledge may be poor or incomplete, it is prudent to represent the uncertainty about our frequency estimation using a probability distribution (Figure 40, left). The consequence of the gas leak event is also uncertain, as it depends on a number of factors such as the size of the gas leak, the system operating pressure at the time of the leak, whether or not the emergency shutdown system malfunctions, whether or not the gas cloud finds an ignition source, etc.. There is uncertainty about all these conditions, and so the consequence is also represented using a probability distribution as shown in Figure 40 (right). The consequence considered in this case is the cost associated with production loss at the facility and is measured in dollars lost per event occurrence.

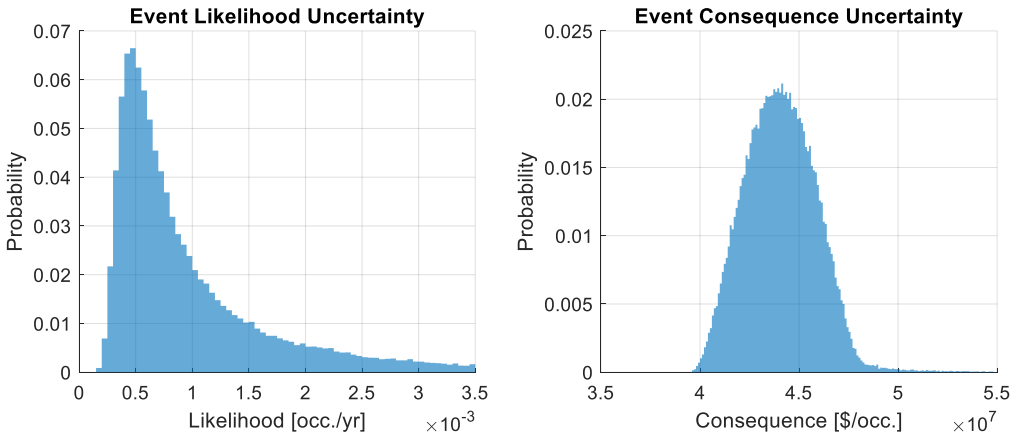

Figure 40. Example Risk Uncertainty

Figure 41 depicts the risk quantification approach used in this work, sometimes referred to as the risk-cost per year (Hastings, 2015). We represent risk as the product of the annual frequency of the undesired event and the financial cost of the consequence(s) if the event occurs. The quantitative measure of risk (R) is therefore the product distribution of the

likelihood and consequence distributions ($p(R_i) = p(l_i) \times p(x_i)$). Note that this measure assumes that the two quantities (likelihood and consequence) are independent.

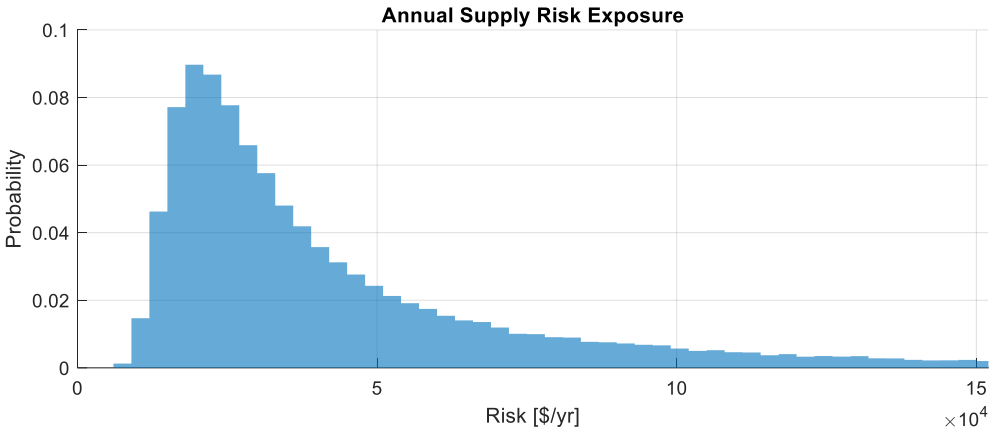

Figure 41. Example Risk Quantification

4.3.1.2 Evaluation

The risk evaluation step requires the decision maker to compare the quantitative measure of risk against tolerability criteria to make a judgement call about whether risk treatment is required. In this section we define risk matrices to support decision-making about the tolerability of risk across three consequence categories in the context of physical asset management; loss of life, loss of production and property loss. We limit the analysis to three consequence categories, though any number may be used depending on the asset management needs. In developing the risk matrices, we use a common scale (i.e. dollars) for all consequences to facilitate comparison across the many types of risk in the scope of physical asset management. Loss of production and property loss may be objectively calculated in dollars lost per undesired event occurrence. Production loss being the revenue generating potential of the product (e.g. natural gas supply), and property loss measured by the cost of repairing any damage resulting from the undesired event (e.g. fire damage to equipment). Loss of life is substantially more difficult to quantify in terms of dollars and deserves special consideration.

Converting loss of life to dollars is done using the value of a statistical life (VSL), which is a measure used to perform cost-benefit analysis for public policy decisions. We use the United States government Environmental Protection Agency benchmark value of $10 million in this work (EPA, 2015). It is important to note that VSL is not meant to reflect the compensation one is willing to accept in exchange for the certainty of one's death as no amount would be considered acceptable. Rather the VSL reflects the amount a decision-maker is willing to

spend to prevent a potential fatality (Aven, 2011). Risk in the asset management context may require a measure of loss of life where the consequence is an injury rather than a fatality (Wijnia, 2016). An objective measure is needed to scale the VSL of $10 million per fatality to injury levels. A reputable source for such scaling is the World Health Organization's (WHO) methods and data sources for global burden of disease estimates (WHO, 2017). The WHO has derived disability weights for a wide range of diseases and injuries that reflect the relative severity as compared to mortality, where disability weight of 1 is equivalent to death and 0 reflects perfect health. Using the WHO disability weights, one can objectively scale a VSL to arrive at dollar equivalents for injuries. It is beyond the scope of this paper to present such analyses. However, in this work we use $1 million as a benchmark for a long-term injury in developing the risk matrix.

Figure 42 and Figure 43 show the risk matrices developed in this work for application in physical asset management decision-making. The matrices span eight orders of magnitude for both consequence and likelihood. The eight orders of magnitude were chosen to cover the many types of risk-informed decisions required for asset management. For example, an engineered system may experience component failures that are high frequency and low consequence. On the other hand, assets within the system may be susceptible to extreme events (low frequency, high consequence). For showing the risk criteria on the matrix we do not use colour-coded cells, which hamper typical risk matrices by causing incorrect prioritization of risks (Cox, 2008). Instead we divide the matrices into regions of intolerable, ALARP and broadly tolerable (see Section 4.2.2) using the concept of a risk limit and risk target.

The United Kingdom's Health and Safety Executive (UK HSE) published a risk-based decision-making process in which a loss of life risk limit for a member of the public is defined as an annual probability (chance) of one in ten thousand. The UK HSE defined the risk target at one in a million chance of fatality per annum (UK HSE, 2001). The UK HSE limit and target and the previously defined VSL of $10 million provide an anchor point for the risk limit and target (Figure 42). At a consequence level of $10 million (i.e. a single fatality), a likelihood equal to or less than 10^{-6} occurrences per year is broadly tolerable. Similarly, at a consequence level of $10 million, a likelihood equal to or greater than 10^{-4} occurrences per year is intolerable. Now considering a neutral attitude towards increasing and decreasing risk, we create the risk limit and target lines. For example, for a lower consequence of $1 million, we would set any likelihood of occurrence greater than or equal to

10^{-3} as intolerable. In other words, for an order of magnitude lower consequence we accept an order of magnitude higher likelihood.

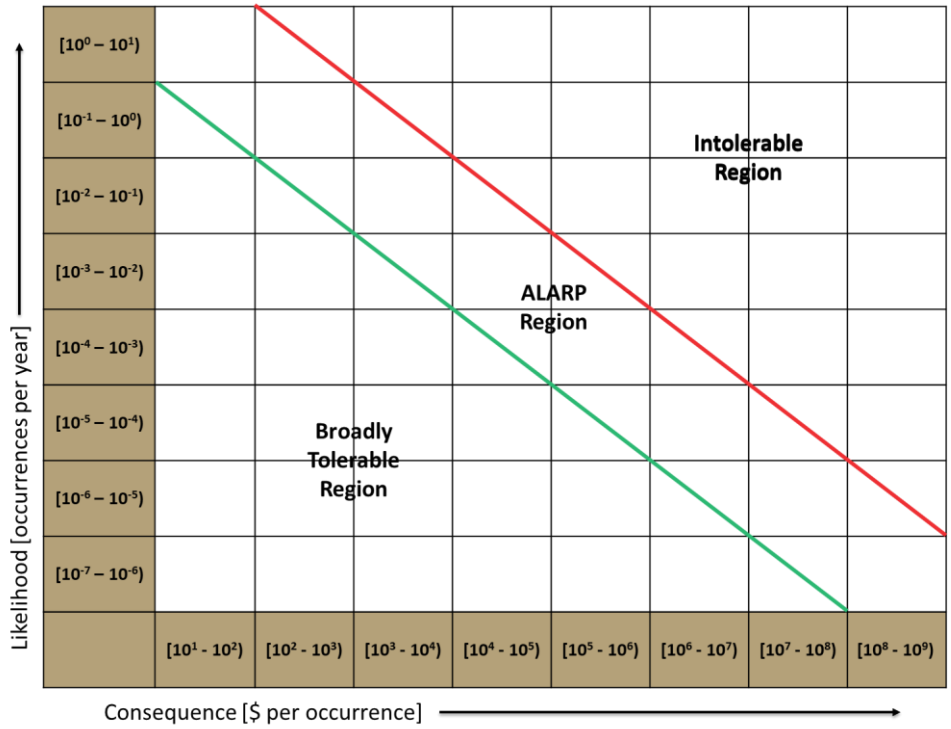

Figure 42. Suggested Risk Matrix for Loss of Life in Physical Asset Management

Risk limits and targets for financial consequences are more company specific than loss of life. A possible approach is to consider a company's annual average historical (or forecasted) net earnings for a length of time equal to the asset management planning horizon. The annual consequence limit can be then set considering a percentage of the average annual net earnings based on the amount the company can absorb given its financial position. A target is somewhat easier to set since a company should always consider a cost-benefit approach when it comes to potential financial losses. As such, we set the target as $10 annual risk exposure in Figure 43.

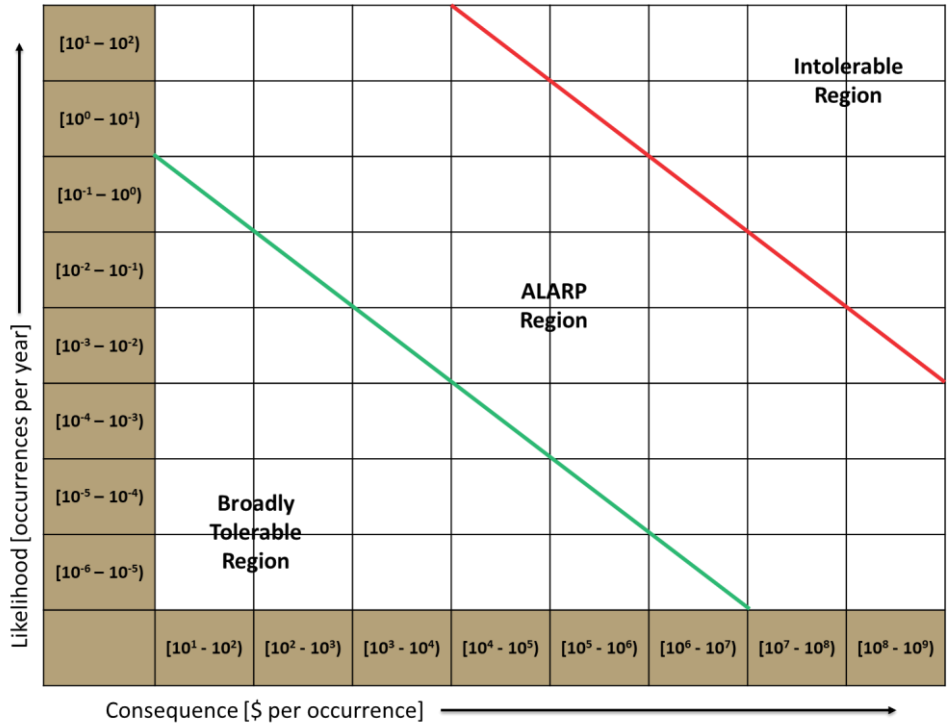

Figure 43. Suggested Risk Matrix for Financial Loss in Physical Asset Management

Risk matrices have been criticized in the literature, with the primary argument being that they fail to prioritize risks and therefore are not effective decision-making tools (Cox, 2008; Wijnia, 2016). Nevertheless, risk matrices have proven to be so effective in risk communication, even with stakeholders with little or no risk management knowledge, that they continue to see widespread use in both academia and industry. In fact, it appears that much of the criticism of risk matrices is rooted in improper application rather than the method itself (Alp, 2006). In this work we take the perspective that risk and risk criteria are nothing more than reference points to inform asset management decisions (Aven, 2011). As such, risk matrices should not be used in a mechanistic decision procedure about the tolerability or intolerability of risk. With this in mind, we augment the risk matrix with additional information about the risk in question, providing a more honest and open picture of the risk, which better supports risk-informed decision-making.

An example risk evaluation dashboard is shown in Figure 44. The top left chart plots the likelihood of an undesired event and associated consequence(s) on a risk matrix along with the 95% prediction intervals for each measure. The top right chart shows the annual risk exposure as the product distribution of the likelihood distribution (bottom left) and consequence distribution (bottom right).

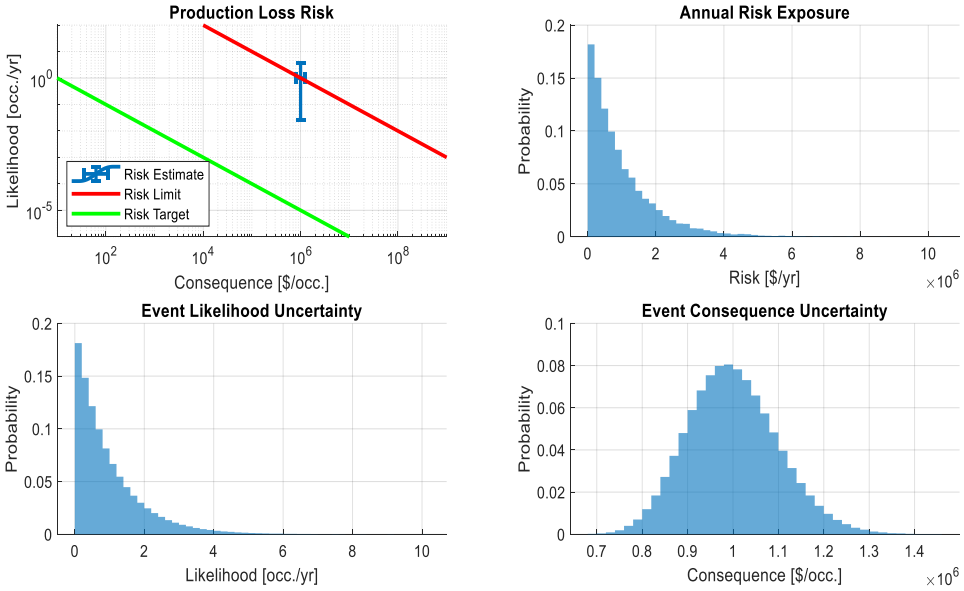

Figure 44. Example Risk Evaluation Dashboard

Representation of the uncertainty ranges as well as distributions for likelihood, consequence and annual risk exposure give the decision-maker a complete picture of the risk. In this way, the decision-maker can use the risk matrix effectively as a visual aid in examining the tolerability of the risk. Evaluation of risk tolerability is not limited to expected values of likelihood and consequence. Instead, the decision-maker may consider the optimistic and pessimistic percentiles and evaluate tolerability based on probability of exceedance of risk limit or target thresholds as defined by the risk matrix.

4.3.1.3 First Decision: Treatment Urgency

Upon completion of Steps 1 and 2 in Figure 1, we reach the first decision point, where a decision-maker must determine the urgency of treatment for the risk in question. If a risk is in the intolerable or ALARP region of the risk matrix, the decision-maker will consider risk treatment options. If the decision-maker has perfect information, then an intolerable risk implies that risk treatment is mandatory, while a risk in the ALARP region is treated if the risk reduction benefits outweigh the treatment costs. Of course, the judgement about whether a risk is intolerable, ALARP or broadly tolerable is often difficult in practice due to the uncertainty in both the likelihood and consequence of a risk. There is a recognition now among stakeholders that risk evaluations must go beyond expected values and take into consideration the uncertainty of the risk estimate (Aven, 2010). As such, we recommend that the decision-maker use the probability of exceedance of the risk limit to determine whether risk treatment is mandatory. Based on the risk matrices defined in Figure 42 and Figure 43,

the annual risk exposure limit for loss of life is $1,000 per year and the limit for financial loss is $1 million per year. The exceedance probability threshold to use is a judgment to be made by the decision-maker that is dependent on his or her aversion to risk. Similarly, the decision-maker may consider the risk treatment in the ALARP region based on the exceedance probability relative to the risk targets as defined by the risk matrix. Once a decision-maker determines whether to proceed with risk treatment, evaluation and prioritization of treatment options is necessary, as will be discussed in the next section.

4.3.2 Risk Treatment

In this section we present a cost-benefit analysis of potential risk treatment options as well as prioritization of the viable options. Cost-benefit analysis (Steps 3 and 4) and the second decision point (see Figure 1) are discussed in sub-section 4.3.2.1. Step 5 in Figure 1, prioritization of viable treatment options using MCDM/A, is discussed in sub-section 4.3.2.3.

4.3.2.1 Cost-Benefit Analysis

Generally, if a risk falls in the ALARP region of the risk matrix (Figure 42 and Figure 43), the decision-maker should perform some form of cost-benefit analysis to determine if a risk treatment option is viable. Whilst treatment of risks in the intolerable region of the risk matrix is considered mandatory, it may be prudent to perform similar cost-benefit analyses, particularly if the risk treatment options are costly. Furthermore, a risk in the broadly tolerable region does not preclude treatment. As discussed in Section 4.3.1, there may be significant uncertainty in a risk analysis. Therefore, a decision-maker may choose to treat a risk by virtue of the precautionary principle, even if the expected values of the likelihood and consequence(s) places the risk in the broadly tolerable region of the risk matrix (Aven, 2011). Considering the discussion above, it would be prudent to perform a cost-benefit analysis of a risk treatment option regardless of the tolerability of the risk being addressed.

For physical asset management, the preferred method of performing cost-benefit analysis is by computing the net present value (NPV) of the treatment option (Hastings, 2015). All costs of the treatment option, including design and commission as well as ongoing running costs must be considered. The risk reduction (dR), calculated as the difference in the expected values of the pre and post-project annual risk exposure ($dR = E(R_{pre}) - E(R_{post})$), can be treated as a cash flow back to the company. Figure 45 illustrates the concept where a capital outlay of $500,000 provides a company with annual risk reductions, treated as positive cash flows, for a 10-year period.

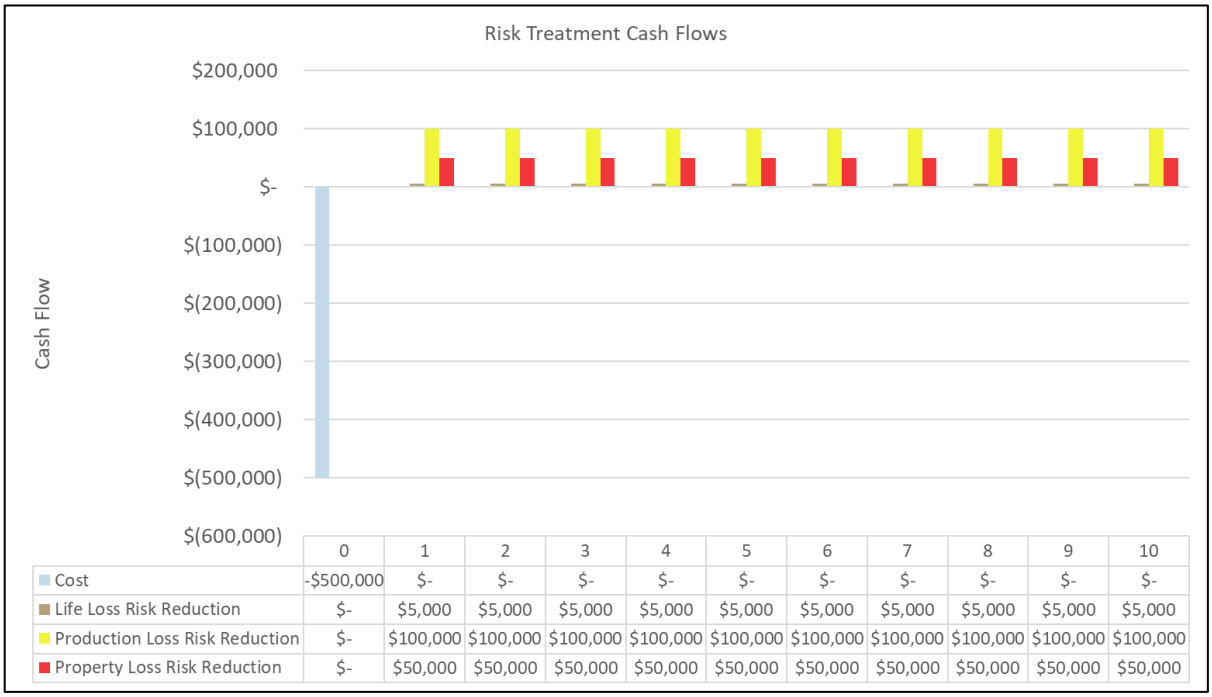

	0	1	2	3	4	5	6	7	8	9	10
Cost	-$500,000	$-	$-	$-	$-	$-	$-	$-	$-	$-	$-
Life Loss Risk Reduction	$-	$5,000	$5,000	$5,000	$5,000	$5,000	$5,000	$5,000	$5,000	$5,000	$5,000
Production Loss Risk Reduction	$-	$100,000	$100,000	$100,000	$100,000	$100,000	$100,000	$100,000	$100,000	$100,000	$100,000
Property Loss Risk Reduction	$-	$50,000	$50,000	$50,000	$50,000	$50,000	$50,000	$50,000	$50,000	$50,000	$50,000

Figure 45. Example of Risk Reductions as Cash Flows

We calculate the NPV as shown by Equation 20 to determine the viability of a risk treatment option. The NPV is the total risk reduction afforded by the treatment minus costs to implement and maintain/run the treatment option. A positive NPV implies that the risk reduction benefit outweighs the cost of the treatment option.

$$\begin{aligned} &NPV \\ &= (Expected\ present\ value\ of\ loss\ of\ life\ risk\ reduction) \\ &+ (Expected\ present\ value\ of\ loss\ of\ production\ risk\ reduction) \\ &+ (Expected\ present\ value\ of\ loss\ of\ property\ risk\ reduction) \\ &- (Expected\ present\ value\ of\ cost\ of\ risk\ treatment\ option). \end{aligned} \tag{20}$$

In the simplest case, one can consider the risk reduction benefit and the risk treatment running costs as constant annual cash flows. In such a scenario, the present values of the cash flows can be calculated using the discounting factor for an annuity as shown in Equation 21 (Fraser, Bernhardt, Jewkes, & Tajima, 2000).

$$NPV = dR_{life} \times \left[\frac{1-(1+r)^{-n}}{r}\right] + dR_{prod} \times \left[\frac{1-(1+r)^{-n}}{r}\right] + dR_{prop} \times \left[\frac{1-(1+r)^{-n}}{r}\right] - C_1 - C_2 \times \left[\frac{1-(1+r)^{-n}}{r}\right], \quad (21)$$

where dR_{life}, dR_{prod} and dR_{prop} represent the annual risk exposure reductions for loss of life, loss of production and loss of property afforded by the risk treatment option in question. C_1 is the initial capital outlay to implement the treatment option, and C_2 is the ongoing running cost of the treatment. The number of periods (n) is based on the duration for which the risk reduction benefit will be received. If for example, a modification is being made to improve the reliability of a critical asset, the remaining useful life of the asset may be considered as the duration of the risk benefit. For a new asset, such as a new safety system in a production facility, the duration may be the useful life of the safety system or the planned life of the production facility (whichever is shorter). If the risk treatment requires periodic re-investment (e.g. maintenance capital) then the duration of the benefit should be equal to the re-investment period, provided it is shorter than the remaining life of the asset. Lastly, r is the appropriate risk-adjusted discount factor. However, discussion on how the discount factor should be defined is beyond the scope of this paper.

4.3.2.2 Second Decision: Treatment Viability

Upon completion of Steps 3 and 4 in Figure 1, we reach the second decision point, where a decision-maker must determine the viability of the treatment option. Strictly speaking, any treatment with an NPV greater than zero is considered viable. However, considering the uncertainty in risk analysis (and even discounted cash flow analysis), a decision-maker must apply his/her judgement about the required NPV for a treatment option to be considered viable. We have indicated an iterative process at this step in Figure 1 as a decision-maker may consider modifications to the treatment option if the NPV does not suggest viability. Once a decision-maker determines whether to proceed with risk treatment, prioritization of treatment options is necessary, as will be discussed in the next section.

4.3.2.3 Prioritization

A decision-maker may be faced with multiple project alternatives to treat a single risk or multiple projects to treat many different risks. It is inevitable that in the asset management context, the number of potential projects will be greater than the operating budget can

accommodate. As a result, there is a need for an objective method of prioritizing projects while taking into consideration decision-maker preferences and multiple project prioritization criteria. In this section we discuss how MCDM/A may be used to prioritize risk treatment options (i.e. projects or alternatives).

We implement a MCDM/A method known as the Technique for Order Preference by Similarity to Ideal Solution (TOPSIS) (Yoon & Hwang, 1995). As the name suggests, the method prioritizes decision alternatives based on the idea that the best solution is one that is the shortest Euclidian distance from the ideal solution and farthest distance from the anti-ideal solution. The only inputs required for the TOPSIS method are weights for each of the decision criteria, and specification about whether a decision criterion must be maximized or minimized for the ideal solution. In the TOPSIS method, the weight for each decision criterion is meant to be reflective of the decision-maker's preferences (e.g. valuing life risk reduction more than property risk reduction). The Analytic Hierarchy Process (AHP) is a natural fit for determination of such weights. AHP is a MCDM/A methodology that has been widely used in both academia and industry (Saaty, 1980). The method breaks the objective (selection of the best alternative) into decision criteria and sub-criteria. The decision-maker performs pairwise comparison of the decision criteria, followed by pairwise comparison of the sub-criteria. The decision-maker expresses his/her preference towards a certain criteria using Saaty's numeric scale shown in Table 1 (Saaty, 1980). The overall weight of each decision criterion is then calculated.

Table 12. AHP Numeric Scale with Linguistic Interpretation

Intensity of Importance	Definition	Explanation
1	Equal importance	Two factors contribute equally to the objective.
3	Somewhat more important	Experience and judgement slightly favour one over the other.
5	Much more important	Experience and judgement strongly favour one over the other.
7	Very much more important	Experience and judgement very strongly favour one over the other. Its importance is demonstrated in practice.

Intensity of Importance	Definition	Explanation
9	Absolutely more important	The evidence favouring one over the other is of the highest possible validity.
2,4,6,8	Intermediate values	When compromise is needed.

Both AHP and TOPSIS methods have been widely used in the academic literature, and in the risk and asset management contexts (Kabir, Sadiq, & Tesfamariam, 2014; de Almeida, Alencar, Garcez, & Ferreira, 2017). Many researchers have used a hybrid approach to MCDM/A by combining AHP and TOPSIS in the way we do in this work (Ak & Gul, 2019; Samvedi, Jain, & Chan, 2013; Prakash & Barua, 2015; Zyoud, Kaufmann, Shaheen, Samhan, & Fuchs-Hanusch, 2016). In the remainder of this section we provide a brief review of the AHP and TOPSIS methods in the context of application in this work. For full details of the methodology, we refer the reader to the many MCDM/A textbooks that discuss these popular methods (Ishizaka & Nemery, 2013).

Suggested decision criteria are shown in Figure 46, consisting of three risk criteria and one cost criteria. The three risk criteria are each evaluated using three sub-criteria: cumulative risk reduction (i.e. the present value of the annual risk exposure reduction), reduction in the probability of exceeding the risk limit, and reduction in the probability of exceeding the risk target. Decision-maker preferences are determined first for the criteria by performing a pairwise comparison and eliciting how much more importance the decision-maker places on one criterion over another. Similarly, pairwise comparison is performed for each group of sub-criteria. The AHP calculation is then performed by constructing the comparison matrices for the criteria and sub-criteria, calculating criteria weights, calculating the sub-criteria weights, and finally the overall weighting of each sub-criteria (Saaty & Vargas, 2012). We have provided the comparison matrices used in this work in the supplementary material (Chapter 7). Note that the importance should be evaluated conditional on the risk treatment already determined to be viable from a cost-benefit perspective. The objective now is prioritization of viable alternatives.

Table 13 provides a summary of the prioritization criteria applied in the TOPSIS method, along with overall weights derived from the AHP pairwise comparison described previously. Cumulative risk reduction measures are calculated as the present value of the annual risk reduction: $PV = dR \times \left[\frac{1-(1+r)^{-n}}{r}\right]$. The present value of costs associated with a risk

treatment is similarly calculated. To capture the uncertainty in the risk analysis in our decision-making we consider the change in exceedance probability of the annual risk exposure compared to the risk limit and target (see Section 4.3.1). Table 13 also indicates whether we want to maximize or minimize a measure for the ideal solution, and vice-versa for the anti-ideal solution. The TOPSIS method may then be applied to prioritize a list of alternatives using objective measures derived from quantitative risk analysis. By deriving the weights through the AHP method described previously, we ensure that the prioritization will be consistent with decision-maker preferences.

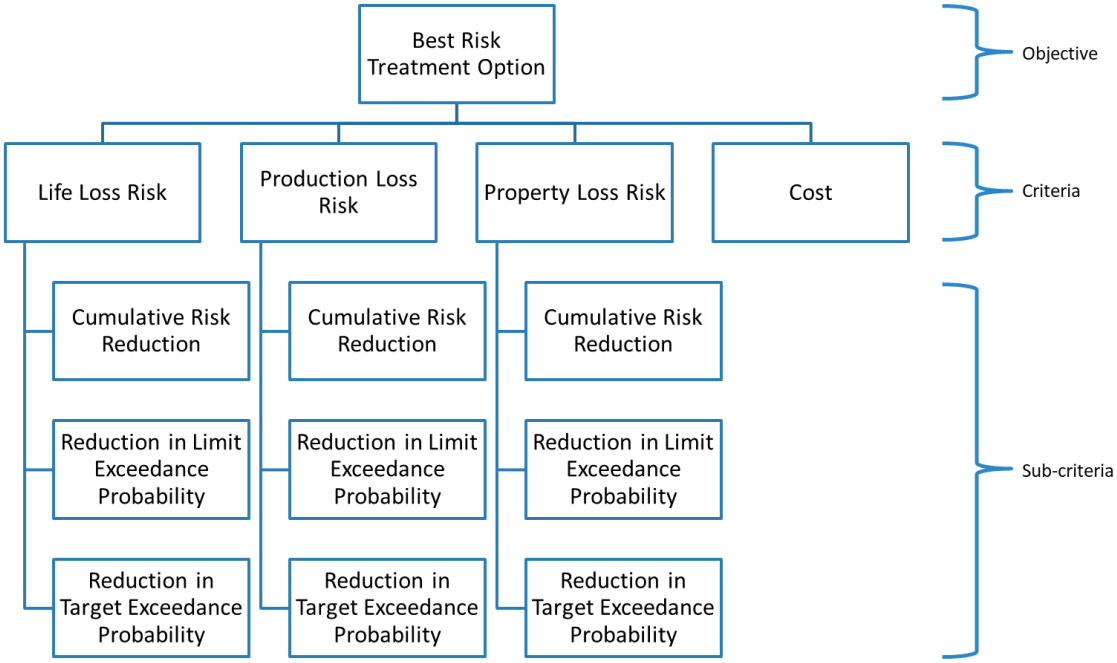

Figure 46. AHP Decision Structure

Table 13. TOPSIS Prioritization Criteria

Criteria	Sub-Criteria	Measure	Ideal Solution	Weight
Life Loss Risk	Cumulative Risk Reduction	$PV(\Delta R_{life})$	Maximize	37.3%
	Reduction in Limit Exceedance Probability	$p(R_{life}^{pre} > 1000) - p(R_{life}^{post} > 1000)$	Maximize	15.7%
	Reduction in Target Exceedance Probability	$p(R_{life}^{pre} > 10) - p(R_{life}^{post} > 10)$	Maximize	3.3%

Criteria	Sub-Criteria	Measure	Ideal Solution	Weight
Production Loss Risk	Cumulative Risk Reduction	$PV(\Delta R_{prod})$	Maximize	8.0%
	Reduction in Limit Exceedance Probability	$p(R_{prod}^{pre} > 1mil) - p(R_{prod}^{post} > 1mil)$	Maximize	1.7%
	Reduction in Target Exceedance Probability	$p(R_{prod}^{pre} > 10) - p(R_{prod}^{post} > 10)$	Maximize	0.7%
Property Loss Risk	Cumulative Risk Reduction	$PV(\Delta R_{prop})$	Maximize	8.1%
	Reduction in Limit Exceedance Probability	$p(R_{prop}^{pre} > 1mil) - p(R_{prop}^{post} > 1mil)$	Maximize	1.5%
	Reduction in Target Exceedance Probability	$p(R_{prop}^{pre} > 10) - p(R_{prop}^{post} > 10)$	Maximize	0.7%
Cost	n/a	$PV(Cost)$	Minimize	23%

A typical TOPSIS decision matrix may be constructed as shown in Table 14, where the performance measure of the i[th] alternative against the j[th] criterion is given by x_{ij}. Performance measures are calculated as specified in Table 13.

Table 14. Example TOPSIS Decision Matrix

Decision Matrix	Criterion 1	Criterion 2	Criterion 3
Alternative 1	x_{11}	x_{12}	x_{13}
Alternative 2	x_{21}	x_{22}	x_{23}
Alternative 3	x_{31}	x_{32}	x_{33}

The performance measures for the decision criteria vary in units and scale. A such we must first normalize the decision matrix using Equation 22, where a is the number of alternatives (Ishizaka & Nemery, 2013):

$$r_{ij} = \frac{x_{ij}}{\sqrt{\sum_{i=1}^{a} x_{ij}^2}}. \tag{22}$$

A weighted normalized decision matrix is calculated by multiplying each normalized measure with the weight of the criteria ($v_{ij} = w_j \times r_{ij}$) as calculated using the AHP method and given in Table 13. For each criterion we define the ideal as $v_j^+ = max_j(v_{1j}, \dots, v_{aj})$ and the anti-ideal as $v_j^- = min_j(v_{1j}, \dots, v_{aj})$ if the criterion is to be maximized. Conversely, if the

criterion is to be minimized, the ideal and anti-ideal are defined as $v_j^+ = min_j(v_{1j}, \dots, v_{aj})$ and $v_j^- = max_j(v_{1j}, \dots, v_{aj})$. The distance of each alternative from the ideal (d_i^+) and anti-ideal (d_i^-) is calculated using Equation 23 (Ishizaka & Nemery, 2013).

$$d_i^+ = \sqrt{\sum_{j=1}^{c} (v_j^+ - v_{ij})^2} \; and \; d_i^- = \sqrt{\sum_{j=1}^{c} (v_j^- - v_{ij})^2}. \qquad (23)$$

Finally, the closeness coefficient of each alternative is calculated as $C_i = d_i^-/(d_i^+ + d_i^-)$. The closeness coefficient approaches one the closer the alternative is to the ideal solution, and zero the closer it is to the anti-ideal. The closeness coefficient is then used to prioritize risk treatment alternatives (Ishizaka & Nemery, 2013).

4.4 Numerical Example

In this section we illustrate the decision-making framework described in Section 4.3 using a numerical example. In this case we consider a natural gas compression facility for which we must prioritize investments for risk treatment of critical assets. Degradation of high-pressure gas containing pipework within the facility has led to concerns of potential gas leaks in the facility, which has the potential to cause loss of life, property damage and result in significant production interruption. Furthermore, the aging fleet of compressors are experiencing major failures annually (sometimes more) resulting in production interruption. The decision-making process begins by first obtaining a baseline measure of the risk in the facility using quantitative risk analysis. The results are summarized in sub-section 4.4.1.1. Potential risk treatment options and their effect on the facility risk exposure is discussed in sub-section 4.4.1.2. We do not discuss the quantification approach in detail as risk analysis methods are not the topic of this paper. The focus is on how the results of a quantitative risk analysis may be used to support decision-making in the physical asset management context, to which end we provide a detailed discussion of risk treatment prioritization in sub-section 4.4.1.3.

4.4.1.1 Baseline Results

Figure 47 through Figure 49 show the risk results for a potential gas leak event. Loss of life (Figure 47) exceeds the $1000 risk limit with a probability of exceedance of 80%. With such a high exceedance probability, the decision-maker may consider risk treatment mandatory. Production loss risk (Figure 48) and property loss risk (Figure 49) are in the ALARP region of the risk matrix, meaning risk treatment options will be subject to cost-benefit consideration. Figure 50 and Figure 51 show the production loss and property loss risk associated with potential compressor failure events. Production loss (Figure 50) risk exceeds

the risk limit with a probability of exceedance of 36.5%. Given the (relatively) low exceedance probability, the decision-maker may require cost-benefit analysis in this case. Property loss risk (Figure 51) is in the ALARP region. As such, treatment options will require cost-benefit analysis. Risk treatment options are discussed in the next sub-section.

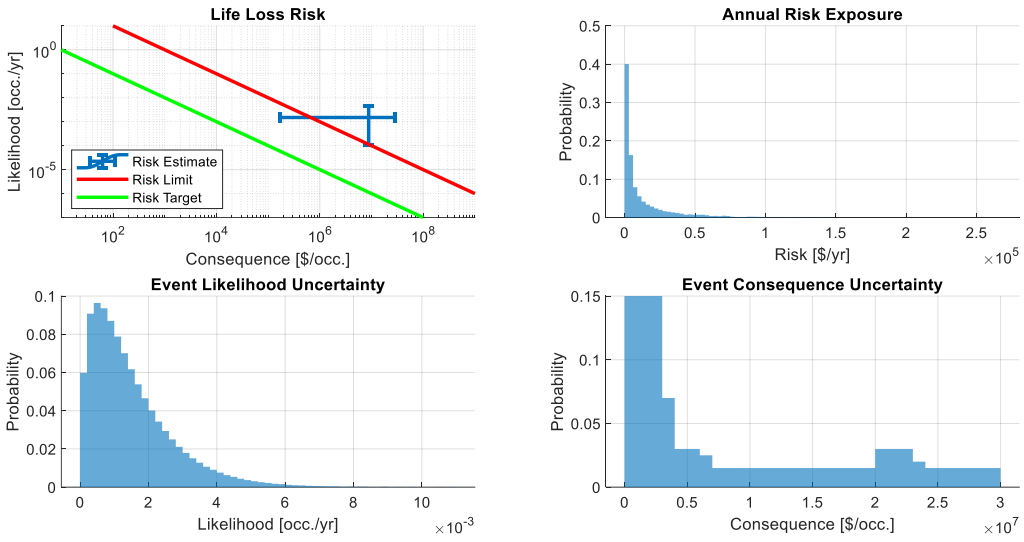

Figure 47. Gas Leak - Loss of Life - Baseline Risk Results

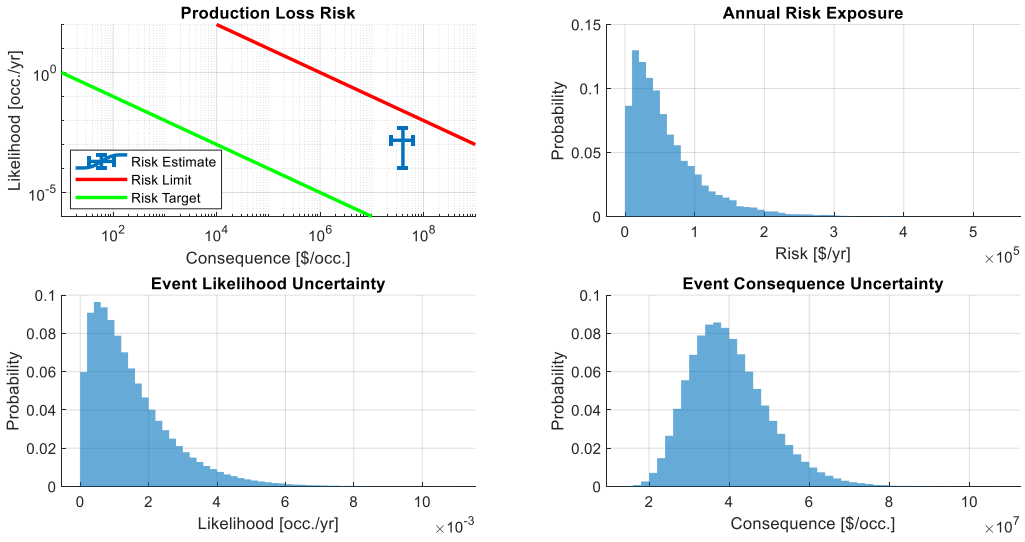

Figure 48. Gas Leak - Loss of Production - Baseline Risk Results

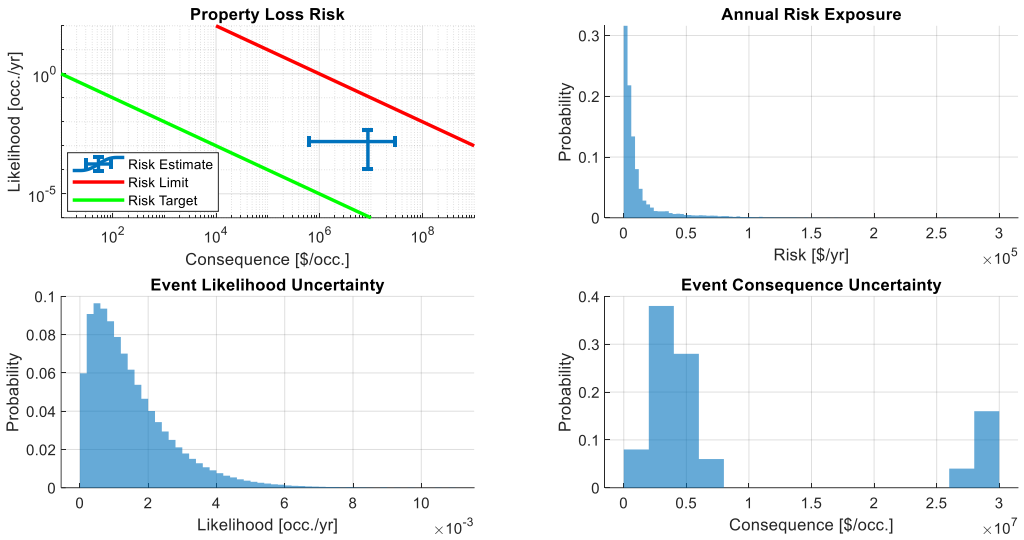

Figure 49. Gas Leak - Loss of Property - Baseline Risk Results

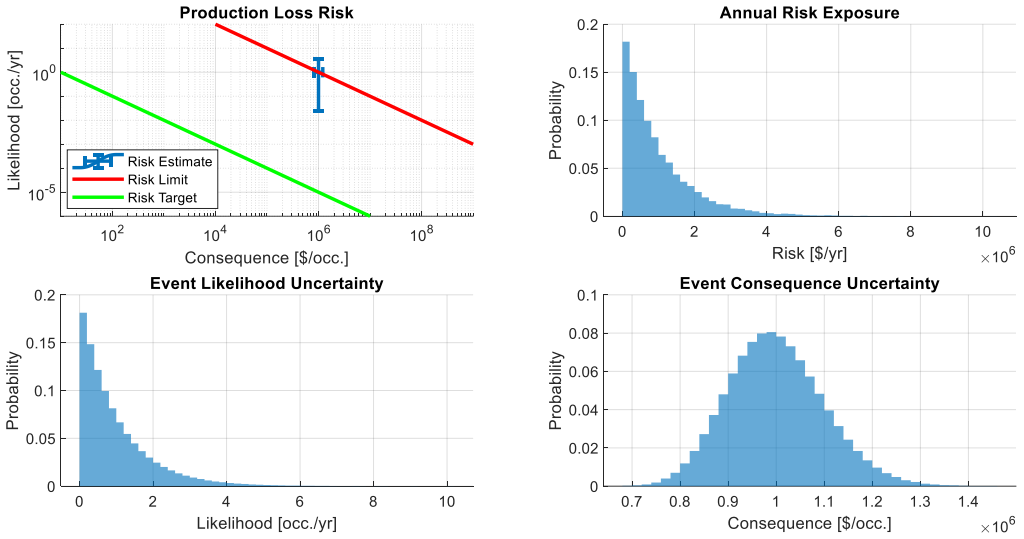

Figure 50. Compressor Failure - Loss of Production - Baseline Risk Results

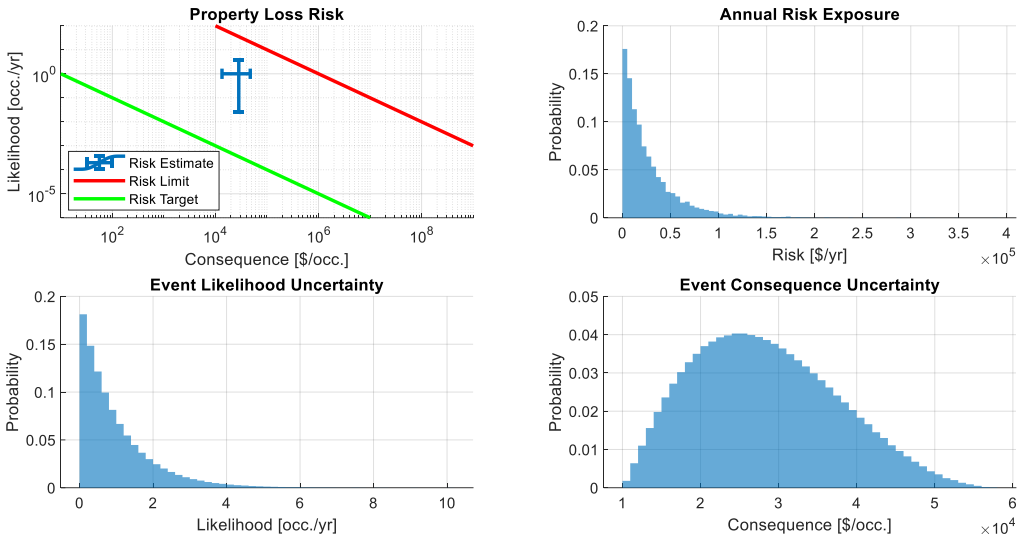

Figure 51. Compressor Failure - Loss of Property - Baseline Risk Results

4.4.1.2 Risk Treatments

Potential risk treatments for gas leak events and compressor failures are summarized in Table 15, along with the present value of the cost of the options. The risk reduction benefits of each option are summarized in Table 16. Figure 52 is a graphical representation of the risk reduction benefit with respect to loss of life afforded by treatment option 1 (automation upgrades). Risk results pre- and post-treatment are plotted on the same charts to demonstrate the benefit. Automation upgrades essentially reduces the occupancy level within the facility, resulting in a reduction in the consequence of a gas leak event. The likelihood is not affected. We can then obtain the annual risk reduction by comparing the difference in the expected values of the annual risk exposure. The present value of the risk reduction can be calculated as described in Section 4.3.2.1. Results in Table 15 and Table 16 for the other treatment options were similarly obtained.

Strictly speaking, cost-benefit analysis would eliminate treatment options 2 and 5 due to a negative NPV. Option 5 is eliminated because option 4 reduces the production loss risk due to compressor failure to below the risk limit. However, since treatment option 1 does not reduce the loss of life risk below the limit (see Figure 52), we consider option 2 for prioritization, discussed in the next section. We evaluate the risk reduction afforded by option 2 under the assumption that option 1 has been implemented.

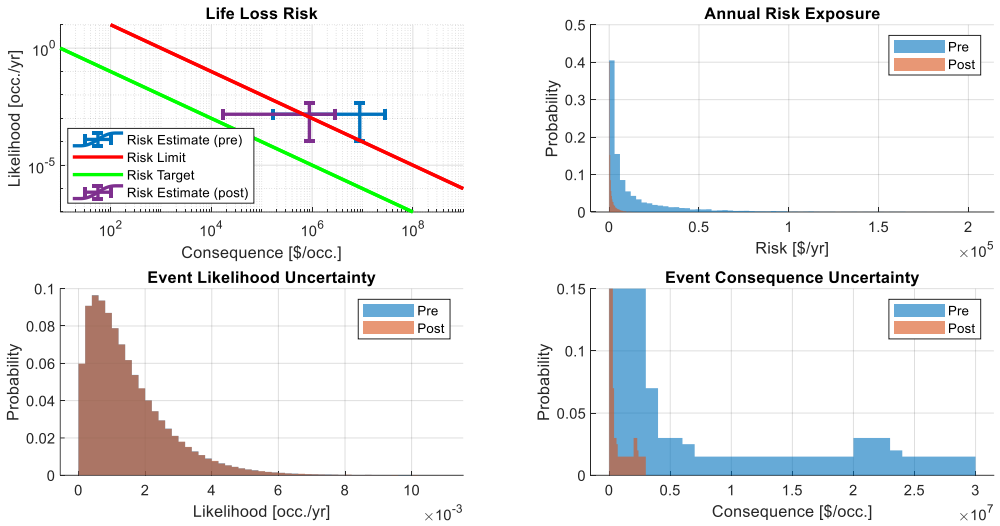

Figure 52. Loss of Life Risk Reduction – Automation Upgrades (Treatment No. 1)

Table 15. Risk Treatment Options

Treatment No.	Name	Description	Risk Addressed	$PV(Cost)$
1	Automation Upgrades	Automation for the facility will reduce the amount of time personnel need to spend within the facility.	Loss of Life due to Gas Leak	$400,000
2	Pipework Replacements	Replacement of aging pipework within the facility.	Loss of Life/ Production/ Property due to Gas Leak	$10,000,000
3	Fire Suppression System	Installation of a fire suppression system that reduces the potential for extensive damage and extended production outage in the event of a gas leak.	Loss of Production/ Property due to Gas Leak	$350,000
4	Compressor Improvements	Reliability improvements that reduce the number of unexpected failures of compressor units.	Loss of Production/ Property due to Compressor Failure	$6,000,000
5	Redundant Compressor Unit	A standby compressor unit that can be brought online in the event of a compressor failure.	Loss of Production/ Property due to Compressor Failure	$30,000,000

Table 16. Risk Treatment Benefits Summary

No.	Life Loss		
	$PV(\Delta R_{life})$	$\Delta p(Exceed\ Limit)$	$\Delta p(Exceed\ Target)$
1	$357,750	0.46	0.025
2	$35,775	0.33	0.025
3	0	0	0
4	0	0	0
5	0	0	0
No.	**Production Loss**		
	$PV(\Delta R_{prod})$	$\Delta p(Exceed\ Limit)$	$\Delta p(Exceed\ Target)$
1	0	0	0
2	$743,300	0	0
3	$291,370	0	0
4	$5,888,070	0.36	0.011
5	$12,388,350	0.36	0
No.	**Property Loss**		
	$PV(\Delta R_{prop})$	$\Delta p(Exceed\ Limit)$	$\Delta p(Exceed\ Target)$
1	0	0	0
2	$162,600	0	0
3	$67,880	0	0
4	$166,830	0	0
5	0	0	0

4.4.1.3 Prioritization

Prioritization of risk treatment options 1 through 4 (see Table 15) is done using the TOPSIS method and with weights derived using AHP as described in Section 4.3.2.3. The TOPSIS decision matrix is developed using the values for the first four alternatives in Table 16. The weights used for each criterion are summarized in Table 13. We do not review the details of the TOPSIS calculation in this paper. However, the TOPSIS decision matrix, normalized decision matrix, and treatment option closeness coefficients are provided in the supplementary material (Chapter 7). Final rankings of the treatment options are as follows:

1. Option 1 – Automation Upgrades
2. Option 3 – Fire Suppression System
3. Option 4 – Compressor Improvements
4. Option 2 – Pipework Replacements

The result of the prioritization exercise appears to be logically consistent. Automation upgrades provide the largest reduction in loss of life risk, as well as reducing the risk limit exceedance probability with respect to loss of life. Both measures are heavily weighted according to the decision-maker preferences assumed in this work. Options 3 and 4 improve

production and property loss risk. Option 3 is ranked higher due to the lower cost, which is more heavily weighted than production and property loss risk reduction. Option 2 is ranked lowest, which is expected considering its high cost and relatively little risk reduction. That being said, since the project reduces the probability of exceeding the loss of life risk limit, the decision-maker could consider this project by virtue of the precautionary principle.

4.5 Conclusions

In this work we have presented a method for risk-informed decision-making in the physical asset management context. The methodology uses quantitative risk measures for loss of life, loss of production and loss of property. A risk matrix is used to classify risk as intolerable, ALARP or broadly tolerable. Risks in the intolerable and ALARP region require risk treatment, and risk treatment options are generated. Risk reduction benefit of the treatment options is quantified, and cost-benefit analysis is performed using discounted cashflow analysis. Viable projects, as determined by positive NPV calculated in the cost-benefit analysis, are then prioritized using a combination of the AHP and TOPSIS MCDM/A methods. AHP is used to derive weights for prioritization criteria based on decision-maker preferences. The weights, along with prioritization criteria for risk reduction, tolerance criteria and project cost, are used to prioritize projects using the TOPSIS method. The usefulness of the methodology for improved decision-making is illustrated using a numerical example. Decision-making is improved by the full transparency of the methodology. Risk and associated uncertainty of the likelihood and consequence(s) are clearly demonstrated visually through a risk results dashboard. Furthermore, the utilization of AHP and TOPSIS provide a direct “line of sight” between decision-maker preferences and prioritization measures. Application of the proposed methodology will promote transparent risk-informed decision-making in the physical asset management context.

5 CONCLUSIONS AND FUTURE WORK

5.1 Contributions

The primary objective of this thesis was to develop a framework and computer models to facilitate risk-informed and data-driven management of physical assets for natural gas storage and transmission assets. The main contributions of the thesis are the methodologies and computer models discussed in three manuscripts. Each manuscript addresses significant gaps in the asset management literature by providing an effective means of incorporating tacit knowledge in asset reliability analysis, using simulation to facilitate system-level risk analysis of gas storage and transmission assets, and presenting a unified framework for risk-informed decision-making in the asset management context.

a) The first paper presented a novel practical approach that can be used in reliability assessment and risk analysis. A Bayesian framework was implemented to cohesively integrate objective data with expert opinion and tacit knowledge with the aim toward deriving life distributions for physical assets. As has been illustrated, when dealing with limited, incomplete and missing data, classical methods such as MLE produce inadequate results with a high level of uncertainty. This uncertainty, coupled with the significant capital or operating expenditures at stake, essentially prohibits the decision-maker from properly deciding on a course of action. The methodology presented provides an elegant and powerful way of addressing uncertainty by allowing the analyst to take into consideration all types of available information.

b) The second paper presented a quantitative risk analysis model to study operational reliability risk of an underground gas storage facility. The model combines a thermo-hydraulic performance model for a gas storage facility consisting of a gathering system, compression system and transmission system with a Monte Carlo simulation of potential disruption events. The proposed model is highly configurable and can be used to quantitatively assess operational reliability risk for natural gas storage and transmission assets. This model can be used to analyse a multitude of potential events that can affect an underground gas storage facility. The integrated physics model means the user does not have to explicitly account for changes in system performance resulting from disruption events. As such, many combinations of asset configurations (performance parameters), system states (inventory levels, asset availability) and disruption events (concurrent events, event timings) can be analysed within a single modelling framework.

c) In the third paper we presented a method for risk-informed decision-making in the physical asset management context whereby risk evaluation and cost-benefit analysis are considered in a common framework. The methodology uses quantitative risk measures to prioritize projects based on a combination of risk tolerance criteria, cost-benefit analysis and uncertainty reduction metrics. Decision-making is improved by the full transparency of the methodology. Risk and associated uncertainty of the likelihood and consequence(s) are clearly demonstrated visually through a risk results dashboard. Furthermore, the utilization of AHP and TOPSIS provide a direct "line of sight" between decision-maker preferences and prioritization measures. Application of the proposed methodology will promote transparent risk-informed decision-making in the physical asset management context.

5.2 Future Work

The proposed future work is focused on further development as well as broader applications of the methodologies presented in this thesis. As such, the following potential extensions are proposed.

1. While the methodology in the first paper focused on incorporating expert opinion for the construction of priors, the methodology is flexible and can be easily extended to other sources of information. Such information can include accelerated life tests, analogous data from similar assets, physics of failure computer simulations, etc. AHP

may be used as a means of weighting and aggregating the information from such sources.

2. The methodology in the first paper focused on using expert knowledge to derive a Weibull life distribution for a physical asset, and one that experiences wear out failures. Expansion of the methodology to other distributions used to model time-to-failure such as exponential and log-normal would provide greater modelling flexibility. Furthermore, an expert elicitation methodology for the modelling of complex repairable systems, commonly done using a non-homogeneous Poisson process, would broaden the applicability of the methodology.
3. Elicitation of expert opinion to support Bayesian statistical inference is an approach taken in other disciplines as well, including finance and medicine. The first paper presents an expert selection and opinion aggregation method using AHP as a framework. This approach may be applied in other disciplines as well to support the construction of prior distributions using expert opinion.
4. The methodology in the second paper analyses operational reliability risk for an underground gas storage facility. The physics-based model implicitly considers changes in the performance of the system due to asset failures. Currently, the reliability model considers each asset as either available or unavailable. Considering intermediate states, such as asset level performance degradations, would be a useful expansion of the methodology.
5. As was discussed in the second paper, integration of physics-based performance models with asset system reliability models is seldom done in literature. Extension of the methodology to other aspects of natural gas infrastructure, and even other industries will contribute significantly to the body of knowledge in risk and asset management literature. A similar physics-based approach can be taken for gas, water and electric utilities. Oil and other chemical production supply chains may also benefit from physics-based risk and reliability modelling.
6. The specific model for an underground gas storage facility presented in the second paper has broader applicability beyond physical asset management. Gas producers and consumers are regularly balancing gas supply with demand. The output of the model presented in the second paper can be used in a larger decision framework to support consideration of reliability of supply from storage facilities. For example, electric utilities relying on natural gas powerplants may consider reliability of gas supply from storage in decision-making for natural gas futures contracts.

7. The third paper presented a transparent methodology that utilizes risk measures and decision-maker preferences to prioritize asset investment projects. Augmenting the decision process with a multi-objective optimization procedure would be a valuable extension of the methodology. The challenge will be to retain transparency in the optimization step of the decision process.
8. The problem of multi-criteria decision-making considering risk and uncertainty is not limited to the discipline of physical asset management. Communication of risk and uncertainty and factoring that into the decision process are important for environmental management, project management, process safety management and enterprise risk management to name a few. Application of the methodology presented in the third paper to such fields is not only possible but would contribute greatly towards improving decision-making.

6 REFERENCES

Ak, M. F., & Gul, M. (2019). AHP-TOPSIS integration extended with Pythagorean fuzzy sets for information security risk analysis. *Complex & Intelligent Systems, Vol. 5, No. 2*, 113-126.

Alp, E. (2006). Risk Matrices - The Good, the Bad, and the Ugly. *Air & Waste Management Association 2006 Annual Conference.* New Orleans, LA.

Aouam, T., Rardin, R., & Abrache, J. (2010). Robust strategies for natural gas procurement. *European Journal of Operational Research*, 151-158.

Aven, T. (2010). *Misconceptions of Risk.* Chichester, West Sussex, United Kingdom: John Wiley & Sons, Ltd.

Aven, T. (2011). *Quantitative Risk Assessment - The Scientific Platform.* New York, NY: Cambridge University Press.

Bauckhage, C. (2013). *Computing the Kullback-Leibler Divergence between two Weibull Distributions.* Cornell University.

Bedford, T., & Cooke, R. (2001). *Probabilistic Risk Analysis: Foundations and Methods.* Cambridge: Cambridge University Press.

Bedford, T., Quigley, J., & Walls, L. (2006). Expert Elicitation for Reliable System Design. *Statistical Science, Vol. 21, No. 4*, 428-450.

Bentley, J. (1999). *Introduction to Reliability and Quality Engineering 2nd Edition.* Harlow, England: Pearson Education Limited.

Bharadwaj, U. R., Silberschmidt, V. V., & Wintle, J. B. (2012). A risk based approach to asset integrity management. *Journal of Quality in Maintenance Engineering 18*, 417-431.

Brigham Young University Thermophysical Properties Laboratory. (2018). *Home Page - DIPPR801*. Retrieved 2018, from https://dippr.aiche.org/

Cagno, E., Caron, F., Mancini, M., & Ruggeri, F. (2000). Using AHP in determining the prior distributions on gas pipeline failures in a robust Bayesian approach. *Reliability Engineering & System Safety 67*, 275-284.

Cengel, Y. A., & Boles, M. A. (2006). *Thermodynamics An Engineering Approach.* New York, NY: McGraw Hill.

Chib, S., & Greenberg, E. (1995). Understanding the Metropolis-Hastings Algorithm. *American Statistician* , 327-335.

Coolen, F., Mertens, P., & Newby, M. (1990). *A Bayes-competing risk model for the use of expert judgement in reliability estimation.* Eindhoven: Technische Universiteit Eindhoven.

Cox, L. A. (2008). What's Wrong with Risk Matrices? *Risk Analysis, Vol. 28, No. 2*, 497-512.

CSChE. (2004). *Risk Assessment - Recommended Practices for Municipalities and Industry.* Ottawa: Canadian Society for Chemical Engineering.

de Almeida, A. T., Alencar, M. H., Garcez, T. V., & Ferreira, R. J. (2017). A systematic literature review of multicriteria and multi-objective models applied in risk management. *IMA Journal of Management Mathematics 28*, 153-184.

de Almeida, A. T., Cavalcante, C. A., Alencar, M. H., Ferreira, R. J., de Almeida-Filho, A. T., & Garcez, T. V. (2015). *Multicriteria and Multiobjective Models for Risk, Reliability and Maintenance Decision Analysis.* New York: Springer.

Duben, A., & Ricks, J. (2015). The Application of the Analytic Hierarchy Process in Sales Personnel Recruitment. *Proceedings of the 1992 Academy of Marketing Science Annual Conference* (pp. 417-421). Springer, Cham.

Emura, T., & Shiu, S.-K. (2014). *Estimation and model selection for left-trucated and right censored lifetime data with application to electic power transformers analysis.* Taiwan: Graduate Institute of Statistics, National Central University.

EPA. (2015). *Regulatory Impact Analysis of the Final Revisions to the National Ambient Air Quality Standards for Ground-Level Ozone.* Research Triangle Park, NC: Environmental Protection Agency.

Evans, J. (1989). *Bias in human reasoning: Causes and consequences.* Hillsdale, NJ: Erlbaum Associates, Inc.

Falk, M., Husler, J., & Reiss, R. (2011). *Laws of Small Numbers: Extremes and Rare Events 3rd Edition.* Berlin: Springer Basel.

Fodstad, M., Midthun, K. T., & Tomasgard, A. (2015). Adding flexibility in a natural gas transportation network using interruptible transportation services. *European Journal of Operational Research*, 647-657.

Fraser, N. M., Bernhardt, I., Jewkes, E. M., & Tajima, M. (2000). *Engineering Economics in Canada, 2nd Edition.* Toronto, ON, Canada: Prentice-Hall Canada, Inc.

Gelman, A., & Rubin, D. (1992). Inference from iterative simulation using multiple sequences. *Statistical science*, 457-472.

GFMAM. (2014). *The Asset Management Landscape, 2nd Edition.* Zurich: Global Forum On Maintenance & Asset Management.

Guo, B., & Ghalambor, A. (2005). *Natural Gas Engineering Handbook.* Houston, TX: Gulf Publishing Company.

Gustavsson, M., & Shahriari, M. L. (2010). Evaluating EML Modeling Tools for Insurance Purposes: A Case Study. *International Journal of Chemical Engineering*.

Gutierrez-Pulido, H., Aguirre-Torres, V., & Christen, J. A. (2005). A Practical Method for Obtaining Prior Distributions in Reliability. *IEEE Transactions on Reliability, Vol. 54, No. 2*, 262-269.

Hamada, M. S., Wilson, A. G., Reese, C. S., & Martz, H. F. (2008). *Bayesian Reliability.* New York, NY: Springer.

Han, Z., & Weng, W. (2010). An integrated quantitative risk analysis method for natural gas pipeline network. *Journal of Loss Prevention*, 428-436.

Hastings, N. A. (2015). *Physical Asset Management 2nd Edition.* New York, NY: Springler International Publishing.

Hong, Y., Meeker, W. Q., & McCalley, J. D. (2009). Prediction of remaining life of power transformers based on left truncated and right censored lifetime data. *Annals of Applied Statistics, Vol. 3, No. 2*, 857-879.

IAM. (2015). *Asset Management - an anatomy Version 3.* Bristol, UK: The Institute of Asset Management.

IEA. (2018). *Natural Gas Information.* Paris: International Energy Agency Publications.

InQvis, Inc. (2011). *Overview of the Natural Gas Industry.* Toronto: Enbridge Gas Distribution, Inc.

Ishizaka, A., & Nemery, P. (2013). *Multi-Criteria Decision Analysis Methods and Software.* Chichester, West Sussex, UK: John Wiley & Sons Ltd.

ISO. (2014). *ISO 55000 - Asset Management.* Geneva: International Standards Organization.

ISO. (2018). *ISO 31000 - Risk Management 2nd Edition.* Vernier, Geneva: International Standards Organization.

Jardine, A. K., & Tsang, A. H. (2013). *Maintenance, Replacement, and Reliability Theory and Applications 2nd Edition.* Boca Raton, FL: CRC Press.

Johnson, S., Tomlinson, G., Hawker, G., Granton, J., & Feldman, B. (2010). Methods to elicit beliefs for Bayesian priors: a systematic review. *Journal of Clinical Epidemiology, Vol 63*, 355-369.

Kabir, G., Sadiq, R., & Tesfamariam, S. (2014). A review of multi-criteria decision-making methods for infrastructure management. *Structure and Infrastructure Engineering, Vol. 10, No. 9*, 1176-1210.

Kaplan, S. (1997). The Words of Risk Analysis. *Risk Analysis, Vol. 17, No. 4*, 407-417.

Kaplan, S., & Garrick, B. J. (1981). On The Quantitative Definition of Risk. *Risk Analysis, Vol. 1, No. 1*, 11-27.

Knox, S. W. (2018). *Machine Learning: a Concise Introduction.* Hoboken, NJ: John Wiley & Sons, Inc.

Komljenovic, D., Gaha, M., Abdul-Nour, G., Langheit, C., & Bourgeois, M. (2016). Risks of extreme and rare events in Asset Management. *Safety Science 88*, 129-145.

Kundu, D., & Mitra, D. (2016). Bayesian inference of Weibull distribution based on left truncated and right censored data. *Computational Statistics and Data Analysis 99*, 38-50.

Lad, B. K., & Kulkarni, M. S. (2010). A parameter estimation method for machine tool reliability analysis using expert judgement. *International Journal of Data Analysis Techniques and Strategies, Vol. 2, No. 2*, 155-169.

Lambert, B. (2018). *A Student's Guide to Bayesian Statistics.* Thousand Oaks, CA: SAGE Publications, Inc.

Leimeister, M., & Kolios, A. (2018). A review of reliability-based methods for risk analysis and their application in the offshore wind industry. *Renewable and Sustainable Energy Reviews 91*, 1065-1076.

Li, M., & Meeker, W. Q. (2014). Application of Bayesian Methods in Reliability Data Analyses. *Journal of Quality Technology, Vol. 46, No. 1*, 1-23.

Lindhe, A., Rosen, L., Norberg, T., Rostum, J., & Pettersson, T. J. (2013). Uncertainty modelling in multi-criteria analysis of water safety measures. *Environment Systems and Decisions 33*, 195-208.

Louit, D., Pascual, R., & Jardine, A. (2009). A practical procedure for the selection of time-to-failure models based on the assessment of trends in maintenance data. *Reliability Engineering and System Safety, 94*, 1618-1628.

Lynden-Bell, D. (1971). A method of allowing for known observational selection in small samples applied to 3CR quasars. *Monthly Notices of the Royal Astronomical Society 155*, 95-118.

March, J., & Shapira, Z. (1987). Managerial perspectives on risk and risk taking. *Management Science*, 1404-1418.

Markowitz, H. (1952). Portfolio selection. *Journal of Finance*, 77-91.

MathWorks, Inc. (2018). *Statistics and Machine Learning Toolbox User's Guide.* Natick, MA: Mathworks, Inc.

McBride, B. J., Zehe, D. M., & Gordon, S. (2002). *NASA Glenn Coefficients for Calculating Thermodynamic Properties of Individual Species.* Washington, DC: National Aeronautics and Space Administration.

McNeish, D. (2016). On Using Bayesian Methods to Address Small Sample Problems. *StructuralEquation Modeling: A Multidisciplinary Journal, Vol. 23, No. 5*, 750-773.

Menon, E. S. (2005). *Gas Pipeline Hydraulics.* Boca Raton, FL: Taylor & Francis.

Mettas, A. (2013). Asset Management Supported by Reliability Engineering. *Journal of KONBiN 1(25)*, 117-128.

Mitra, D. (2012). *Likelihood Inference for Left Truncated and Right Censored Lifetime Data.* Hamilton: McMaster University .

Modisette, J. L., & Modisette, J. P. (2001). Transient and Succession-of-Steady-States Pipeline Flow Models. *Pipeline Simulation Interest Group Conference.* Pipeline Simulation Interest Group.

Nesic, S. (2007). Key issues related to modelling of internal corrosion of oil and gas pipelines - A review. *Corrosion Science*, 4308-4338.

Nishiumi, H., Arai, T., & Takeuchi, K. (1988). Generalization of the binary interaction parameter of the Peng-Robinson equation of state by component family. *Fluid Phase Equilibria*, 43-62.

Nordgard, D. E. (2012). A framework for risk-informed decision support in electricity distribution companies utilizing input from quantitative risk assessment. *Electrical Power and Energy Systems 43*, 255-261.

Nordgard, D., & Catrinu, M. (2011). Integrating risk analysis and multi-criteria decision support under uncertainty in electricity distribution system asset management. *Reliability Engineering and System Safety 96*, 663-670.

Parlikad, A., & Jafari, M. (2016). Challenges in infrastructure asset management. *International Federation of Automatic Control Conference* (pp. 185-190). Elsevier.

Peng, D.-Y., & Robinson, D. B. (1976). A New Two-Constant Equation of State. *Industrial & Engineering Chemistry Fundamentals*, 59-64.

Petchrompo, S., & Parlikad, A. K. (2019). A review of asset management literature on multi-asset systems. *Reliability Engineering and System Safety 181*, 181-201.

Plaat, H. (2009). Underground gas storage: Why and how. *Underground Gas Storage: Worldwide Experiences and Future Development in the UK and Europe*, 25-37.

Prakash, C., & Barua, M. (2015). Integration of AHP-TOPSIS method for prioritizing the solutions of reverse logistics adoption to overcome its barriers under fuzzy environment. *Journal of Manufacturing Systems, Vol. 37*, 599-615.

Praks, P., Kopustinskas, V., & Masera, M. (2015). Probabilistic modelling of security of supply in gas networks and evaluation of new infrastructure. *Reliability Engineering and System Safety*, 254-264.

Quigley, J., Bedford, T., & Walls, L. (2008). Prior Distribution Elicitation. In F. Ruggeri, R. Kenett, & F. Faltin, *Encyclopedia of Statistics in Quality and Reliability.*

Rao, M. S., & Naikan, V. N. (2016). Review of simulation approaches in reliability and availability modeling. *International Journal of Performability Engineering, Vol. 12, No. 4*, 369-388.

Rausand, M. (2011). *Risk Assessment: Theory, Methods, and Applications.* Hoboken: John Wiley & Sons.

Redman, T. (2018). If Your Data Is Bad, Your Machine Learning Tools Are Useless. *Harvard Business Review*.

Saaty, T. L. (1980). *The analytic hierarchy process: planning, priority setting, resource allocation.* New York: McGraw-Hill International Book Co.

Saaty, T. L., & Vargas, L. G. (2012). *Models, Methods, Concepts & Applications of the Analytic Hierarchy Process.* New York: Springer.

Samvedi, A., Jain, V., & Chan, F. T. (2013). Quantifying risks in a supply chain through integration of fuzzy AHP and fuzzy TOPSIS. *International Journal of Production Research, Vol. 51, No. 8*, 2433-2442.

Sandler, S. I. (1999). *Chemical and Engineering Thermodynamics, 3rd Edition.* New York, NY: Wiley.

Singpurwalla, N. D. (1988). An Interactive PC-Based Procedure for Reliability Assessment Incorporating Expert Opinion and Survival Data. *Journal of the American Statistical Association, 83:401*, 43-51.

Sridhar, N. (2018). Knowledge-Based Predictive Analytics in Corrosion. *Corrosion, Vol 74*, 181-196.

Tobias, P. A., & Trindade, D. C. (2012). *Applied Reliability, 3rd Edition.* Boca Raton, FL: CRC Press.

Tran, T. H., French, S., Ashman, R., & Kent, E. (2018). Impact of compressor failures on gas transmission network capability. *Applied Mathematical Modelling*, 741-757.

Tversky, A., & Kahneman, D. (1982). *A Judgement Under Uncertainty: Heuristics and Biases.* Cambridge: Cambridge University Press.

UK HSE. (2001). *Reducing risks, protecting people HSE's decision-making process.* Colegate, Norwich: United Kingdom Health and Safety Executive.

van de Schoot, R., Denissen, J., Neyer, F., Kaplan, D., Assendorpf, J., & van Aken, M. (2013). A Gentle Introduction to Bayesian Analysis: Applications to Developmental Research. *Child Development*, 1-19.

van der Lei, T., Herder, P., & Wijnia, Y. (2012). *Asset Management - The State of the Art in Europe from a Life Cycle Perspective.* New York, NY: Springer.

von Lanzenauer, C. H., James, W. G., & Wright, D. D. (1992). Insufficient supply in a natural gas distribution system: A risk analysis. *European Journal of Operational Research*, 41-53.

von Lanzenauer, C. H., James, W. G., & Wright, D. D. (1995). Service level risk in a pipeline system: A stochastic analysis. *European Journal of Operational Research*, 489-499.

Vose, D. (2008). *Risk Analysis - A quantitative guide, 3rd Edition.* Chichester, West Sussex: John Wiley & Sons Ltd.

Wang, J., Zuo, W., Rhode-Barbarigos, L., Lu, X., Wang, J., & Lin, Y. (2019). Literature review on modeling and simulation of energy infrastructures from a resilience perspective. *Reliability Engineering and System Safety, 183*, 360-373.

Wang, X., & Economides, M. (2009). *Advanced Natural Gas Engineering.* Houston, TX: Gulf Publishing Company.

WHO. (2017). *WHO methods and data sources for global burden of disease estimates 2000-2015.* Geneva: World Health Organization.

Wijnia, Y. (2016). *Processing Risk in Asset Management.* Delft, Netherlands: Technische Universiteit Delft.

Wilson, A., & Fronczyk, K. (2016). *Bayesian Reliability: Combining Information.* Alexandria, VA: Institute for Defense Analyses.

Wu, J. (2017). *Reliability analysis for small wind turbines using Bayesian hierarchical modelling.* Edinburgh: The University of Edinburgh.

Yang, C., Jing, W., Daemen, J., Zhang, G., & Du, C. (2013). Analysis of major risks associated with hydrocarbon storage caverns in bedded salt rock. *Reliability Engineering and System Safety*, 94-111.

Yoon, K. P., & Hwang, C.-L. (1995). *Multiple Attribute Decision Making An Introduction.* Thousand Oaks, CA: SAGE Publications, Inc.

Zyoud, S. H., Kaufmann, L. G., Shaheen, H., Samhan, S., & Fuchs-Hanusch, D. (2016). A framework for water loss management in developing countries under fuzzy environment: Integration of Fuzzy AHP with Fuzzy TOPSIS. *Expert Systems With Applications, Vol. 61*, 86-105.

7 APPENDICES

APPENDIX 1 CHAPTER 2 SUPPLEMENTARY MATERIAL

Table 17. Full Simulation Data Set

Samples 1 to 40			Samples 41 to 80		
Age at Removal t_i	**Truncation τ_i**	**Censoring Indicator δ_i**	**Age at Removal t_i**	**Truncation Age τ_i**	**Censoring Indicator δ_i**
32	4	0	38	10	1
18	1	1	36	8	1
32	28	1	34	6	1
26	1	1	29	23	1
36	10	1	37	9	0
33	23	1	14	10	1
23	13	1	27	15	1
22	0	1	27	0	0
20	0	1	30	12	1
28	27	1	39	25	1
27	0	0	19	6	1
27	0	0	29	24	1
32	4	0	34	15	1
26	18	1	29	8	1
5	0	1	29	1	0
33	5	0	27	0	0
27	0	0	42	23	1
38	10	0	31	3	0
31	3	0	30	24	1
19	0	1	17	4	1
18	9	1	48	24	1
16	6	1	28	0	0
34	6	0	36	20	1
29	19	1	23	11	1
33	10	1	28	16	1
28	8	1	25	20	1
36	23	1	31	3	0
33	31	1	20	12	1
37	29	1	36	13	1
32	4	0	22	0	1
16	8	1	36	22	1
25	21	1	30	6	1
25	0	1	23	6	1
37	31	1	41	13	1
23	19	1	27	14	1
30	6	1	28	5	1
26	5	1	28	0	1
29	26	1	32	28	1
41	15	1	26	13	1
34	17	1	26	16	1

Table 18. 10 Sample Subset

Age at Removal t_i	Truncation Age τ_i	Censoring Indicator δ_i
36	8	1
32	4	0
32	28	1
36	22	1
31	3	0
27	0	0
28	0	0
29	1	0
32	4	0
25	20	1

APPENDIX 2 CHAPTER 3 SUPPLEMENTARY MATERIAL

PR-EOS Constants and Mixing Rules

The constants for the PR-EOS are calculated using the following set of equations for a pure component (Peng & Robinson, 1976):

$$a(T) = 0.45724 \frac{R^2 T_{cr}^2}{P_{cr}} \alpha(T) \left[Pa \left(\frac{m^3}{mol} \right)^2 \right], \tag{24}$$

$$\alpha(T) = \left[1 + \kappa \left(1 - \frac{T}{T_{cr}} \right)^{\frac{1}{2}} \right]^2, \tag{25}$$

$$\kappa = 0.37464 + 1.54226\omega - 0.26992\omega^2, \tag{26}$$

$$b = 0.07780 \frac{RT_{cr}}{P_{cr}} \left[\frac{m^3}{mol} \right], \tag{27}$$

where T_{cr} is the fluid critical temperature, P_{cr} is the fluid critical pressure, and ω is the unitless fluid Pitzer acentric factor. Critical properties (temperature and pressure) and the Pitzer acentric factor were obtained from the DIPPR database (Brigham Young University Thermophysical Properties Laboratory, 2018). Properties for each component of the fluid are summarized in Table 19 below.

Table 19. Pure Component Properties

Pure Component Name	mol %	Molecular Weight [kg/kmol]	Critical Temperature [K]	Critical Pressure [kPa]	Acentric Factor
Methane	95.1%	16.04	190.6	4,599	0.0115
Ethane	3.1%	30.07	305.3	4,872	0.0995
Propane	0.3%	44.10	369.8	4,248	0.1523
Isobutane	0.0%	58.12	407.8	3,640	0.1835
n-Butane	0.0%	58.12	425.1	3,796	0.2002
n-Pentane	0.0%	72.15	469.7	3,370	0.2515
n-Hexane	0.0%	86.18	507.6	3,025	0.3013
Nitrogen	0.9%	28.01	126.2	3,400	0.0377
Carbon Dioxide	0.6%	44.01	304.2	7,383	0.2236
Hydrogen Sulphide	0.0%	34.08	373.5	8,963	0.0942

Since we are working with a fluid that is a mixture of many pure components, it is necessary to use mixing rules to obtain the PR-EOS constants for the mixture. The mixing rules used in this model are summarized below for completeness (Peng & Robinson, 1976).

$$a = \sum_i \sum_j x_i x_j (1 - \delta_{ij}) a_i^{0.5} a_j^{0.5}, \quad (28)$$

$$b = \sum_i x_i b_i, \quad (29)$$

where x_i is the mole fraction of pure component i, a_i is a PR-EOS constant for pure component i, b_i is a PR-EOS constant for pure component i, δ_{ij} is the empirically derived binary interaction coefficient for pure components i and j. The binary interaction coefficients used in this study are summarized in Table 20 for each pure component pair.

Table 20. Binary Interaction Coefficients (Nishiumi, Arai, & Takeuchi, 1988)

Component	Methane	Ethane	Propane	Isobutane	n-Butane	n-Pentane	n-Hexane	Nitrogen	Carbon Dioxide	Hydrogen Sulphide
Methane	0	0.056	0.015	0.031	0.025	0.031	0.038	0.044	0.114	0.081
Ethane	0.056	0	0.005	0.016	0.011	0.014	0.018	0.058	0.113	0.076
Propane	0.015	0.005	0	0.003[1]	0.003	0.004	0.007	0.071	0.111	0.07
Isobutane	0.031	0.016	0.003	0	0	0	0	0.088	0.11	0.063
n-Butane	0.025	0.011	0.003	0	0	0	0	0.086	0.11	0.064
n-Pentane	0.031	0.014	0.004	0	0	0	0	0.101	0.109	0.058
n-Hexane	0.038	0.018	0.007	0	0	0	0	0.117	0.109	0.058
Nitrogen	0.044	0.058	0.071	0.088	0.086	0.101	0.117	0	0.152	0.152
Carbon Dioxide	0.114	0.113	0.111	0.11	0.11	0.109	0.109	0.152	0	0.106
Hydrogen Sulphide	0.081	0.076	0.07	0.063	0.064	0.058	0.058	0.152	0.106	0

NASA Ideal Gas Thermodynamic Properties

The ideal gas property functions and coefficients were adopted from a NASA Glenn report for the Chemical Equilibrium with Applications computer program (McBride, Zehe, & Gordon, 2002). The ideal gas specific heat at constant pressure (c_p^*) in units of Joules/mole-Kelvin is given by

$$\frac{c_p^*(T)}{R} = a_1T^{-2} + a_2T^{-1} + a_3 + a_4T + a_5T^2 + a_6T^3 + a_7T^4, \qquad (30)$$

where R is the universal gas constant and T is the gas temperature. The constants a_1 through a_7 are empirically derived and summarized in Table 21 for each pure component. The specific heat at constant volume is calculated simply as $c_v^*(T) = c_p^*(T) - R$. The ideal gas enthalpy (h^*) in Joules/mole is

$$\frac{h^*(T)}{RT} = -a_1T^{-2} + a_2\frac{lnT}{T} + a_3 + a_4\frac{T}{2} + a_5\frac{T^2}{3} + a_6\frac{T^3}{4} + a_7\frac{T^4}{5} + \frac{b_1}{T}, \qquad (31)$$

and the ideal gas entropy (s^*) in Joules/mole-Kelvin is

$$\frac{s^*(T)}{R} = \frac{-a_1T^{-2}}{2} - a_2T^{-1} + a_3lnT + a_4T + a_5\frac{T^2}{2} + a_6\frac{T^3}{3} + a_7\frac{T^4}{4} + b_2, \qquad (32)$$

The integration constants b_1 and b_2 are summarized in Table 21 below as provided in the NASA report.

Table 21. NASA Glenn Ideal Gas Coefficients (McBride, Zehe, & Gordon, 2002)

	a_1	a_2	a_3	a_4	a_5
Methane	-1.767E+05	2.786E+03	-1.203E+01	3.918E-02	-3.619E-05
Ethane	-1.862E+05	3.406E+03	-1.952E+01	7.566E-02	-8.204E-05
Propane	-2.433E+05	4.656E+03	-2.939E+01	1.189E-01	-1.376E-04
Isobutane	-3.834E+05	7.000E+03	-4.440E+01	1.746E-01	-2.078E-04
n-Butane	-3.176E+05	6.176E+03	-3.892E+01	1.585E-01	-1.860E-04
n-Pentane	-2.769E+05	5.834E+03	-3.618E+01	1.533E-01	-1.528E-04

	a_1	a_2	a_3	a_4	a_5
n-Hexane	-5.816E+05	1.079E+04	-6.634E+01	2.524E-01	-2.904E-04
Nitrogen	2.210E+04	-3.818E+02	6.083E+00	-8.531E-03	1.385E-05
Carbon Dioxide	4.944E+04	-6.264E+02	5.301E+00	2.504E-03	-2.127E-07
Hydrogen Sulphide	9.544E+03	-6.875E+01	4.055E+00	-3.015E-04	3.768E-06

	a_6	a_7	b_1	b_2
Methane	2.027E-08	-4.977E-12	-2.331E+04	8.904E+01
Ethane	5.061E-08	-1.319E-11	-2.703E+04	1.298E+02
Propane	8.815E-08	-2.343E-11	-3.540E+04	1.842E+02
Isobutane	1.340E-07	-3.552E-11	-5.034E+04	2.659E+02
n-Butane	1.200E-07	-3.202E-11	-4.540E+04	2.379E+02
n-Pentane	8.191E-08	-1.792E-11	-4.665E+04	2.266E+02
n-Hexane	1.802E-07	-4.617E-11	-7.272E+04	3.938E+02
Nitrogen	-9.626E-09	2.520E-12	7.108E+02	-1.076E+01
Carbon Dioxide	-7.690E-10	2.850E-13	-4.528E+04	-7.048E+00
Hydrogen Sulfide	-2.239E-09	3.087E-13	-3.278E+03	1.415E+00

Distribution Parameterizations

Table 22 provides the parameterizations programmed into the DEM. The exponential and Weibull distributions (Tobias & Trindade, 2012) are used for modelling asset failures, while the uniform, triangular and generalized Pareto distributions (MathWorks, Inc., 2018) are used for modelling recovery times.

Table 22. Probability Distribution Parameterizations

Name	pdf	Parameters
Uniform	$f(t) = \begin{cases} \frac{1}{b-a} \; for \; a \leq t \leq b \\ 0 \; otherwise \end{cases}$	a is the lower bound and b is the upper bound with $-\infty < a < b < +\infty$
Triangular	$f(t) = \begin{cases} \frac{2(x-a)}{(b-a)(c-a)} \; for \; a \leq t < c \\ \frac{2}{b-a} \; for \; t = c \\ \frac{2(b-x)}{(b-a)(b-c)} \; for \; c < t \leq b \\ 0 \; otherwise \end{cases}$	a is the lower bound with $-\infty < a < +\infty$ b is the upper bound with $a < b$ c is the peak with $a \leq c \leq b$
Exponential	$f(t) = \lambda e^{-\lambda t}$	λ is the rate parameter with $\lambda > 0$
2-parameter Weibull	$f(t) = \frac{\beta}{\eta}\left(\frac{t}{\eta}\right)^{\beta-1} e^{-\left(\frac{t}{\eta}\right)^{\beta}}$	β is the shape parameter with $\beta > 0$ η is the scale parameter with $\eta > 0$

Name	pdf	Parameters
3-parameter Weibull	$f(t) = \frac{\beta}{\eta}\left(\frac{t-\gamma}{\eta}\right)^{\beta-1} e^{-\left(\frac{t-\gamma}{\eta}\right)^{\beta}}$	β is the shape parameter with $\beta > 0$ η is the scale parameter with $\eta > 0$ γ is the location parameter with $-\infty < \gamma < +\infty$
Generalized Pareto	$f(t) = \left(\frac{1}{\sigma}\right)\left(1 + k\frac{(x-\theta)}{\sigma}\right)^{-1-\frac{1}{k}}$	k is the shape parameter with $k \neq 0$ σ is the scale parameter with $\sigma > 0$ θ is the location parameter with $-\infty < \theta < +\infty$

Stochastic Process Parameterizations

Parameterizations for NHPP intensity functions used in the DEM are provided in Table 23 (Tobias & Trindade, 2012).

Table 23. Stochastic Process Parameterizations

Name	Intensity	Parameters
NHPP Power Law	$\lambda(t) = \alpha\beta t^{\beta-1}$	β is the shape parameter with $\beta > 0$ α is the scale parameter with $\alpha > 0$

Name	Intensity	Parameters
NHPP Log Linear	$\lambda(t) = e^{\alpha+\beta t}$	β is the shape parameter with $-\infty < \beta < +\infty$ α is the scale parameter with $-\infty < \alpha < +\infty$

Storage System Configuration

The required delivery pressure on withdrawal or injection is 4,926 kPa. A simulation time step of 12 hours was used in the TPM.

Table 24. Transmission System Configuration

Asset Name	Length [m]	Inner Diameter [m]	Efficiency	Maximum Operating Pressure [kPa]
Transmission Pipeline A	30,000	0.6096	95%	6,232
Transmission Pipeline B	30,000	0.6096	95%	6,232
Transmission Pipeline C	30,000	0.6096	95%	6,232

Table 25. Compressor Unit Configuration

Asset Name	Rated Power [kW]	Rated Pressure [kPa]	Pressure Ratio Limit	Efficiency	Usage Priority
Compressor MP	8,948	8,377	2	80%	1
Compressor LP	8,948	6,998	2	85%	2
Compressor HP	8,948	10,791	2	85%	3

Table 26. Reservoir Configuration

Asset Name	Cushion Pressure [kPa]	Maximum Operating Pressure [kPa]	Gas in Place @ Maximum [SCM]	Reservoir Temp. [K]	Flow Coeff.	Flow Exponent	Draw Down Limit
Reservoir A	2,512	9,751	10E+08	290	5E-01	0.9	0.33
Reservoir B	2,512	8,373	8E+08	290	8E-01	0.6	0.33
Reservoir C	2,512	8,373	8E+08	290	7E-01	0.7	0.33
Reservoir D	2,512	9,751	6E+08	290	3E+00	0.6	0.33

Table 27. Reservoir Pipeline Configuration

Asset Name	Length [m]	Inner Diameter [m]	Efficiency	Maximum Operating Pressure [kPa]
Reservoir A	3,000	0.6096	95%	9,751
Reservoir B	1,000	0.6096	95%	8,373
Reservoir C	1,000	0.6096	95%	8,373
Reservoir D	500	0.6096	95%	9,751

Table 28. Storage Field Withdrawal/Injection Priorities

Asset Name	Withdrawal Priority	Injection Priority
Reservoir A	1	1
Reservoir B	2	2
Reservoir C	2	3
Reservoir D	3	4

Table 29. Disruption Event Configuration

Event Name	Time at Risk	Probability Model	Clock	Units	Parameters	
SF A Meter Minor Failure	Calendar	Exponential	0	Y	10	
SF A Meter Major Failure	Calendar	Exponential	0	Y	50	
SF A Field Valve Failure	Calendar	Weibull 2-Parameter	40	Y	1.2	50
SF B Meter Minor Failure	Calendar	Exponential	0	Y	10	
SF B Meter Major Failure	Calendar	Exponential	0	Y	50	
SF B Field Valve Failure	Calendar	Weibull 2-Parameter	40	Y	1.2	50
SF C Meter Minor Failure	Calendar	Exponential	0	Y	10	
SF C Meter Major Failure	Calendar	Exponential	0	Y	50	
SF C Field Valve Failure	Calendar	Weibull 2-Parameter	40	Y	1.2	50
SF D Meter Minor Failure	Calendar	Exponential	0	Y	10	
SF D Meter Major Failure	Calendar	Exponential	0	Y	50	
SF D Field Valve Failure	Calendar	Weibull 2-Parameter	40	Y	1.2	50
Compressor MP Minor Failures	Usage	NHPP Power Law	50000	H	1	0.001

Event Name	Time at Risk	Probability Model	Clock	Units	Parameters		
Compressor MP Main Bearings	Usage	Weibull 2-Parameter	50000	H	10	95000	
Compressor MP Cylinder Liner	Usage	Weibull 3-Parameter	50000	H	4	48000	30000
Compressor LP Minor Failures	Usage	NHPP Power Law	25000	H	1	0.001	
Compressor LP Main Bearings	Usage	Weibull 2-Parameter	25000	H	10	95000	
Compressor LP Cylinder Liner	Usage	Weibull 3-Parameter	25000	H	3.6	32000	25000
Compressor HP Minor Failures	Usage	NHPP Power Law	25000	H	1	0.0005	
Compressor HP Main Bearings	Usage	Weibull 2-Parameter	75000	H	10	95000	
Compressor HP Cylinder Liner	Usage	Weibull 3-Parameter	25000	H	4	48000	30000
Transmission Pipeline A Failure	Calendar	Exponential	0	Y	1000		
Transmission Pipeline B Failure	Calendar	Exponential	0	Y	1000		
Transmission Pipeline C Failure	Calendar	Exponential	0	Y	1000		

Event Name	Recovery Lag Time	Units	Parameters			Recovery Active Time	Units	Parameters		
SF A Meter Minor Failure	Uniform	H	1	12		Uniform	H	1	24	
SF A Meter Major Failure	Uniform	H	1	24		Generalized Pareto	D	0.01	60	0
SF A Field Valve Failure	Triangular	D	0	14	1	Triangular	D	0	14	1
SF B Meter Minor Failure	Uniform	H	1	12		Uniform	H	1	24	
SF B Meter Major Failure	Uniform	H	1	24		Generalized Pareto	D	0.01	60	0
SF B Field Valve Failure	Triangular	D	0	14	1	Triangular	D	0	14	1
SF C Meter Minor Failure	Uniform	H	1	12		Uniform	H	1	24	
SF C Meter Major Failure	Uniform	H	1	24		Generalized Pareto	D	0.01	60	0
SF C Field Valve Failure	Triangular	D	0	14	1	Triangular	D	0	14	1
SF D Meter Minor Failure	Uniform	H	1	12		Uniform	H	1	24	
SF D Meter Major Failure	Uniform	H	1	24		Generalized Pareto	D	0.01	60	0
SF D Field Valve Failure	Triangular	D	0	14	1	Triangular	D	0	14	1
Compressor MP Minor Failures	Uniform	H	0	12		Generalized Pareto	H	0.05	48	0
Compressor MP Main Bearings	Uniform	D	7	14		Triangular	D	3	10	5

Event Name	Recovery Lag Time	Units	Parameters			Recovery Active Time	Units	Parameters		
Compressor MP Cylinder Liner	Uniform	D	7	14		Triangular	D	3	10	5
Compressor LP Minor Failures	Uniform	H	0	12		Generalized Pareto	H	0.05	48	0
Compressor LP Main Bearings	Uniform	D	7	14		Triangular	D	3	10	5
Compressor LP Cylinder Liner	Uniform	D	7	14		Triangular	D	3	10	5
Compressor HP Minor Failures	Uniform	H	0	12		Generalized Pareto	H	0.05	48	0
Compressor HP Main Bearings	Uniform	D	7	14		Triangular	D	3	10	5
Compressor HP Cylinder Liner	Uniform	D	7	14		Triangular	D	3	10	5
Transmission Pipeline A Failure	Triangular	D	1	5	2	Triangular	Y	0.5	1.5	1
Transmission Pipeline B Failure	Triangular	D	1	5	2	Triangular	Y	0.5	1.5	1
Transmission Pipeline C Failure	Triangular	D	1	5	2	Triangular	Y	0.5	1.5	1

Note that units of H is hours, D is days and Y is years.

Table 30. Impact Matrix Configuration

	SF A	SF B	SF C	SF D	COMP MP	COMP LP	COMP HP	TR PL A	TR PL B	TR PL C
SF A Meter Minor Failure	1									
SF A Meter Major Failure	1									
SF A Field Valve Failure	1									
SF B Meter Minor Failure		1								
SF B Meter Major Failure		1								
SF B Field Valve Failure		1								
SF C Meter Minor Failure			1							
SF C Meter Major Failure			1							
SF C Field Valve Failure			1							
SF D Meter Minor Failure				1						
SF D Meter Major Failure				1						
SF D Field Valve Failure				1						
Compressor MP Minor Failures					1					
Compressor MP Main Bearings					1					
Compressor MP Cylinder Liner					1					
Compressor LP Minor Failures						1				
Compressor LP Main Bearings						1				
Compressor LP Cylinder Liner						1				
Compressor HP Minor Failures							1			
Compressor HP Main Bearings							1			
Compressor HP Cylinder Liner							1			
Transmission Pipeline A Failure								1	1	
Transmission Pipeline B Failure								1	1	1
Transmission Pipeline C Failure									1	1

APPENDIX 3 CHAPTER 4 SUPPLEMENTARY MATERIAL

Table 31. Criteria Comparison Matrix with Consistency Ratio (CR)

CR = 0.076	Cost	Life Loss Risk	Production Loss Risk	Property Loss Risk
Cost	1	1/2	2	2
Life Loss Risk	2	1	6	6
Production Loss Risk	1/2	1/6	1	1
Property Loss Risk	1/2	1/6	1	1

Table 32. Life Loss Risk Comparison Matrix with Consistency Ratio (CR)

CR = 0.056	Cumulative Risk Reduction	Reduction in Limit Exceedance Probability	Reduction in Target Exceedance Probability
Cumulative Risk Reduction	1	3	9
Reduction in Limit Exceedance Probability	1/3	1	6
Reduction in Target Exceedance Probability	1/9	1/6	1

Table 33. Production Loss Risk Comparison Matrix with Consistency Ratio

CR = 0.039	Cumulative Risk Reduction	Reduction in Limit Exceedance Probability	Reduction in Target Exceedance Probability
Cumulative Risk Reduction	1	6	9
Reduction in Limit Exceedance Probability	1/6	1	3
Reduction in Target Exceedance Probability	1/9	1/3	1

Table 34. Property Loss Risk Comparison Matrix with Consistency Ratio

CR = 0.074	Cumulative Risk Reduction	Reduction in Limit Exceedance Probability	Reduction in Target Exceedance Probability
Cumulative Risk Reduction	1	7	9
Reduction in Limit Exceedance Probability	1/7	1	3
Reduction in Target Exceedance Probability	1/9	1/3	1

Table 35. TOPSIS Decision Matrix Analysis Results

	Life			Production		
Decision Criteria	**Cumulative Risk Reduction**	**Reduction in Limit Exceedance Probability**	**Reduction in Target Exceedance Probability**	**Cumulative Risk Reduction**	**Reduction in Limit Exceedance Probability**	**Reduction in Target Exceedance Probability**
Option 1	$357,750	46.0%	2.5%	$-	0.0%	0.0%
Option 2	$35,775	33.0%	0.0%	$743,300	0.0%	0.0%
Option 3	$-	0.0%	0.0%	$291,370	0.0%	0.0%
Option 4	$-	0.0%	0.0%	$5,888,070	36.0%	1.1%
Normalization Constant	1.29265E+11	0.3205	0.000625	3.53068E+13	0.1296	0.000121
Weight	37.3%	15.7%	3.3%	8.0%	1.7%	0.7%
Normalized-Weighted Option 1	0.3715041	0.127416561	0.032926	0	0	0
Normalized-Weighted Option 2	0.03715041	0.091407533	0	0.009962832	0	0
Normalized-Weighted Option 3	0	0	0	0.003905382	0	0
Normalized-Weighted Option 4	0	0	0	0.07892083	0.016725	0.007024
Ideal	0.3715041	0.127416561	0.032926	0.07892083	0.016725	0.007024
Anti Ideal	0	0	0	0	0	0

Decision Criteria	Property: Cumulative Risk Reduction	Reduction in Limit Exceedance Probability	Reduction in Target Exceedance Probability	Cost
Option 1	$-	0.0%	0.0%	$400,000
Option 2	$162,600	0.0%	0.0%	$10,000,000
Option 3	$67,880	0.0%	0.0%	$350,000
Option 4	$166,830	0.0%	0.0%	$6,000,000
Normalization Constant	58878703300	0	0	1.36283E+14
Weight	8.1%	1.5%	0.7%	23.0%
Normalized-Weighted Option 1	0	0	0	0.007884866
Normalized-Weighted Option 2	0.054413686	0	0	0.197121647
Normalized-Weighted Option 3	0.022715873	0	0	0.006899258
Normalized-Weighted Option 4	0.055829245	0	0	0.118272988
Ideal	0.055829245	0	0	0.006899258
Anti Ideal	0	0	0	0.197121647

Table 36. TOPSIS Option Rankings

Alternatives	DA+	DA-	CA
Option 1	0.10	0.44	0.82
Option 2	0.39	0.11	0.22
Option 3	0.40	0.19	0.32
Option 4	0.41	0.13	0.24

APPENDIX 4 CASE STUDY

This appendix presents a numerical example that incorporates all the models and methods developed in this work. A major component of a compressor unit within an underground gas storage facility is thought to be nearing end of life. An unexpected failure of this component can result in an extended outage of the compressor unit, potentially resulting in gas supply shortfalls. On the other hand, a proactive replacement plan can allow the outage window to be shortened and timed such that no gas supply shortfalls can occur. In the past, only two failures have been recorded for this type major component, and so the sample is not enough to infer probable future failures. In addition, the two failures occurred at a different facility and so the data is not directly applicable to this facility. Nevertheless, we are tasked with quantitatively evaluating the risk associated with a failure of this major component such that the capital expenditure to replace the component can be prioritized against other competing capital projects.

Probability of Failure

We must first determine the probability of failure of this major component during the capital planning horizon of 10 years. For this we need to determine a time to failure distribution for this component. However, the limited data precluded classical statistical analysis. Knowing that the component exhibits a wear out failure, we can apply the methodology presented in Chapter 2 and augment the limited failure data with expert knowledge about the degradation and eventual failure of the component.

With the knowledge of the failure mode and root cause of this major component, we determine the criteria scores presented in Table 37. Given the rarity of such failures, we put most importance on years of experience of our experts. In addition, we give significant weight to experts that have observed such failures. Finally, we give least importance to formal training since the failure mechanism is rare and not covered by most training programs. Scoring each expert against the AHP decision criterion, we derive the weights presented in Table 38. Time to failure estimates in units of 1000s of operating hours are obtained through independent interviews with each expert (Table 39) and aggregated using the derived weights (Table 40).

Table 37. AHP Criteria Comparison Matrix

Comparison Matrix	Years of Experience	Observed Failures	Relevant Training
Years of Experience	1	3	7
Observed Failures	1/3	1	5
Relevant Training	1/7	1/5	1

Table 38. Expert Ratings and Weights

Expert	Years of Experience	Observed Failures	Relevant Training	Weight
Expert 1	20	1	5	22.10%
Expert 2	30	1	5	50.78%
Expert 3	15	0	7	7.62%
Expert 4	12	0	7	6.04%
Expert 5	20	0	7	13.46%

Table 39. Expert Estimates for Time to Failure

Expert	Time to Failure Estimates (1000 hours)					
	Mode			Maximum		
	Lower Bound	Best Estimate	Upper Bound	Lower Bound	Best Estimate	Upper Bound
Expert 1	110	120	130	150	175	200
Expert 2	75	80	100	110	130	150
Expert 3	110	130	150	175	220	220
Expert 4	80	100	120	150	175	200
Expert 5	80	90	100	110	130	150

Table 40. Aggregated Time to Failure Estimates

Estimate	Lower Bound	Best Estimate	Upper Bound
$\bar{T}_{mode}$	86.4	95.2	112
$\bar{T}_{max}$	126	150	169

With the aggregated expert estimates for time to failure, we can perform Bayesian inference using informative prior distributions and the limited two-sample data set. The two observed failures were recorded to have occurred after 98,000 and 80,000 operating hours. The prior, likelihood and posterior distribution for the Weibull shape and scale parameters are shown in Figure 53 and Figure 54, with the median and central posterior density intervals summarized in Table 41.

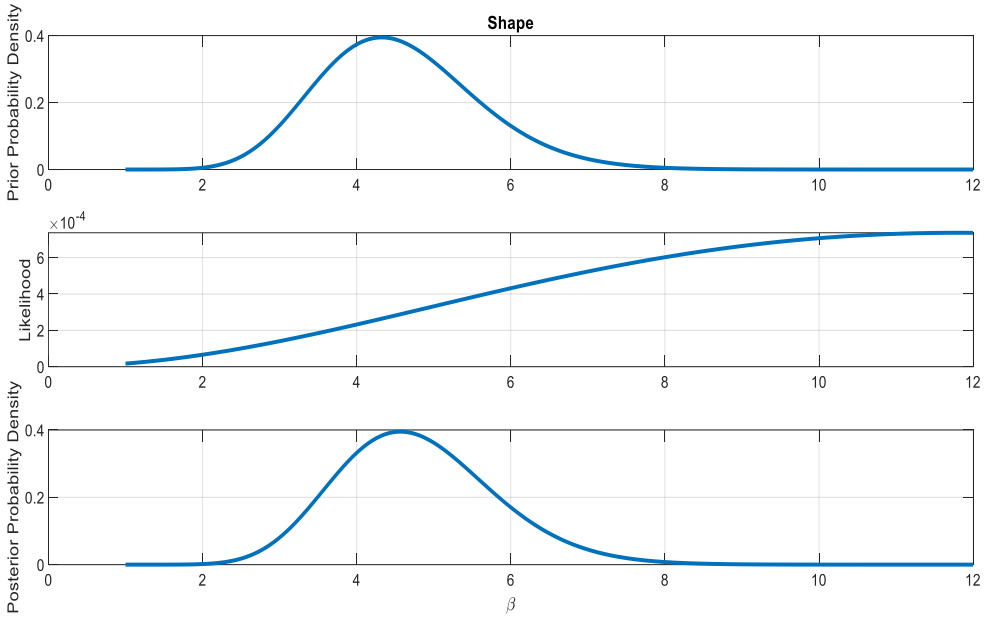

Figure 53. PLP Plot for Shape Parameter

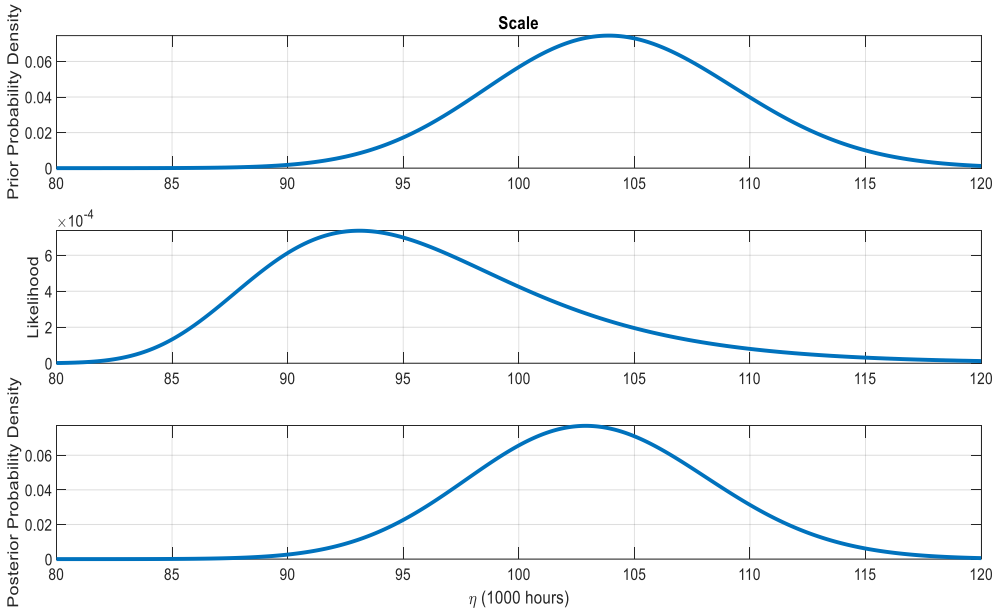

Figure 54. PLP Plot for Scale Parameter

Table 41. Posterior Parameter Estimates

Parameter	Median	95% CPD Interval	
β	4.716	2.987	7.009
η	103.1	93.24	113.6

The posterior distributions capture the uncertainty about the model parameters, which can then be propagated to the time to failure prediction. Figure 55 shows the cumulative probability of failure with 95% prediction intervals. We will use this uncertainty in our risk analysis later in the case study.

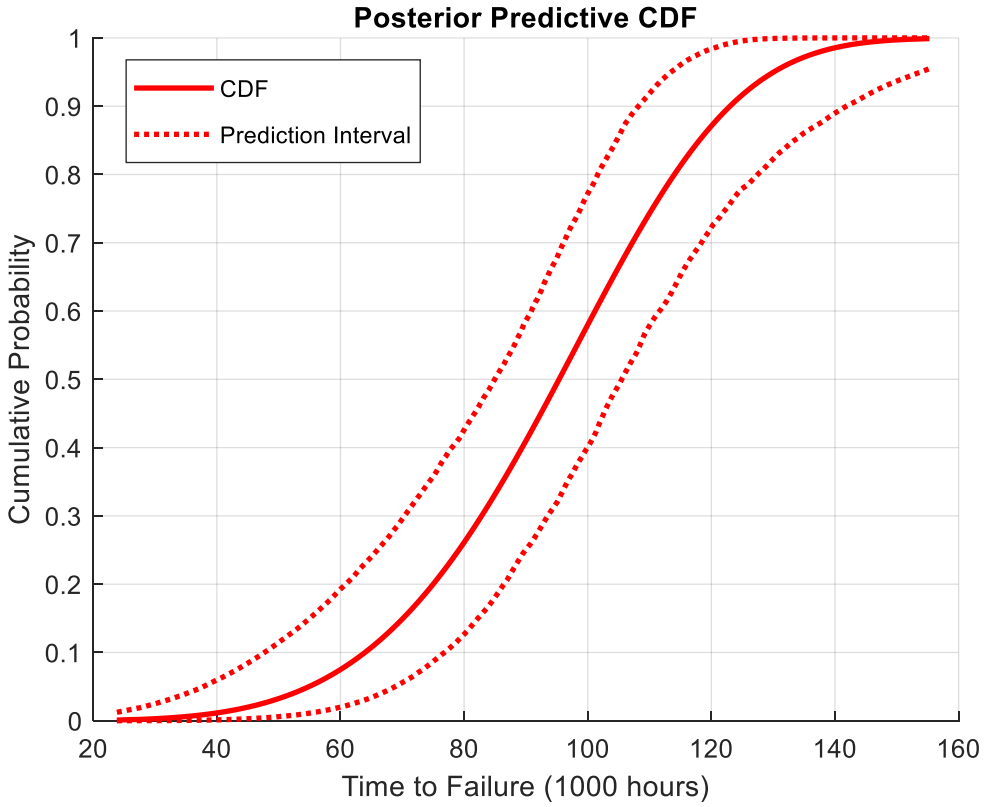

Figure 55. Predictive Distribution with 95% Interval

Consequence of Failure

We must now determine the consequence if the major component were to fail unexpectedly. By first gaining a qualitative understanding of the consequence, perhaps through a hazard or risk identification exercise, we conclude that an unexpected failure of this component can result in an extended shutdown of a compressor unit, which can cause significant shortfalls in gas supply. To quantify the potential gas supply shortfall, we use the simulation model presented in Chapter 3 of this thesis. The configuration of the thermo-physical performance model (TPM) is summarized in Figure 56 and Table 42 through Table 46. The required delivery pressure on withdrawal or injection is 4,926 kPa. A simulation time step of 12 hours was used in the TPM.

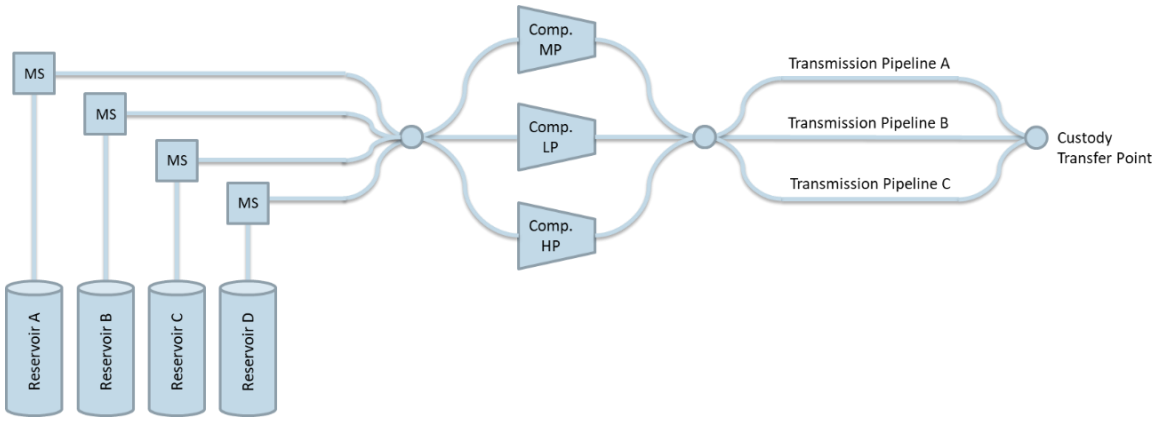

Figure 56. UGS Facility Configuration

Table 42. Transmission System Configuration

Asset Name	Length [m]	Inner Diameter [m]	Efficiency	Maximum Operating Pressure [kPa]
Transmission Pipeline A	30,000	0.6096	95%	6,232
Transmission Pipeline B	30,000	0.6096	95%	6,232
Transmission Pipeline C	30,000	0.6096	95%	6,232

Table 43. Compressor Unit Configuration

Asset Name	Rated Power [kW]	Rated Pressure [kPa]	Pressure Ratio Limit	Efficiency	Usage Priority
Compressor MP	2,610	8,377	2	80%	1
Compressor LP	2,610	6,998	2	80%	2
Compressor HP	2,610	10,791	2	80%	3

Table 44. Reservoir Configuration

Asset Name	Cushion Pressure [kPa]	Maximum Operating Pressure [kPa]	Gas in Place @ Maximum [SCM]	Reservoir Temp. [K]	Flow Coeff.	Flow Exponent	Draw Down Limit
Reservoir A	2,512	9,751	10E+08	290	5E-01	0.9	0.33
Reservoir B	2,512	8,373	8E+08	290	8E-01	0.6	0.33
Reservoir C	2,512	8,373	8E+08	290	7E-01	0.7	0.33
Reservoir D	2,512	9,751	6E+08	290	3E+00	0.6	0.33

Table 45. Reservoir Pipeline Configuration

Asset Name	Length [m]	Inner Diameter [m]	Efficiency	Maximum Operating Pressure [kPa]
Reservoir A	3,000	0.6096	95%	9,751
Reservoir B	1,000	0.6096	95%	8,373
Reservoir C	1,000	0.6096	95%	8,373
Reservoir D	500	0.6096	95%	9,751

Table 46. Storage Field Withdrawal/Injection Priorities

Asset Name	Withdrawal Priority	Injection Priority
Reservoir A	1	1
Reservoir B	2	2
Reservoir C	2	3
Reservoir D	3	4

The major component of concern in this case study is part of the MP compressor (see Figure 56). We consider minor failures of all compressor units (MP, LP, HP) as well as a major component failure of the MP unit. Minor failures of the compressor units are considered to account for potential synergistic effects of concurrent compressor unit failures. All other assets in the system (pipelines, reservoirs, etc.) are considered reliable. The configuration of the disruption event model (DEM) is summarized in Table 47 through Table 49. We draw attention to the MP Major Failure event, which represents the major component failure of concern in this case study. Note the parameters for this disruption event (Table 47) matches the median values of the parameters obtained in the Probability of Failure section of this case study. Other parameters for configuration of the disruption events and recovery times are assigned for illustration purposes.

Table 47. Disruption Event Configuration

Event Name	Time at Risk	Probability Model	Clock	Units	Parameters	
MP Minor Failure	Usage	NHPP Power Law	95,310	H	1	1/1500
LP Minor Failure	Usage	NHPP Power Law	76,695	H	1	1/1500
HP Minor Failure	Usage	NHPP Power Law	55,110	H	1	1/1500
MP Major Failure	Usage	Weibull 2-Parameter	95,310	H	4.716	103100

Table 48. Disruption Event Recovery Configuration

Event Name	Lag Time	Units	Parameters		Active Time	Units	Parameters	
MP Minor Failure	Uniform	H	0	12	Generalized Pareto	H	0.05	48

Event Name	Lag Time	Units	Parameters		Active Time	Units	Parameters		
LP Minor Failure	Uniform	H	0	12	Generalized Pareto	H	0.05	48	
HP Minor Failure	Uniform	H	0	12	Generalized Pareto	H	0.05	48	
MP Major Failure	None				Triangular	D	90	365	180

Note that units of H is hours, D is days and Y is years.

Table 49. Impact Matrix Configuration

	MP Unit	LP Unit	HP Unit
MP Minor Failure	1		
LP Minor Failure		1	
HP Minor Failure			1
MP Major Failure	1		

Finally, the risk simulation is run for 150 iterations and 3 years per iteration. The demand pattern (Figure 57) is assumed identical in each of the three years. Note that this is the same demand pattern presented in the scenario analysis in Chapter 3.

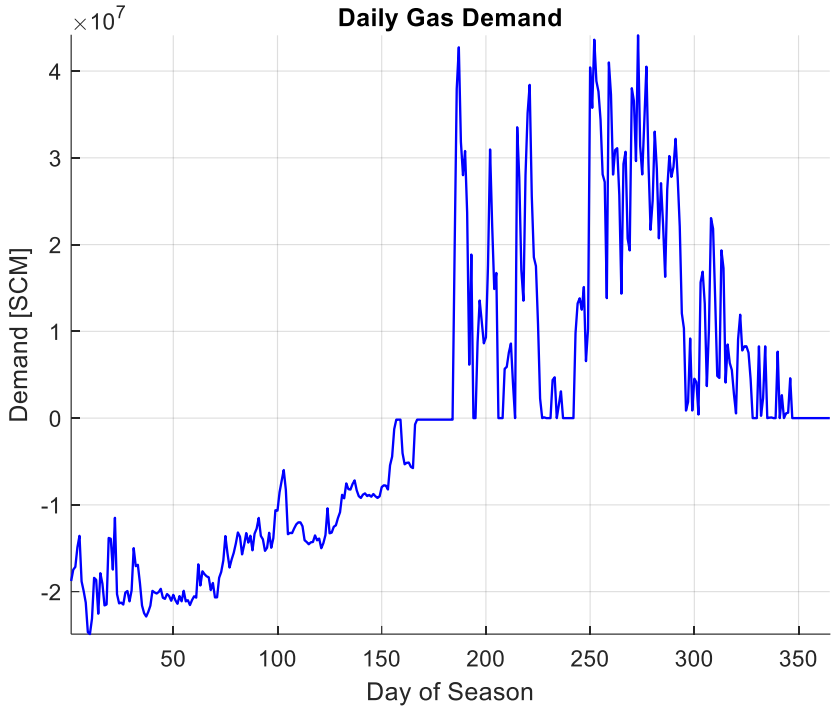

Figure 57. Daily Gas Flow Demand

Processing the results of the simulation we obtain the following histogram (Figure 58) for the cumulative gas supply shortfall during an outage of the MP compressor unit due to each occurrence of a major component failure event. This result is used in the risk analysis presented in the next section.

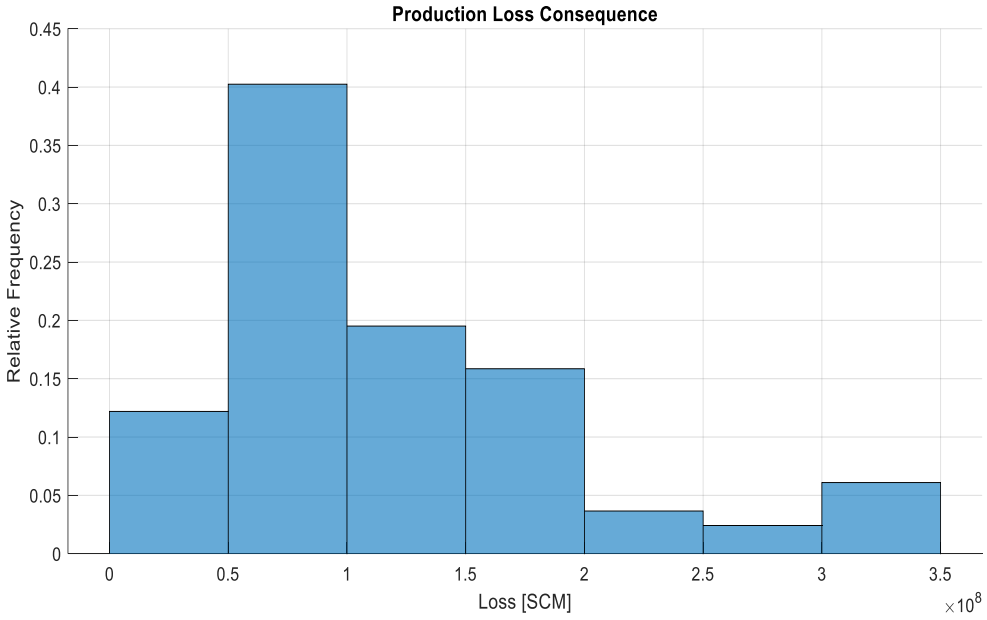

Figure 58. Production Loss Consequence Histogram

Risk Assessment

Recall that risk is calculated by multiplying the annual likelihood of event occurrence with the consequence associated with the event. If the likelihood and consequence are represented using probability distributions, then the annual risk exposure is represented as the product distribution of the two quantities.

The annual likelihood of event occurrence is calculated as the conditional probability of failure over one year. If we assume that the MP compressor's major component currently has 95,310 hours on it, and it averages 6,354 run hours per year, then we can calculate the run hours at year end as summarized in Table 50. Using the median values of the Weibull parameters (see Probability of Failure section), we then obtain the conditional probability of failure over each year, given that the component has survived up to the end-of-year hours from the previous year. Assuming our planning horizon is 10 years, we look at the 10-year average annual probability of failure for risk analysis purposes.

The Weibull parameters obtained previously are uncertain, which is represented using the posterior distributions of the parameters. We may propagate that uncertainty through the calculation described above using Monte Carlo simulation and arrive at the distribution shown in Figure 59. This distribution quantifies our uncertainty about the annual probability of occurrence of the event (i.e. major component failure).

Table 50. Component Run Hours and Probability of Failure

Year	Run Hours	Conditional Probability of Failure
1	101,664	0.217774
2	108,018	0.266394
3	114,372	0.31984
4	120,726	0.377344
5	127,080	0.437889
6	133,434	0.500242
7	139,788	0.563013
8	146,142	0.624741
9	152,496	0.683982
10	158,850	0.739412

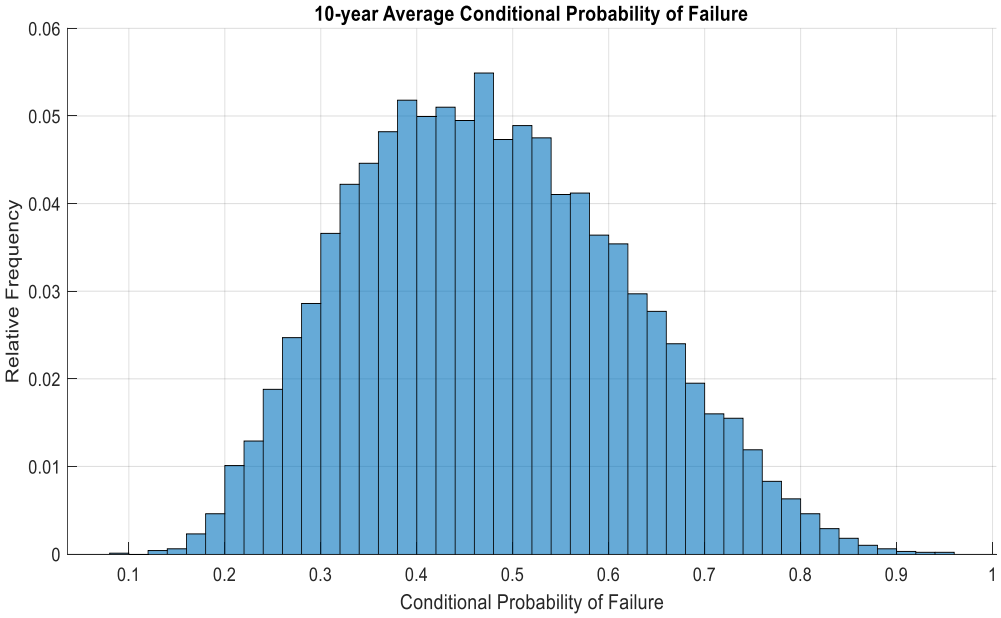

Figure 59. Component Probability of Failure Uncertainty

Combining the annual probability of event occurrence (likelihood) with the consequence of event occurrence, we can obtain the risk results shown in Figure 60. The event likelihood was obtained from Figure 59 and the event consequence was obtained from Figure 58. The SCM of gas supply loss was converted to dollars using a $53/SCM factor. The baseline risk analysis results show that the risk is above the tolerability limit, and therefore requires risk treatment.

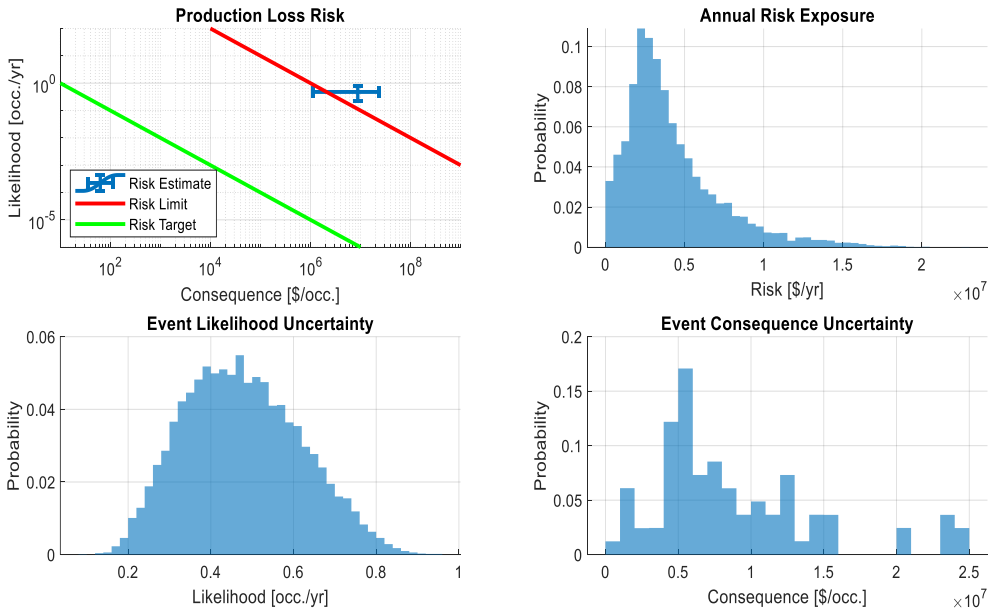

Figure 60. Major Component Failure Production Loss Risk Results

Since the risk has been evaluated to require treatment, we consider the risk exposure if the major component were to be replaced or renewed. The potential risk reduction is shown in Figure 61. The reduction in annual risk exposure is significant, attributed entirely to the reduced probability of failure for a renewed major component. As discussed in Chapter 4 of this thesis, a decision-maker may choose to make such renewal mandatory, given the risk is reduced from the intolerable region to the ALARP region. A cost-benefit analysis is also warranted to ensure that a proactive component replacement project has a positive net present value. Furthermore, if multiple options or competing capital investments are seeking funding, a prioritization exercise such as the one described in Chapter 4 may also be undertaken.

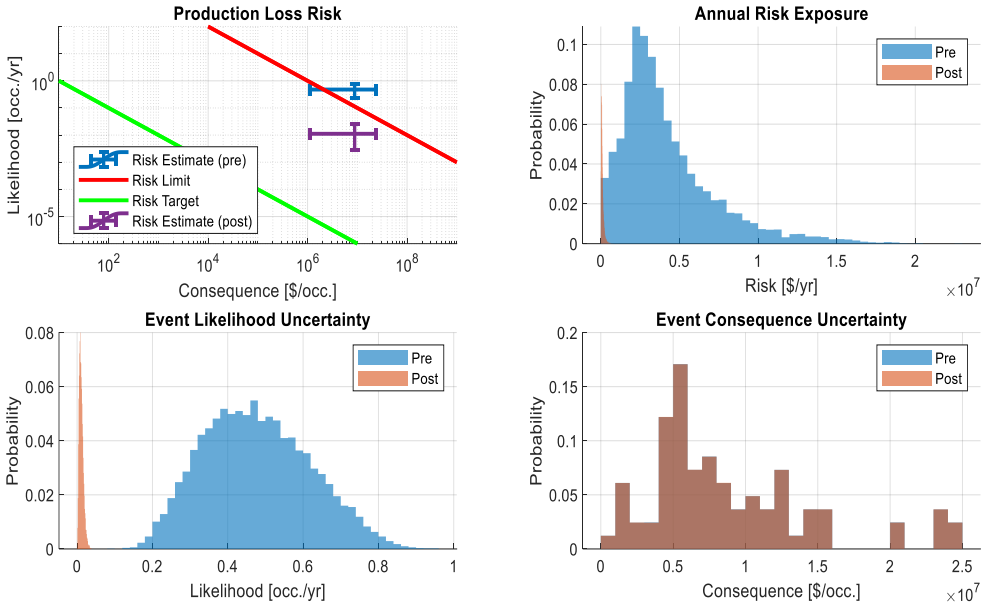

Figure 61. Major Component Replacement Production Loss Risk Reduction